Multiple Substituent Effects on the Rate Constants for N(2)-N(3) Restricted Rotation of *cis*-1,3-Diphenyltriazenes

by

Herlina Lim

A thesis

presented to the University of Waterloo

in fulfillment of the

thesis requirement for the degree of

Master of Science

in

Chemistry

Waterloo, Ontario, Canada, 2006

AUTHOR'S DECLARATION FOR ELECTRONIC SUBMISSION OF A THESIS

I hereby declare that I am the sole author of this thesis. This is a true copy of the thesis, including any required final revisions, as accepted by my examiners.

I understand that my thesis may be made electronically available to the public.

Abstract

Triazenes represent an interesting class of organic photochromic materials based on *cis-trans* isomerization around a nitrogen-containing double bond, and are of potential use in optical memory devices. One structural property of triazenes related to *cis-trans* isomerization is restricted rotation around the N(2)-N(3) bond. The purpose of the study presented in this thesis is to investigate the influence of aryl substitution on the N(2)-N(3) rotational barrier of *meta* and/or *para* substituted *cis*-1,3-diphenyltriazenes. Rate constants for restricted rotation in *cis*-triazenes were measured by means of a laser-flash photolysis system, via *trans*-to-*cis* photoisomerization of corresponding *trans*-triazenes (which were synthesized either by classical or non-classical diazonium coupling reactions). A quantitative structure-reactivity correlation analysis of rate constants for restricted rotation of *cis*-triazenes was carried out in terms of an extended Hammett equation. Resulting Hammett reaction constants for restricted rotation are -1.88 ± 0.08 and 0.70 ± 0.08 for N(1) and N(3), respectively, indicating that restricted rotation of *cis*-triazenes is more sensitive to the electronic character of the aryl group at N(1) than to that at N(3). Interestingly, the observed rate constants for restricted rotation in cyano-containing substrates are found to be pH-dependent. The latter is attributed to a change in the ionization state of the substrate, which is supported by solvent isotope effects. Furthermore, the pH dependence observed for unsymmetrical cyano-containing substrates indicates that upon deprotonation of the amino group, the negative charge concentrates either on the 4-CN substituent attached to the phenyl ring at N(3) or on the triazeno moiety. Thus, the primary *cis*-anionic 4-cyano-containing forms are not the same ions and do not equilibrate rapidly, since they undergo *cis*-to-*trans* isomerization. Finally, an extended Hammett equation was also employed in the analysis of p*Ka* values of *trans*-triazenes. The results show that there is a direct mesomeric interaction between the charge at N(3) in the triazeno moiety with 4-CN and 4-NO_2 groups in the systems studied. Consequently, the Yukawa-Tsuno modification of the Hammett equation is introduced to correlate p*Ka* values and Hammett substituent constants.

Acknowledgements

I would like to greatly thank my supervisor, Professor Mónica Barra. Her support, guidance and friendship over the past two years have made my research study a rewarding experience. Special thanks are given to my committee members, Professors Gary Dmitrienko and Xiangdong Fang for their valuable advice. Thanks are also due to Mrs. Jan Venne for her great help in acquiring NMR spectra and to Mrs. Cathy Van Esch for her help with administrative issues.

I would also like to acknowledge all the undergraduate students who worked and who are working in our laboratory: Atefeh Asadi, Marianne Heppleston, Kelvin Lau, and Ryan Tabone. Special thanks are given to all my friends, particularly Minh Nguyen and Jarrod Johnson for their support.

Last but not least, I would like to express my appreciation to my parents for their unconditional love and support that allowed me to pursue a higher education level.

This thesis is dedicated to my dearest and beloved parents, brother and sister.

Table of Contents

List of Tables

List of Figures

List of Schemes

List of Charts

List of Abbreviations, Acronyms, and Symbols

A	absorbance
AN	acetonitrile
aq	aqueous
A1	acid-catalyzed unimolecular process
BHT	2,6-di-*tert*-butyl-4-methylphenol
Bz	benzene
Calc.	calculated
δ	chemical shift
d	doublet (NMR)
d	deuterium
dd	doublet of doublets (NMR)
e.u.	entropy units
ΔA	change in absorbance
$\Delta G^{\ddagger}$	free energy of activation
ΔH	standard molar enthalpy change
ΔH_f	heat of formation
DMSO	dimethylsulfoxide
ε	extinction coefficient; dielectric constant
EAS	electrophilic aromatic substitution
EI MS	electron impact mass spectrum
g	gram
HRMS	high resolution mass spectrometry

Hz	hertz
IUPAC	international union of pure and applied chemistry
J	coupling constant (NMR)
Ka	acid dissociation equilibrium constant
k_{obs}	observed rate constant
k_{rot}	rotational rate constant for neutral species
k_{rot}^{-}	rotational rate constant for anionic species
K_T	tautomeric equilibrium constant
Kw	self-ionization constant of water
laser	light amplification by stimulated emission of radiation
LFP	laser flash photolysis
lit.	literature
λ	wavelength
λ_{max}	wavelength of maximum absorption
m	*meta*
MeOH	methanol
μ	ionic strength
mg	milligram
MC	monochromator
MHz	megahertz
mL	milliliter
mmol	millimole
mp	melting point

MS	mass spectrometry
NMR	nuclear magnetic resonance
p	*para*
PE	petroleum ether
Ph	phenyl
pH	negative logarithm of hydrogen ion activity
p*Ka*	negative logarithm of ionization equilibrium constant
PMT	photomultiplier tube
ppm	part per million
rel.	relative
ρ	Hammett reaction constant
rt	room temperature
s	singlet (NMR)
S_AN	two-step addition-elimination reaction
SHNC	sodium hexanitrocobaltate (III)
σ	Hammett substituent constant
S_N1	unimolecular nucleophilic substitution reaction
t	triplet (NMR)
T	temperature
THF	tetrahydrofuran
TLC	thin layer chromatography
UV	ultraviolet
v	volume

vis	visible
w	weight
YAG	yttrium aluminium garnet

Chapter 1. Introduction

Triazenes are compounds characterized by having a N=N-N functional group, referred to as the triazeno moiety.[1] The general structure of triazenes is shown in Scheme 1.1, where R can be any alkyl group, aryl group, and hydrogen.

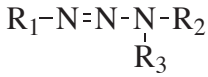

Scheme 1.1 General structure of triazenes.

According to the IUPAC system of nomenclature, the nitrogen atoms in the triazeno moiety are numbered consecutively from one end to the other, assigning the smallest numbers to the double bond, i.e., N(1)=N(2)-N(3).[2] For example, the triazene with $R_1 = R_2$ = phenyl and R_3 = hydrogen is named as 1,3-diphenyltriazene (**1**). Derivatives of **1** are the target substrates for the studies conducted for the purpose of this thesis.

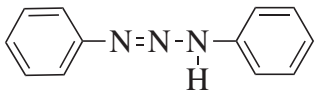

1

Triazenes are examples of photochromic organic materials. Photochromism, by definition, is a reversible transformation of a chemical species induced, at least in one direction, by absorption of electromagnetic radiation (light) between two forms having

different absorption spectra.[3] The representation of photochromism can be then illustrated as shown in Scheme 1.2.

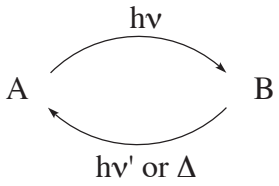

Scheme 1.2 Photochromic system.

One possible application of photochromic organic materials is their commercial usage in ophthalmic lenses.[4] These lenses are unique; the lenses are colorless when they are not exposed to bright light, and darken in a bright environment. These lenses contain a photochromic organic compound that is colorless when there is no bright light exposure. In a bright environment, this material undergoes an isomerization reaction to form a colored species. When taken back indoors, this activated form isomerizes back to its original form and the lenses become colorless again.

There are six classes of chemical processes involved in photochromism:[5] (a) pericyclic reactions, (b) *cis-trans* (*Z*/*E*) isomerization, (c) intramolecular H-transfer (H-tautomerism), (d) dimerization processes, (e) dissociation processes, and (f) electron transfers (oxido-reduction). Triazenes represent photochromic organic materials based on *cis-trans* isomerization of nitrogen-containing double bonds. Photochromic materials of this type are of interest for potential applications, among others, in molecular electronic devices.[5] In fact, triazenes are potential photochromic candidates for making high density, high signal/noise ratio optical memory materials.[6]

Other than being photochromic materials, triazenes have been extensively used both in the medical and industrial fields. In the medical research area, triazenes such as 1-aryl-3,3-dialkyltriazenes and 3-acyl-1,3-dialkyltriazenes are used in the development of anticancer drugs.[2,7] In several industrial sectors, *para*-substituted 1,3-diphenyltriazenes are used as versatile metal complexing agents as well as chemical blowing agents in a variety of polymer systems, such as in the manufacture of foam rubbers.[8] Last but not least, triazenes are also used as intermediates in heterocycle synthesis[7] and as protecting groups for secondary amines.[9]

As already mentioned, triazenes can undergo reversible *cis-trans* isomerization. One structural property of triazenes related to the *cis-trans* isomerization mechanism is the restricted or hindered rotation around the N(2)-N(3) bond. The work presented in this thesis concentrates on a structure-reactivity correlation analysis of rate constants for restricted rotation around the N(2)-N(3) bond of *cis*-**1** and its derivatives. Properties of triazenes significant to the study presented in this thesis are described in the next sections.

1.1 Properties of Triazenes

1.1.1 Stability of Triazenes

While studying triazene systems, one should take into account their stability towards not only heat and light, but also towards acids.[1,2] 1,3-Diaryltriazenes can undergo photoinduced decomposition (i.e., photolysis).[10] The mechanism that has been proposed for the photolysis of symmetrical 1,3-diaryltriazenes involves homolytic cleavage of the N(2)-N(3) single bond as shown in Scheme 1.3.[11,12]

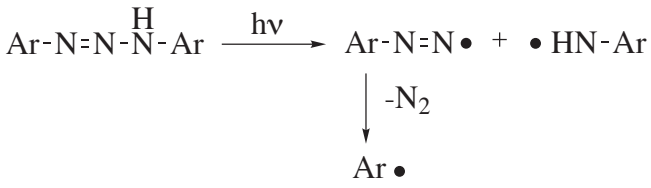

Scheme 1.3 Photoinduced decomposition of symmetrical 1,3-diaryltriazenes.

This radical pathway for photolysis of 1,3-diaryltriazenes yields the corresponding arylamino and aryldiazenyl radicals. Subsequently, the aryldiazenyl radicals can decompose to aryl radicals and nitrogen gas. Depending on the nature of the solvent (i.e., non-aromatic vs. aromatic solvent), these radicals can either combine with each other or react with solvent molecules to form various decomposition products (such as aminoazobenzenes, arylamines, and aminobiphenyls).[11,12] In all solvents, the major products formed are from the radical recombination of the aryl and arylamino radicals within the solvent cage and from hydrogen abstraction by arylamino radicals. Only in the case of aromatic solvents, biaryls are also observed as a result of radical substitution on the solvent molecules by the aryl radicals. The quantum yield of photolysis of **1**, upon continuous light irradiation at 360 nm, is measured to be approximately 0.02 in cyclohexane and 0.001 in methanol.[12] However, the quantum yield of photolysis of **1** is approximately 2.85 in benzene, clearly showing that in aromatic solvents, a free radical chain process is involved.[11]

Besides photoinduced decomposition, 1,3-diaryltriazenes can also undergo thermal decomposition. Just as for the photolysis mechanism, a homolytic cleavage of the N(2)-N(3) bond has been proposed for the thermal decomposition of 1,3-diaryltriazenes.[13] Thus, the primary decomposition products of 1,3-diaryltriazenes at high temperature are arylamino and aryldiazenyl radicals, the latter decomposing to yield aryl radicals and nitrogen gas. Since there

are two distinguishable tautomers for unsymmetrical 1,3-diaryltriazenes (Scheme 1.4), the primary decomposition products at high temperature involve two different arylamino, aryldiazenyl, and aryl radicals (the latter formed via decomposition of the corresponding aryldiazenyl radicals).[14,15]

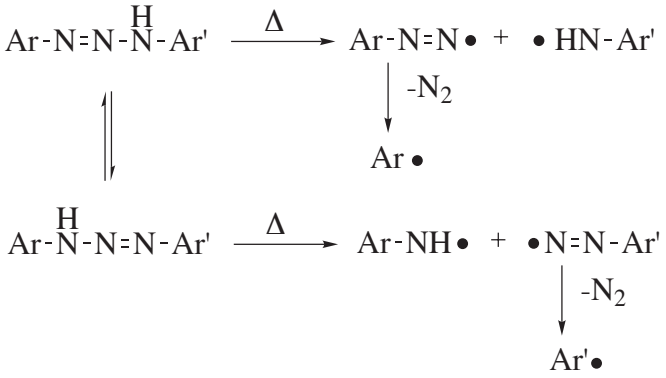

Scheme 1.4 Thermal decomposition of unsymmetrical 1,3-diaryltriazenes.

Besides photolysis and thermal decomposition, triazenes are also sensitive to the presence of acids. Although triazenes are stable in aprotic media, they can be readily decomposed upon the addition of acids, yielding diazonium ions and corresponding anilines.[16] Most studies agree that the acid catalyzed decomposition of triazenes involves protonation of N(3), followed by the breakage of the N(2)-N(3) single bond to yield the corresponding decomposition products, aniline and diazonium ions.[17-19] Results from the studies on the acid-catalyzed decomposition of 1,3-diaryltriazenes are interpreted in terms of an *A1* (acid catalyzed unimolecular) mechanism in which the rate-limiting step is the cleavage of the N(2)-N(3) single bond.[17-20] Thus, as indicated in Scheme 1.5, protonation takes place at N(3) by acids to give a 1,3-diaryltriazene cation **2**. This step is fast and reversible. Subsequently, cation **2** slowly decomposes to yield a diazonium ion **3** and its corresponding aniline **4** through a

heterolytic cleavage of the N(2)-N(3) single bond. It is known that triazene stability increases with increasing electron-withdrawing character of *para* substituents.[19,20] This is due to the difficulty to protonate N(3) since electron-withdrawing substituents decrease the electron density on N(3) (i.e., the basicity of the amino nitrogen decreases). Furthermore, the stability of diazonium ions is also decreased with electron-withdrawing substituents.

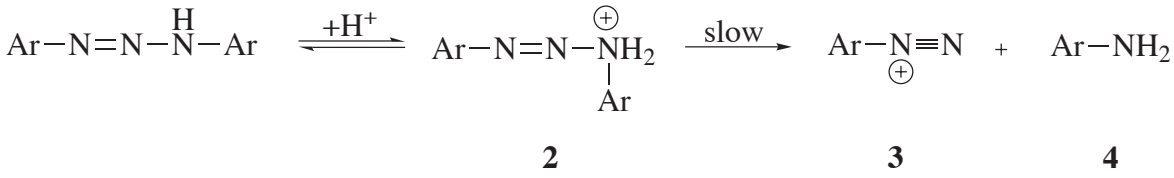

Scheme 1.5 Acid-catalyzed decomposition of 1,3-diaryltriazenes.

The final decomposition products of symmetrical 1,3-diaryltriazenes are usually aniline and phenol. Since there are two distinguishable tautomers for unsymmetrical 1,3-diaryltriazenes (Scheme 1.6), the final decomposition products involve two distinct anilines and phenols.[21]

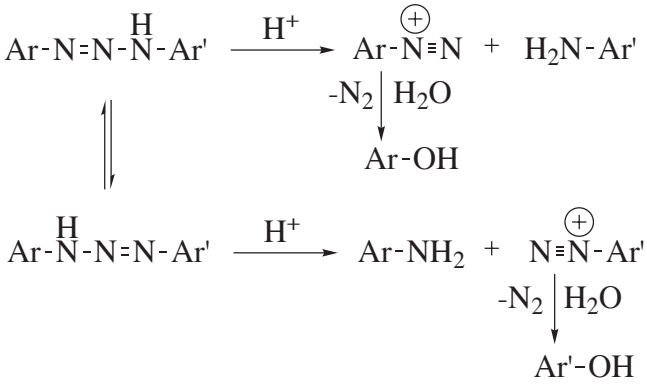

Scheme 1.6 Acid-catalyzed decomposition of unsymmetrical 1,3-diaryltriazenes.

Studies on the decomposition of triazenes derivatives in acidic media have also been performed by means of quantum chemical calculations, i.e., *ab initio* and PM3 semiempirical methods.[16,22,23] Calculations indicate that protonation of N(3) competes with protonation of N(1) and that both are energetically more favorable than protonation of N(2).[16,22,23] This can be seen from the corresponding heat of formation, ΔH_f, data (Table 1.1) calculated from the PM3 semiempirical method.[23] Protonation of N(1) does not lead, however, to 1,3-diaryltriazene decomposition, as it allows charge delocalization over the three nitrogen atoms. On the other hand, protonation of N(3) destabilizes the N(2)-N(3) bond by preventing electron delocalization over the three nitrogen atoms. It is also noticed from Table 1.1 that protonation of N(3) occurs more readily with electron donating substituents since an electron donating group stabilizes the positive charge on N(3). Interestingly, calculations also indicate that protonation on N(3) results in a considerable bond-lengthening of the N(2)-N(3) bond and, as a consequence, the N(1)=N(2) bond is shortened (Table 1.2).[16,23] Thus, protonation of N(3) is a crucial step that eventually leads to the decomposition of triazenes.[16,22,23]

Table 1.1 Calculated heat of formation of protonated *p,p'*-disubstituted 1,3-diphenyltriazenes.[23]

Substituent	ΔH_f (N(1)) (kcal/mol)	ΔH_f (N(2)) (kcal/mol)	ΔH_f (N(3)) (kcal/mol)
OCH_3	183.1	195.3	187.4
H	264.4	276.5	266.5
NO_2	267.4	280.1	267.8

Table 1.2 Calculated bond lengths for neutral and N(3)-protonated *p,p'*-disubstituted 1,3-diphenyltriazenes.[23]

Substituent	neutral 1,3-diphenyltriazene		N(3)-protonated 1,3-diphenyltriazene	
	N(1)=N(2) (Å)	N(2)-N(3) (Å)	N(1)=N(2) (Å)	N(2)-N(3) (Å)
OCH_3	1.236	1.390	1.218	1.596
H	1.237	1.385	1.217	1.580
NO_2	1.237	1.382	1.205	1.927

1.1.2 Restricted Rotation

Restricted or hindered rotation about a single bond, by definition, is the inhibition of rotation of groups about a bond due to the presence of a sufficiently large rotational barrier.[24a] In the case of triazenes, a 1,3-dipolar resonance form is generated when the lone pair electrons on N(3) conjugate with the π electrons on the N(1)=N(2) double bond (Scheme 1.7), which causes an increase in the energy barrier for rotation around the N(2)-N(3) bond.

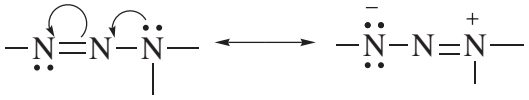

Scheme 1.7 Resonance delocalization of the triazeno moiety.

The first observation on restricted rotation of a series of *trans*-1-(4-X-phenyl)-3,3-dimethyltriazenes (**5**) is documented by Akhtar *et al.*[25] and Marullo *et al.*[26] in the late 1960s. In the ^{1}H NMR spectrum of **5,** the methyl signal is a singlet at room temperature. Cooling the

sample results in a broadening of the methyl signal and eventually two distinct peaks of equal intensity appear. From the corresponding temperature dependent NMR spectrum of **5**, the free energy activation of rotation, $\Delta G^{\ddagger}$, is derived. Values of $\Delta G^{\ddagger}$ given in Table 1.3 show that as the electron-withdrawing character of the substituent placed in the *para* position of the phenyl ring increases, the rotational barrier of the restricted rotation around N(2)-N(3) bond increases. Thus, this suggests that the influence of the 1,3-dipolar resonance structure is greater in the presence of electron-withdrawing substituents on the phenyl ring.[25-29]

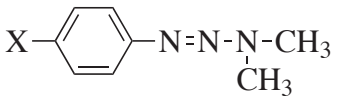

5

Table 1.3 Free energy of activation for restricted rotation of *trans*-1-(4-X-phenyl)-3,3-dimethyl triazenes in $CDCl_3$ at 298 K.

X	$\Delta G^{\ddagger}$ (kcal/mol)[a]	$\Delta G^{\ddagger}$ (kcal/mol)[b]
OCH_3	12.7	
CH_3	13.0	12.1
H	13.7	12.7
Cl	13.9	13.3
NO_2	15.7	15.7

[a]Data taken from ref. 25. [b]Data taken from ref. 26.

Results from X-ray diffraction studies (Table 1.4) clearly show that the bond length of the N(1)=N(2) double bond in disubstituted *trans*-1,3-diphenyltriazenes **6** is longer than the characteristic N=N double bond (1.24 Å).[30] On the contrary, the N(2)-N(3) single bond in disubstituted *trans*-1,3-diphenyltriazenes is shorter than the characteristic N-N single bond (1.44 Å).[30]

Table 1.4 Bond lengths for N(1)=N(2) and N(2)-N(3) for various 1,3-diphenyltriazene derivatives.

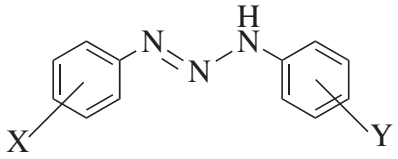

6

	X	Y	N(1)=N(2) (Å)	N(2)-N(3)(Å)
6a[a]	4-CH_3	4-F	1.2803	1.3163
6b[a]	4-CH_3	4-CH_3	1.2777	1.3344
6c[b]	H	H	1.27	1.31
6d[c]	3-NO_2	3-NO_2	1.2612	1.3262
6e[d]	4-NO_2	4-NO_2	1.2632	1.3402
6f[a]	4-F	4-Cl	1.3178	1.3217

[a]Data taken from ref. 31. [b]Data taken from ref. 32. [c]Data taken from ref. 33. [d]Data taken from ref. 34.

Furthermore, a theoretical study on 1-aryl-3,3-diethyltriazenes indicates that the calculated bond orders for N(1)=N(2) are smaller than 2 (typically between 1.683 and 1.829), while the calculated bond orders for N(2)-N(3) are larger than 1 (typically between 1.009 and 1.187).[35] These results are consistent with the 1,3-dipolar resonance contribution. There is a linear correlation between the bond orders of the N(2)-N(3) bond and the free energy of rotation, $\Delta G^{\ddagger}$; i.e., the bond order of the N(2)-N(3) bond increases with $\Delta G^{\ddagger}$.[35]

The free energies of activation of rotation, $\Delta G^{\ddagger}$, can also be correlated by means of the Hammett equation (see Section 1.2). In the case of *trans*-1-(4-X-phenyl)-3,3-dimethyltriazenes (**6**), Akhtar *et al.*[25] report that an excellent linear relationship against the Hammett substituent constants σ is observed, with a slope (ρ) value of -2.1, whereas Marullo *et al.*[26] report that the observed ρ values at 25°C and 0°C are –2.01 and –2.03, respectively. Furthermore, in the case of *trans*-1-aryl-3,3-dialkyltriazenes, observed ρ values of –2.04[36] and –1.95[28] are in excellent agreement with the results obtained by both Akhtar *et al.*[25] and Marullo *et al.*.[26] The negative ρ values observed in all cases suggest that (the restricted) rotation around the N(2)-N(3) bond causes the electron density at N(1) to decrease on going from the ground to the transition state.[26,28,36]

Restricted rotation is also observed with *cis*-triazenes, although the studies are very limited. The only documented experimental study on the influence of substituents and solvents on the energy barrier corresponding to the N(2)-N(3) restricted rotation on *cis*-triazenes focuses on *cis*-1,3-di(4-X-phenyl)triazenes.[37] It is noticed from the $\Delta G^{\ddagger}$ values given in Table 1.5 that increasing the electron-withdrawing character of the X substituents results in an increase in the rotational barrier. Increasing the electron-withdrawing character of X substituents will stabilize the negative charge on N(1) and destabilize the positive charge on

N(3). Thus, the trend observed implies that the restricted rotation of *cis*-1,3-di(4-X-phenyl)triazenes is more sensitive to the electronic character of the aryl group attached to N(1) than of that bonded to N(3).[37]

Table 1.5 Free energy of activation for restricted rotation of *cis*-1,3-di(4-X-phenyl)triazenes in 30% v/v THF:H_2O solution at 21ºC.[37]

X	CH_3O	CH_3	H	Cl	CF_3
$\Delta G^{\ddagger}$ (kcal/mol)	10.6 ± 0.1	11.1 ± 0.3	11.1 ± 0.8	11.7 ± 0.2	11.9 ± 0.3

Solvent effects on the restricted rotation of *cis*-1,3-di(4-X-phenyl) triazenes have also been studied experimentally.[37] As depicted in Table 1.6, not only decreasing polarity of the organic co-solvent, but also increasing the organic co-solvent concentration lead to an increase in the rotational barrier about the N(2)-N(3) bond. This clearly indicates an increase in dipole moment on rotation from the ground state to the transition state.[37]

Table 1.6 Free energy of activation for N(2)-N(3) restricted rotation of *cis*-1,3-diphenyltriazene in aqueous solution at 21ºC.[37]

Co-Solvent	30 % MeOH	30% AN	30% THF	20% THF	15% THF
$\Delta G^{\ddagger}$ (kcal/mol)	10.1 ± 0.4	10.5 ± 0.4	11.1 ± 0.8	10.5 ± 0.1	10.2 ± 0.2

1.1.3 Tautomerization

Besides restricted rotation around the N(2)-N(3) bond of triazenes, tautomerization is also an important aspect for the study presented in this thesis. Tautomerization, by definition, is a process occurring by the migration of a proton and relocation of single and double bonds.[24b] Triazenes with R'' = H, as illustrated in Scheme 1.8, display tautomerism. If the substituents R and R' at N(1) and N(3) are not identical, a mixture of two distinguishable tautomeric forms, **7a** and **7b**, will exist. Tautomeric equilibria depend on the electronic character of the substituents R and R' and are determined by the equilibrium constant, K_T. Studies on tautomeric equilibria of triazenes have been conducted by means of spectroscopic methods, such as IR and NMR.[38-42]

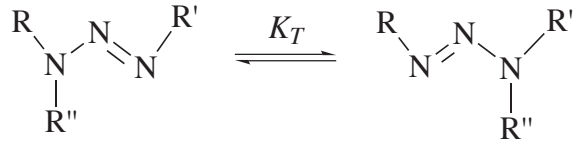

7a **7b**

Scheme 1.8 Tautomerization of *trans*-triazenes.

Substituents effect on a series of unsymmetrical *trans*-1,3-diaryltriazenes have been studied by means of infrared spectroscopy in carbon tetrachloride.[38] In this study, unsymmetrical triazenes labeled with ^{15}N are used to assign the absorption bands due to the N-H stretching vibrations (i.e., Scheme 1.8, RNH-N=^{15}NR′ in **7a** and RN=N-^{15}NHR′ in **7b**).[38] The approximate ratio of the two tautomeric forms, K_T, is obtained based on the IR absorption intensities of the ^{15}NH stretching vibration bands compared to the ^{14}NH stretching vibration

bands (i.e., $K_T = \frac{A(7b)}{A(7a)}$, where A represents the absorption intensity). As given in Table 1.7, the equilibrium constants (K_T) of a series of unsymmetrical *trans*-1,3-diaryltriazenes indicates that *para* groups with an electron-withdrawing mesomeric effect favor tautomer **7a**, whereas *para* groups with an electron-donating mesomeric effect and *meta* groups with an electron-withdrawing inductive effect favor tautomer **7b**.[38]

Table 1.7 Tautomerization equilibrium constants for a series of unsymmetrical *trans*-1,3-diaryltriazenes.[38]

R	R'	R''	$K_T = \frac{A(7b)}{A(7a)}$
p-NO_2-C_6H_4	C_6H_5	H	0.48
m-Cl-C_6H_4	C_6H_5	H	1.33
p-CH_3-C_6H_4	C_6H_5	H	1.64
p-Cl-C_6H_4	C_6H_5	H	2.27

Besides IR, NMR spectroscopy also gives information on the effect of various substituents in shifting the equilibrium in favor of one of the two possible tautomers. The ^{13}C-NMR spectra of 3-methyl-1-*p*-tolyltriazene (Scheme 1.8; R = *p*-CH_3-C_6H_4, R' = CH_3), observed in $CDCl_3$ at temperatures ranging from –40°C to 100°C, demonstrate that while tautomer **7b** predominates, tautomer **7a** is still present in *ca.* 18%.[39] Indeed, this result is consistent with the IR study,[38] i.e., the tautomerization equilibrium shifts to the position where

the N=N double bond is closer to the electron-donating group. A ^{19}F-NMR study on a series of 1-(4-fluorophenyl)-3-(4-X-phenyl)triazenes in THF and pyridine at –90°C and –60°C, respectively, demonstrates that the position of the tautomerization equilibrium depends mainly on the resonance effect of the substituents.[42] Increasing the electron-withdrawing character of the X-substituent causes the tautomerization equilibrium to shift to the position in which the N=N double bond is distant from the X-substituent. These results are supported by *ab initio* calculations of the electron density of a series of 1-(4-fluorophenyl)-3-(4-X-phenyl)triazenes, which have shown that electron-withdrawing X-substituents increase the electron density on the nearest nitrogen atom.[43] Thus, the tautomerization equilibrium is expected to shift to the position in which the N-H bond is closer to the electron-withdrawing X-substituent.

1.1.4 Cis-Trans Isomerization

Many unsaturated N-containing substances, such as azo compounds[44] and carbamates,[45] undergo *cis-trans* isomerizations. The interconversion of *cis* (*Z*) and *trans* (*E*) configurations is known to affect physical properties such as absorption spectra. Owing to the presence of the N=N double bond, triazenes can exist as *cis* and *trans* isomers and can undergo reversible *cis-trans* isomerization (Scheme 1.9).[2,46,47] Triazenes in the *trans* form can be photochemically transformed into the *cis* form. Because of the instability of *cis*-isomers, *cis*-triazenes will revert back to the thermodynamically more stable *trans*-form via a thermal process.[46] In this section, the mechanistic studies on the thermal *cis*-to-*trans* isomerization for series of *p,p′*-disubstituted-1,3-diphenyltriazenes are presented.

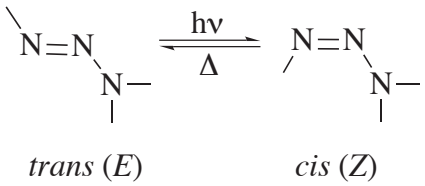

Scheme 1.9 *Cis-trans* isomerization of triazenes.

Kinetic studies on the thermal *cis*-to-*trans* isomerization of series of *p,p′*-disubstituted-1,3-diphenyltriazenes (both symmetrical and unsymmetrical) have been studied systematically by Barra *et al.*[20,37,48,49] *Cis-p,p′*-disubstituted-1,3-diphenyltriazenes were generated upon laser excitation at λ = 355 nm of *trans-p,p′*-disubstituted-1,3-diphenyltriazenes in buffered 30% (v/v) THF:H_2O solutions. The proposed *cis*-to-*trans* isomerization mechanism for symmetrical *p,p′*-disubstituted-1,3-diphenyltriazenes is shown in Scheme 1.10.[20,48]

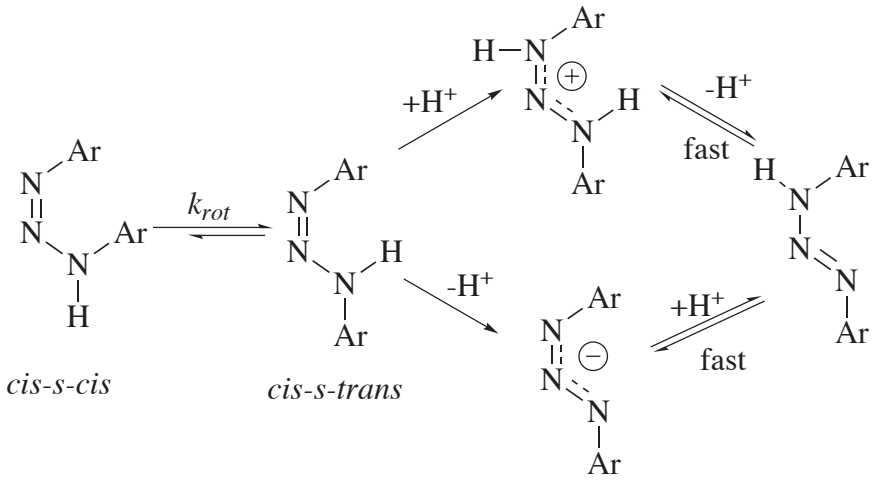

Scheme 1.10 *Cis*-to-*trans* isomerization mechanism for symmetrical triazenes.

According to Scheme 1.10, the mechanism for thermal *cis*-to-*trans* isomerization of 1,3-diphenyltriazenes in aqueous media involves two consecutive processes: restricted rotation

around the N(2)-N(3) bond, followed by 1,3-prototropic rearrangements. It is found that the rate-controlling step depends on the pH of the solution.[48] At pH < 10, the 1,3-prototropic rearrangement, which is catalyzed by general acids and bases, is the rate-controlling step. Acid catalysis is attributed to rate-limiting proton transfer to the diazo group leading to the isomerization. Acid catalysis becomes predominant as the electron donating character of the *para* substituent increases. Base catalysis is attributed to the rate-limiting base-promoted ionization of the amino nitrogen and becomes predominant as the electron withdrawing character of the *para* substituent increases.

On the other hand, at pH > 10, restricted rotation around the N(2)-N(3) bond is the rate-controlling step. The rate of this process is independent of the concentration of acids and bases. As it is already illustrated in Scheme 1.7, the N(2)-N(3) bond of the triazeno moiety possesses a considerable partial double bond character as a result of the 1,3-dipolar resonance form. This resonance hybridization causes an increase in the energy barrier for the rotation about the N(2)-N(3) bond. Thus, *cis*-1,3-diphenyltriazenes, shown in Scheme 1.11, exist as pair of rotamers (*cis-s-cis* and *cis-s-trans*). A 1,3-prototropic rearrangement illustrated in Scheme 1.10 can only lead to a change in the N=N double bond configuration if applied to the *cis-s-trans* rotamer.[20,48]

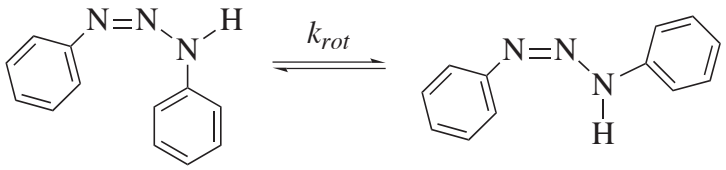

cis-s-cis *cis-s-trans*

Scheme 1.11 Restricted rotation around the N(2)-N(3) bond of *cis*-**1**.

In addition to the symmetrical system, three unsymmetrical *p,p′*-disubstituted 1,3-diphenyltriazenes have also been thoroughly studied.[49] For these systems, it is reasonable to assume that the thermal *cis*-to-*trans* isomerization mechanism is similar to that of symmetrical *p,p′*-disubstituted 1,3-diphenyltriazenes presented in Scheme 1.10. However, one needs to consider a unique geometrical characteristic that arises from the nature of unsymmetrical triazenes, i.e., the existence of unsymmetrical triazenes as a pair of distinguishable tautomers as shown earlier in Scheme 1.8.[49]

The general observations for *cis*-to-*trans* isomerization of unsymmetrical triazenes are in agreement with those for symmetrical triazenes. The proposed *cis*-to-*trans* isomerization mechanism of unsymmetrical *p,p′*-disubstituted 1,3-diphenyltriazenes is shown in Scheme 1.12. At relatively low pH, the observed rate constants are dependent on the pH and buffer concentration, consistent with thermal *cis*-to-*trans* isomerization involving a 1,3-prototropic rearrangement catalyzed by general acids and bases, whereas at relatively high pH, the observed rate constants are independent of pH, in agreement with restricted rotation as the rate controlling step, except for the fact that two pairs of *cis* isomers are observed upon *trans*-to-*cis* photoisomerization.[49]

The two *cis-s-cis* tautomers behave as two independent species, and each one follows the same *cis*-to-*trans* isomerization mechanism as described for symmetrical triazenes (Scheme 1.10). This interpretation implies that the rate of tautomerization of *cis-s-cis* isomers is slower than that of *cis*-to-*trans* isomerization.[49] This consideration is reasonable based on steric hindrance arguments: restricted rotation around the N(2)-N(3) bond followed by a 1,3-protrotopic rearrangement decrease the steric interaction between the phenyl groups.[49]

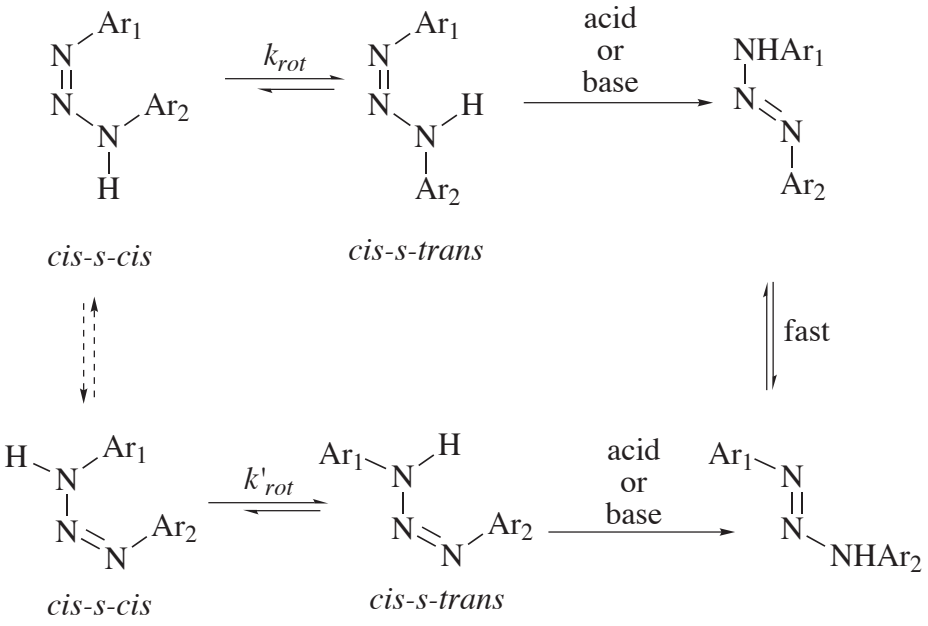

Scheme 1.12 *Cis*-to-*trans* isomerization mechanism for unsymmetrical triazenes.

1.2 Structure-Reactivity Correlation using the Hammett Equation

In order to investigate the effect of substituents on the rate of restricted rotation around the N(2)-N(3) bond, a quantitative structure-reactivity analysis is carried out in terms of the Hammett equation. The Hammett equation describes the influence of *meta* and *para* substituents on the side chain reactions of benzene derivatives. This equation is not applicable for *ortho* substituents due to their steric effects.[50] The Hammett equation can be described in terms of rate constants (eq. 1.1) or equilibrium constants (eq. 1.2),

$$\log (k^X) = \log k^H + \rho\sigma \qquad \text{eq. 1.1}$$

$$\log (K^X) = \log K^H + \rho\sigma \qquad \text{eq. 1.2}$$

where k^X and K^X are the rate constant and equilibrium constant, respectively, for an X substituted aromatic compound, and k^H and K^H are the rate constant and equilibrium constant, respectively, for the parent compound (the unsubstituted aromatic compound). The parameter σ is the substituent constant, which measures the electronic character of the substituent.[51] The parameter σ is defined as $\log(Ka/Ka°)$, where Ka and $Ka°$ are the acid dissociation constants for a substituted benzoic acid and benzoic acid itself, respectively. The substituent constant σ is independent of the nature of the reaction. A negative value of σ implies that the substituent has an electron-donating character. The more negative the value of σ, the stronger the electron-donating character. On the other hand, a positive value of σ specifies that the substituent has an electron-withdrawing character. The parameter ρ measures the susceptibility of a reaction to the electronic effects of substituents and is dependent on the reaction.[51] A positive ρ value implies the electron density on the reaction site increases on going from ground state to transition state, whereas a negative value of ρ specifies that the electron density on the reaction sites decreases on going from ground state to transition state.

The above Hammett equations are not sufficient to describe, for example, unsymmetrical 1,3-diphenyltriazenes, since the substituents are in different rings. Thus, the extended Hammett equation has been proposed to analyze a system having substituents in different rings.[52] Just as the regular Hammett equation, the extended Hammett equation can also be given in terms of rate constants (eq. 1.3) or equilibrium constants (eq. 1.4).

$$\log (k^X) = \log k^H + \rho_i\sigma_i + \rho_j\sigma_j + \rho_{ij}\sigma_i\sigma_j \qquad \text{eq. 1.3}$$

$$\log (K^X) = \log K^H + \rho_i\sigma_i + \rho_j\sigma_j + \rho_{ij}\sigma_i\sigma_j \qquad \text{eq. 1.4}$$

The term $\rho_{ij}\sigma_i\sigma_j$ corresponds to the cross-interaction between the two substituents. The magnitude of ρ_{ij} represents the intensity of the interaction between two substituents through the reaction center in the transition state. Additionally, ρ_{ij} is inversely proportional to the distance between these two substituents in the transition state.[53] The cross-interaction is negligible when (a) the distance between the two substituents is very large, or (b) the distance between the two substituents does not change in the rate limiting step.[53] These two cases can be applied to the characterization of S_N1 and S_AN reactions, respectively. For an S_N1 mechanism such as in the reaction of substituted anilines with substituted 1-phenylethylbenzenesulfonates, in the rate-limiting transition state there is no bond formation, only bond cleavage takes place. Thus, there is no interaction between the substituent on the nucleophile and that on the electrophilic substrate and hence, ρ_{ij} is zero. For an addition-elimination mechanism (S_AN) such as in the reaction of substituted phenoxide ions with chloronitrobenzenes, the elimination step is rate-limiting. Therefore, the distance between the substituent on the nucleophile and that on the electrophile does not change in the rate limiting step (i.e., ρ_{ij} is zero).[53]

Another application of the extended Hammett equation has been on the acid dissociation of N^1-methyl-N^1,N^2-diphenylacetamidinium ions (**8**).[54] It is found that the cross interaction term for the acid dissociation of **8** is negligible, as the distance between the substituents does not change in the rate limiting step.[53,54] Thus, the expression for the extended Hammett equation when applied to **8** is shown in eq 1.5.

$$\log (K^X) = \log K^H + \rho_{im}\sigma_{im} + \rho_{am}\sigma_{am} \qquad \text{eq. 1.5}$$

where K^X and K^H represent equilibrium constants for acid dissociation, and the subscripts "im" and "am" specify the substituent close to N(1) and N(3), respectively. From a regression analysis, the values of ρ_{im} and ρ_{am} for **8** are 2.88 ± 0.18 and 1.42 ± 0.16, respectively. The absolute value of ρ_{im} is clearly higher than that of ρ_{am}, which means that acid dissociation of **8** is more sensitive to the electronic character of the substituent X than that of Y.

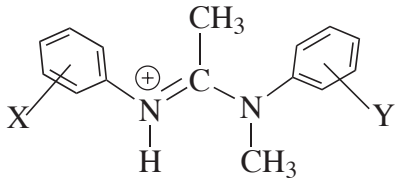

8

The energy barrier of restricted rotation of symmetrical and unsymmetrical *cis*-1,3-diphenyltriazenes is affected by the electronic character of aryl substituents. A quantitative analysis, based on the use of the extended Hammett equation, of the rate constants for restricted rotation around the N(2)-N(3) bond for a series of symmetrical and unsymmetrical *cis*-1,3-diphenyltriazenes, leads to a preliminary ρ_{im} value of –1.93 ± 0.08 and ρ_{am} value of 0.82 ± 0.08.[49] These results are consistent with the 1,3-dipolar resonance model shown in Scheme 1.7. The negative sign of ρ_{im} implies the electron density on N(1) decreases on rotation, and the positive sign of ρ_{am} implies the electron density on N(3) increases on rotation. The rotation around the N(2)-N(3) bond reduces electron delocalization along the nitrogen chain by preventing conjugation. Consequently, the electron density at N(1) decreases and that of N(3) increases on going from ground state to transition state. The absolute ρ_{im} value is obviously higher than the absolute ρ_{am} value. Thus, this indicates that restricted rotation

around the N(2)-N(3) bond is more sensitive to the electronic character of the aryl group at N(1) than to that at N(3).

1.3 Research Objectives

The studies outlined in this thesis are intended to further characterize the influence of aryl substitution on the N(2)-N(3) rotational barrier of *cis*-1,3-diphenyltriazenes. The influence of aryl substitution is investigated by means of a quantitative structure-reactivity analysis in terms of a multiple-substituent Hammett equation. In order to accomplish this, not only a large number of unsymmetrical compounds (in which the phenyl rings contain electron donating and withdrawing groups that have more or less ability for resonance stabilization) are desirable, but also studying some *meta*/*meta* and *meta*/*para* substituted triazenes is important. Target triazenes are listed in Charts 1.1 and 1.2, i.e., symmetrical and unsymmetrical substituted 1,3-diphenyltriazenes, respectively. The experimental conditions for this study are chosen to be identical to those of previous research on symmetrical and unsymmetrical substituted 1,3-diphenyltriazenes so that the results of this study can be combined with the results from previous ones.[20,48,49] The global analysis of all these results will allow a more detailed understanding on the structure-reactivity correlation of the rate constants for restricted rotation of the N(2)-N(3) bond of *cis*-substituted 1,3-diphenyltriazenes.

Chart 1.1 Target symmetrical 1,3-diphenyltriazenes.

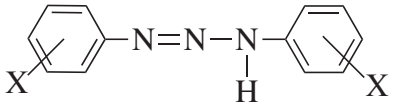

9

9	X	**9**	X	**9**	X
a	3,4-$(CH_3)_2$	**d**	3-CN	**g**	3,4,5-$(Cl)_3$
b	4-CCH	**e**	3-NO_2	**h**	3-CH_3
c	3-CF_3	**f**	3,5-$(Cl)_2$	**i**	3-OCH_3

Chart 1.2 Target unsymmetrical 1,3-diphenyltriazenes.[a]

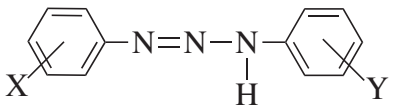

10

10	X	Y	**10**	X	Y
a	3,4,5-$(Cl)_3$	4-CN	**e**	4- OCH_3	4-CN
b	3,5-$(Cl)_2$	4-CN	**f**	4-Cl	4-CF_3
c	3-CF_3	4-CN	**g**	4- CH_3O	4-CH_3
d	4-Cl	4-CN			

[a]For convenience of notation, unsymmetrical 1,3-diphenyltriazenes are referred to by a single name, although these substrates, as mentioned in Section 1.1.3, exist as mixture of tautomeric isomers.

References

(1) Vaughan, K.; Stevens, M. F. G. *Chem. Soc. Rev.* **1978**, *7*, 377-397.

(2) Kolar, G. F. In *Chemical Carcinogens*; 2nd ed.; Searle, C. E., Ed.; American Chemical Society: Washington, D. C., 1984; Vol. 2, pp 869-914.

(3) Dürr, H.; Bouas-Laurent, H. *Pure Appl. Chem.* **2001**, *4*, 639-665.

(4) Such, G.; Evans, R. A.; Yee, L. H.; Davis, T. P. *J. Macromol. Sci.* **2003**, *43*, 547-579.

(5) Martin, P. J. In *Introduction to Molecular Electronics*; Petty, M. C., Bryce, M. R., Bloor, D., Eds.; Oxford University Press: New York, 1995, Chapter 6.

(6) Taniguchi, M.; Uehara, M.; Katsura, Y.; (Seiko Epson Corp.): *Jpn. Kokai Tokyo Koho JP 05 01, 007* 1993; *Chem. Abs.* **118**: 223008q.

(7) Kimball, D. B.; Haley, M. M. *Angew. Chem. Int. Ed.* **2002**, *41*, 3339-3351.

(8) Saunders, K. H.; Allen, R. L. M. *Aromatic Diazo Compounds*; 3rd ed.; Edward Arnold Ltd.: London, 1985, p 415.

(9) Lazny, R.; Sienkiewicz, M.; Brase, S. *Tetrahedron* **2001**, *57*, 5825-5832.

(10) Freeman, H. C.; Le Févre, R. J. W. *J. Chem. Soc.* **1952**, 2932-2934.

(11) Julliard, M.; Scelles, M.; Guillemonat, A.; Vernin, G.; Metzger, J. *Tetrahedron Lett.* **1977**, *18*, 375-378.

(12) Baro, J.; Dudek, D.; Luther, K.; Troe, J. *Ber. Bunsenges. Phys. Chem.* **1983**, *87*, 1155-1161.

(13) Curtin, D. Y.; Druliner, J. D. *J. Org. Chem.* **1967**, *32*, 1552-1557.

(14) Kizber, A. I.; Puchkov, V. A. *J. Gen. Chem. USSR (Engl. Transl. of Zh. Obshch. Khim.)* **1957**, *27*, 2267-2271.

(15) Puchkov, V. A. *J. Gen. Chem. USSR (Engl. Transl. of Zh. Obshch. Khim.)* **1959**, *29*, 3024-3029.

(16) Schmiedekamp, A.; Smith, J., R. H.; Michejda, C. J. *J. Org. Chem.* **1988**, *53*, 3433-3436.

(17) Svoboda, P.; Pytela, O.; Vecera, M. *Collect. Czech. Chem. Commun.* **1986**, *51*, 553-563.

(18) Zverina, V.; Remes, J.; Divis, J.; Marhold, J.; Martka, M. *Collect. Czech. Chem. Commun.* **1973**, *38*, 251-256.

(19) Benes, J.; Beránek, V.; Zimprich, J.; Vetesnik, P. *Collect. Czech. Chem. Commun.* **1977**, *42*, 702-710.

(20) Chen, N.; Barra, M.; Lee, I.; Chahal, N. *J. Org. Chem.* **2002**, *67*, 2271-2277.

(21) Campbell, T. W.; Day, B. F. *Chem. Rev.* **1951**, *48*, 299-317.

(22) Nguyen, M.-T.; Hoesch, L. *Helv. Chim. Acta.* **1986**, *69*, 1627-1637.

(23) Rakotondradany, F.; Williams, C. I.; Whitehead, M. A.; Jean-Claude, B. J. *J. Mol. Struct. (Theochem).* **2001**, *535*, 217-234.

(24) Solomons, T. W. G.; Fryhle, C. B. *Organic Chemistry*; 7th ed.; John Wiley & Sons: New York, 2000, pp (a) 32, (b) 769.

(25) Akhtar, M. H.; McDaniel, R. S.; Feser, M.; Oehlschlager, A. C. *Tetrahedron* **1968**, *24*, 3899-3906.

(26) Marullo, N. P.; Mayfield, C. B.; Wagener, E. H. *J. Am. Chem. Soc.* **1968**, *90*, 510-511.

(27) Lunazzi, L.; Cerioni, G.; Foresti, E.; Macciantelli, D. *J. Chem. Soc., Perkin Trans. 2* **1978**, 686-691.

(28) Lippert, T.; Wokaun, A.; Dauth, J.; Nuyken, O. *Magn. Reson. Chem.* **1992**, *30*, 1178-1185.

(29) Foster, N.; Pestel, B. F. *Magn. Reson. Chem.* **1984**, *23*, 83-85.

(30) Macgillavry, C. H.; Rieck, G. D. *International Tables for X-Ray Crystallography*; The International Union of Crystallography: Birmingham, 1968; Vol. 3, p 270.

(31) Karadyi, N.; Cakmak, S.; Odabasoglu, M.; Büyükgüngör, O. *Acta Crystallogr., Sect. C: Cryst. Struct. Commun.* **2005**, *C61*, O303-O305.

(32) Gladkova, V. F.; Kondrashev, Y. D. *Sov. Phys.-Crystallogr.* **1972**, *16*, 806-809.

(33) Zhang, D.-C.; Fei, Z.-H.; Zhang, T.-Z.; Zhang, Y.-Q.; Yu, K.-B. *Acta Crystallogr., Sect. C: Cryst. Struct. Commun.* **1999**, *C55*, 102-104.

(34) Hörner, M.; Bresolin, L.; Bordinhao, J.; Hartmann, E.; Strähle, J. *Acta Crystallogr., Sect. C: Cryst. Struct. Commun.* **2003**, *C59*, O426-O427.

(35) Panitz, J. C.; Lippert, T.; Stebani, J.; Nuyken, O.; Wokaun, A. *J. Phys. Chem.* **1993**, *97*, 5246-5253.

(36) Sieh, D. H.; Wilbur, D. J.; Michejda, C. J. *J. Amer. Chem. Soc.* **1980**, *102*, 3883-3887.

(37) Barra, M.; Srivastava, S.; Brockman, E. *J. Phys. Org. Chem.* **2004**, *17*, 1057-1060.

(38) Mitsuhashi, T.; Simamura, O. *Chem. Ind. (London)* **1964**, 578-579.

(39) Iwamura, H.; Albert, K.; Rieker, A. *Tetrahedron Lett.* **1976**, *17*, 2627-2630.

(40) Lunazzi, L.; Panciera, G.; Guerra, M. *J. Chem. Soc. Perkin Trans. 2* **1980**, 52-55.

(41) Kelly, M. A.; Murray, M.; Sinnott, M. L. *J. Chem. Soc. Perkin Trans. 2* **1982**, 1649-1654.

(42) Borisov, E. V.; Peregudov, A. S.; Postovoi, S. A.; Fedin, E. I.; Kravtsov, D. N. *Bull. Acad. Sci. USSR, Div. Chem. Sci.* **1986**, *35*, 499-502.

(43) Shcherbakova, O. V.; Kravtsov, D. N.; Peregudov, A. S.; Borisov, Y. A. *Russ. Chem. Bull*. **1998**, *47*, 1835-1386.

(44) Pu, X.; Wong, N.-B.; Zhou, G.; Gu, J.; Tian, A. *Chem. Phys. Lett*. **2005**, *408*, 101-106.

(45) Cox, C.; Lectka, T. *J. Org. Chem*. **1998**, 2426-2427.

(46) Dugave, C.; Demange, L. *Chem. Rev*. **2003**, *7*, 2475-2532.

(47) Pye, C. C.; Vaughan, K.; Glister, J. F. *Can. J. Spectrosc*. **2002**, *80*, 447-454.

(48) Barra, M.; Chen, N. *J. Org. Chem*. **2000**, *65*, 5739-5744.

(49) Zhang, H.; Barra, M. *J. Phys. Org. Chem*. **2005**, *6*, 498-503.

(50) Bansal, R. K. *Organic Reaction Mechanisms*; 3rd ed.; McGraw-Hill: New Delhi, 1998, pp 20-29.

(51) Johnson, C. D. *Hammett Equation*; University Press: Cambridge, 1973.

(52) Shorter, J. In *Similarity Models in organic Chemistry, Biochemistry and Related Fields*; Zalewski, R. I., Krygowski, T. M., Shorter, J., Eds.; Elsevier: Amsterdam, 1991, Chapter 2.

(53) Lee, I. *Adv. Phys. Org. Chem*. **1992**, *27*, 57-117.

(54) Raczynska, E.; Oszczapowicz, J. *Tetrahedron* **1985**, *41*, 5175-5179.

Chapter 2. Synthesis and Acid Dissociation Equilibrium Constants of Substituted 1,3-Diphenyltriazenes

2.1 Synthesis of Substituted 1,3-Diphenyltriazenes

Target symmetrical and unsymmetrical triazenes (listed in Charts 1.1 and 1.2) must be synthesized since they are not commercially available. One of the methods commonly used to synthesize triazenes is the classical diazonium coupling with primary aromatic amines.[1] As a result, N-coupling occurs to give desire products (substituted triazenes).[2,3] Scheme 2.1 (i) shows the classical diazonium reaction for symmetrical triazenes, whereas Scheme 2.1 (ii) shows the classical diazonium reaction for unsymmetrical triazenes.

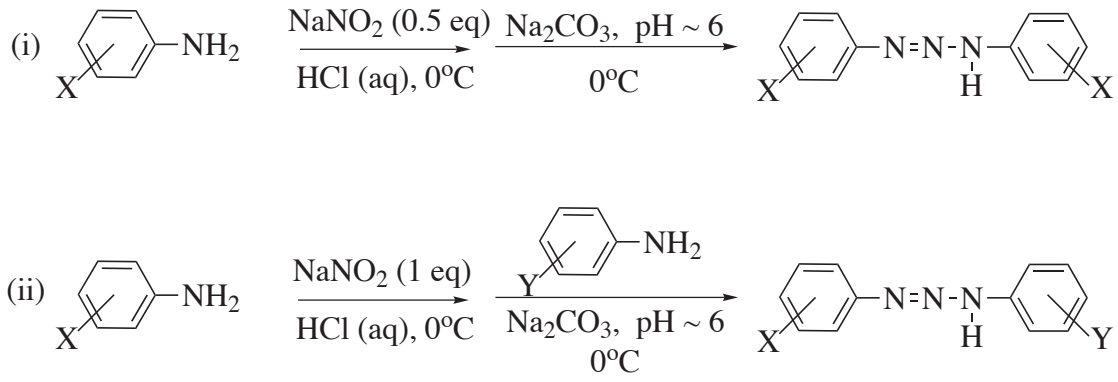

Scheme 2.1 Diazonium coupling reaction for substituted symmetrical (i) and unsymmetrical (ii) 1,3-diphenyltriazenes.

The conditions for these reactions have to be monitored cautiously. A low temperature is required because of the instability of diazonium ions (upon heating, they decomposed

rapidly yielding nitrogen gas and aryl cations).[4a] Also, the pH of the solution needs to be controlled carefully since under acidic condition, the anilines can easily undergo reversible salt formation (anilinium ion). Thus, the addition of sodium bicarbonate (Na_2CO_3) will move the position of equilibrium to the neutral anilines so that the target triazene can be formed.

Another way to synthesize triazenes is by nitrosation of primary aromatic amines with either sodium hexanitrocobaltate (III) (SHNC)[5] or isoamyl nitrite (i-C_5H_{11}-ONO)[6]. Both are typical methods for the synthesis of symmetrical triazenes (Scheme 2.2). The nitrosation reaction with SHNC is carried out under mild acidic conditions. It is claimed to be the simplest and the cleanest reaction to produce symmetrical triazenes.[5]

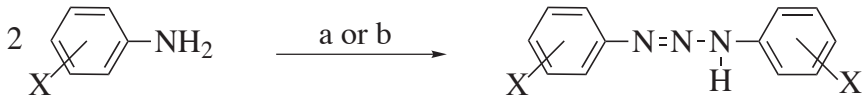

a = SHNC/H_2O, rt

b = i-C_5H_{11}-ONO, PE/Bz, rt

Scheme 2.2 Diazonium coupling reaction of aromatic amines with (a) sodium hexanitrocobaltate (III) or (b) isoamyl nitrite reagents.

As it is displayed in Scheme 2.3, no matter which pair of reagents is used in the synthesis of unsymmetrical 1,3-disubstituted triazenes, the obtained products are the same. This is due to the fact that triazenes with at least one hydrogen atom attached to N(3) can undergo tautomerization, as it is already described in Section 1.1.3. The products obtained from these two pathways can tautomerize easily and rapidly through a 1,3-hydrogen shift. Since either pathway, shown in Scheme 2.3, can be chosen to synthesize unsymmetrical

1,3-disubstituted triazenes, one should consider not only the stability of the diazonium ion and the rate of the diazonium coupling reaction but also the availability of the starting materials.

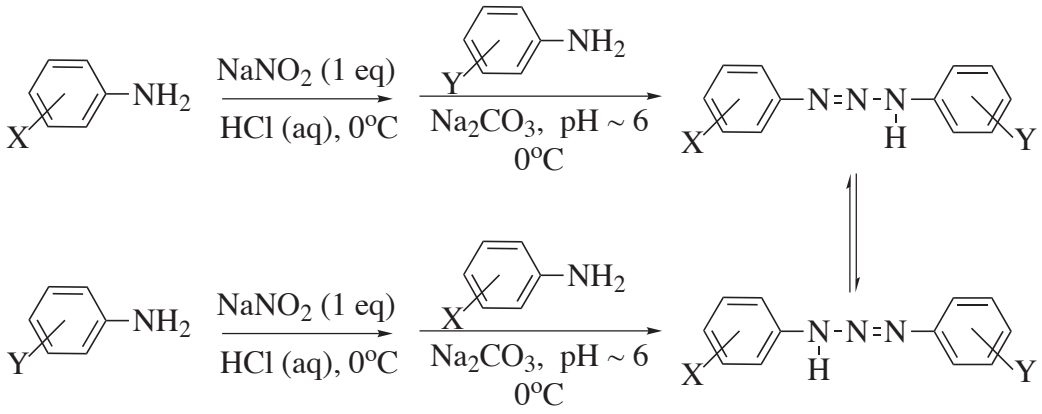

Scheme 2.3 Two different pathways for synthesis of unsymmetrical 1,3-diphenyltriazenes.

Target symmetrical triazenes **9a-c** were synthesized by the classical diazonium coupling method. While triazenes **9d** and **9e** were synthesized by nitrosation reaction with SHNC reagents, triazenes **9f** and **9g** were synthesized by nitrosation reaction with isoamyl nitrite agents. All target unsymmetrical triazenes **10a-g** are synthesized by the classical diazonium coupling method. Detailed descriptions of the corresponding experimental conditions, purification methods (i.e., recrystallization and chromatography), MP, ^{1}H NMR and MS analyses can be found in Section 4.1.

A side reaction of both the classical and non-classical diazonium methods in the synthesis of 1,3-diphenyltriazenes is the coupling of the diazonium ion with the phenyl group (i.e., carbon coupling). This coupling can occur at the *ortho* or *para* positions (Scheme 2.4), and leads to formation of azo compounds. The reaction involved in this case is an electrophilic

aromatic substitution (EAS); due to steric hindrance effects, substitution at the *para* position is preferable.[4b]

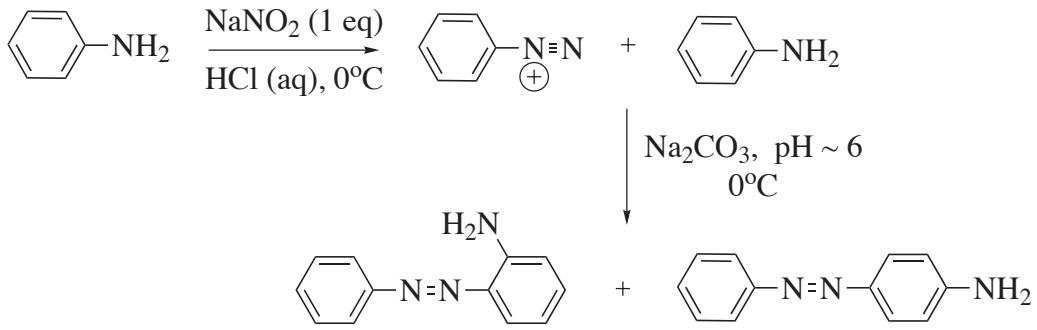

Scheme 2.4 Carbon coupling reaction in the synthesis of 1,3-diphenyltriazenes.

It is important to point out here that not all attempted syntheses led to the desired products. The synthesis of symmetrical triazene **9h** (X = 3-CH_3) has been attempted twice, i.e., by the classical method and by nitrosation with SHNC. As listed in Table 2.1, a mixture of 2-amino-3′,4-dimethyl-azobenzene (**11a**) and 4-amino-2,3′-dimethyl-azobenzene (**11b**) is formed when attempting to synthesize **9h** by the classical method. These azo compounds are separated by means of column chromatography and then characterized by ^{1}H NMR spectroscopy (see Section 4.1). The only separable product obtained from the attempted synthesis of **9h** by the nitrosation method is 4-amino-2,3′-dimethyl-azobenzene (**11b**). The synthesis of **9i** (X = 3-OCH_3) has been attempted utilizing the classical diazonium coupling method, and led only to the formation of 4-amino-2,3′-dimethoxy-azobenzene (**11c**). Again, this azo compound is confirmed by means of ^{1}H NMR spectroscopy. As mentioned above, azo compounds are obtained due to the occurrence of carbon coupling, the main side reaction while synthesizing substituted 1,3-diphenyltriazenes.

Table 2.1 Azo compounds obtained when attempting to synthesize triazenes **9h** and **9i**.

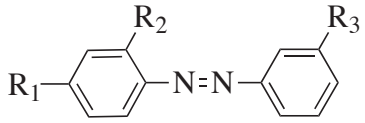

11

11	R_1	R_2	R_3
a	CH_3	NH_2	CH_3
b	NH_2	CH_3	CH_3
c	NH_2	OCH_3	OCH_3

2.2 Determination of Acid Dissociation Equilibrium Constants of Substituted 1,3-Diphenyltriazenes

2.2.1 Results and Discussion

There are many methods to determine acid dissociation equilibrium constants such as potentiometric titration using a glass electrode, conductometry, raman spectroscopy, proton nuclear magnetic resonance spectroscopy, thermometry, and ultraviolet-visible (UV-Vis) spectrophotometry.[7] In order to know the distribution of the neutral and its corresponding anionic form of target triazenes in aqueous solution at different pH, acid dissociation equilibrium constants for target triazenes are required. Under the experimental conditions of the study presented here, the determination of acid dissociation equilibrium constants for target triazenes is done by means of UV-vis spectrophotometry. The idea behind this method is to

find a wavelength (λ) at which the greatest difference between the absorbance of the neutral and anionic species is observed.[7] As displayed in Figure 2.1, as the pH of a 30% THF aqueous solution increases, the wavelength of maximum absorption (λ_{max}) of *trans*-**9b** changes from *ca.* 360 to 450 nm, values which correspond to the λ_{max} for neutral and anionic forms, respectively.

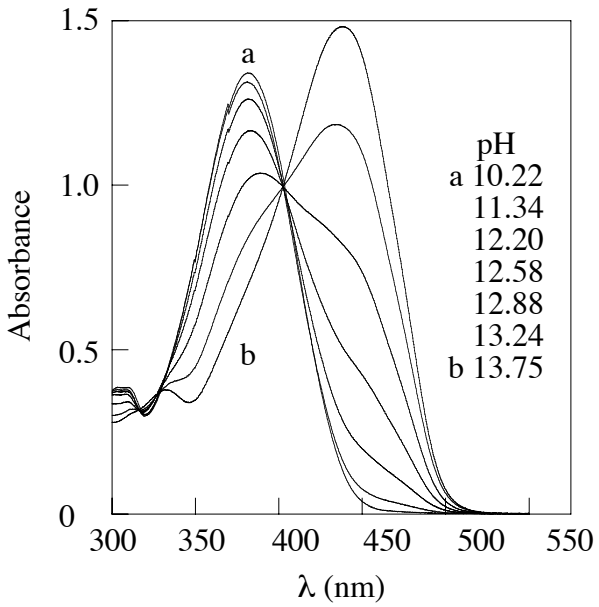

Figure 2.1 UV-visible spectra of **9b** as a function of pH in 30% THF aqueous solution; [**9b**] = 4.75 x 10^{-4} M.

The total absorbance of the solution (A_o), measured as a function of pH at any given λ, can be written mathematically as the sum of the absorbance of the neutral (A_{HT}) and anionic ($A_{T}-$) species as given in eq 2.1. The absorbance of the neutral and anionic forms of triazenes can be related in terms of their molar concentrations according to the Beer-Lambert's law. The law states that at a given wavelength, absorbance is directly proportional to the molar extinction coefficient (ε), path length (b), and molar concentration of the corresponding

absorbing species. Thus, eq 2.1 can be expressed as shown in eq 2.2. The molar concentrations can be expressed in term of their molar fractions and total triazene concentration ($[T]_o$). Consequently, by replacing the molar concentration of neutral and anionic species by their molar fractions and $[T]_o$, eq 2.3 is obtained.

$$A_o = A_{HT} + A_{T^-} \qquad \text{eq 2.1}$$

$$A_o = \varepsilon_{HT} \cdot b \cdot [HT] + \varepsilon_{T^-} \cdot b \cdot [T^-] \qquad \text{eq 2.2}$$

$$A_o = \frac{\varepsilon_{HT} \cdot b \cdot [T]_o \cdot 10^{-pH} + \varepsilon_{T^-} \cdot b \cdot [T]_o \cdot 10^{-pKa}}{10^{-pH} + 10^{-pKa}} \qquad \text{eq 2.3}$$

Values of p*Ka* for triazenes are determined from non-linear curve fittings, according to eq 2.3, of absorbance values as a function of pH (e.g., Figure 2.2). The resulting p*Ka* values for the substrates of the present and of previous studies[8,9] in 30% THF aqueous solution are summarized in Tables 2.2 and 2.3.

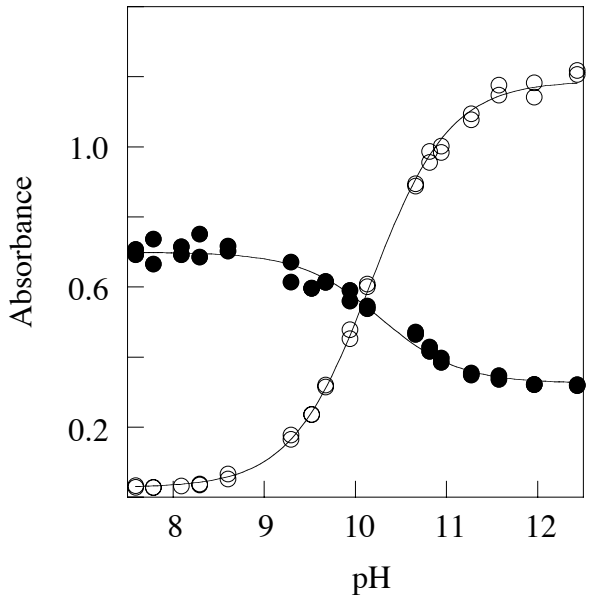

Figure 2.2 Plot of absorbance of *trans*-**10b** against pH at the λ_{max} of the corresponding neutral (●, λ = 367.72 nm) and anionic (❍, λ = 429.60 nm) species.

Table 2.2 p*Ka* values of substituted symmetrical *trans*-1,3-diphenyltriazenes.[a]

9	X	p*Ka*	**9**	X	p*Ka*[b]
a	3,4-$(CH_3)_2$	>14	**j**	4-OCH_3	>14
b	4-CCH	13.03 ± 0.03	**k**	4-CH_3	>14
c	3-CF_3	12.09 ± 0.05	**l**	4-H	>14
d	3-CN	11.49 ± 0.02	**m**	4-Cl	13.2 ± 0.1
e	3-NO_2	10.81 ± 0.03	**n**	4-CF_3	11.71 ± 0.05
f	3,5-$(Cl)_2$	10.59 ± 0.04	**o**	4-CN	10.52 ± 0.02
g	3,4,5-$(Cl)_3$	9.77 ± 0.05	**p**	4-NO_2	9.46 ± 0.04

[a]Solvent contains 30% THF aqueous solution, μ = 0.5 M (NaCl). [b]Values taken from ref. 8.

Table 2.3 p*Ka* values of substituted unsymmetrical *trans*-1,3-diphenyltriazenes.[a]

10	X	Y	p*Ka*	**10**	X	Y	p*Ka*
a	3,4,5-$(Cl)_3$	4-CN	10.22 ± 0.03	**f**	4-Cl	4-CF_3	12.38 ± 0.05
b	3,5-$(Cl)_2$	4-CN	10.69 ± 0.03	**g**	4-OCH_3	4-CH_3	>14
c	3-CF_3	4-CN	11.31 ± 0.04	**h**	4-OCH_3	4-H	>14[b]
d	4-Cl	4-CN	11.81 ± 0.06	**i**	4-OCH_3	4-CF_3	13.48 ± 0.05[b]
e	4-OCH_3	4-CN	13.06 ± 0.02	**j**	4-H	4-CF_3	13.05 ± 0.05[b]

[a]Solvent contains 30% THF aqueous solution, μ = 0.5 M (NaCl). [b]Values taken from ref. 9.

The p*Ka* values summarized in Tables 2.2 and 2.3 are indeed macroscopic acidity equilibrium constants. Deprotonation of tautomerizing triazenes (i.e., HT_1 and HT_2) yields the same anion (T^-), as displayed in Scheme 2.5. The corresponding two microscopic acid dissociation equilibrium constants, Ka^{HT1} and Ka^{HT2}, are described mathematically as in eq 2.4 and 2.5, respectively, while the equilibrium constant measured experimentally by means of UV-vis spectrophotometry is expressed as in eq 2.6. Substitution of eq 2.4 and eq 2.5 into eq 2.6 yield eq 2.7, which shows the relationship between the macroscopic and microscopic acidity constants.

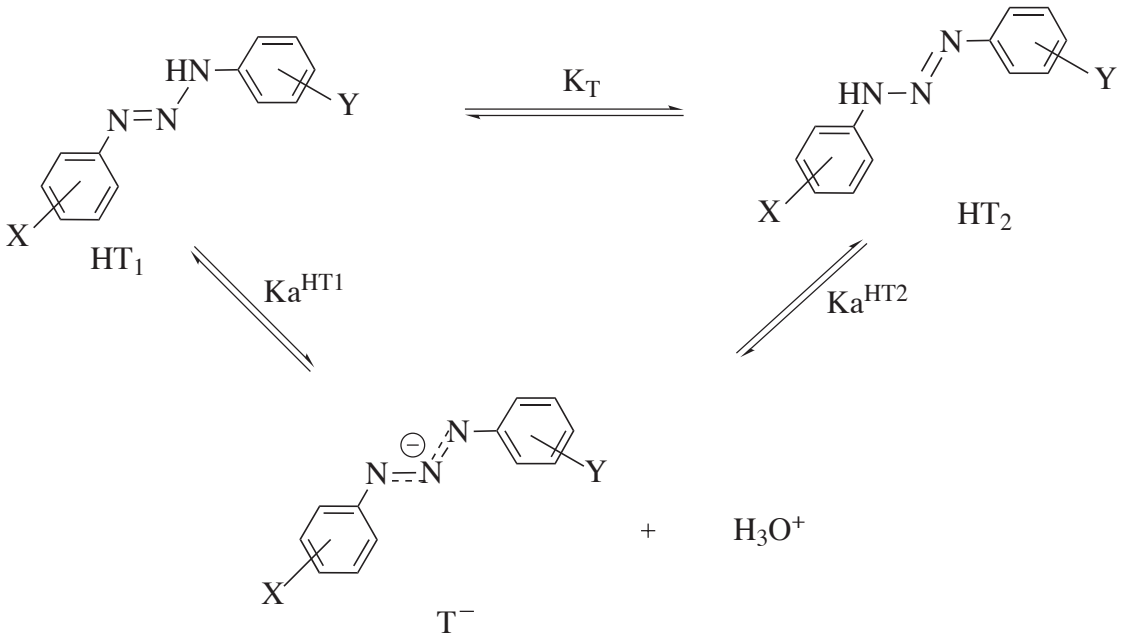

Scheme 2.5 Acid-base equilibria of 1,3-diphenyltriazenes.

$$K_a^{HT_1} = \frac{[T^-]\cdot[H_3O^+]}{[HT_1]} \qquad \text{eq 2.4}$$

$$K_a^{HT_2} = \frac{[T^-]\cdot[H_3O^+]}{[HT_2]} \qquad \text{eq 2.5}$$

$$K_a = \frac{[T^-]\cdot[H_3O^+]}{[HT_1]+[HT_2]} \qquad \text{eq 2.6}$$

$$K_a = \frac{K_a^{HT_1}\cdot K_a^{HT_2}}{K_a^{HT_1}+K_a^{HT_2}} \qquad \text{eq 2.7}$$

The p*Ka* values of substituted triazenes can be interpreted in terms of an extended Hammett equation. The p*Ka* values for both tautomers HT_1 and HT_2 should follow eq 2.8 and 2.9, respectively, in which pKa^{o} represents the p*Ka* value of 1,3-diphenyltriazene (i.e., X = Y = H), and the subscripts "im" and "am" indicate the substituent close to the imino nitrogen and the amino nitrogen, respectively.

$$pK_a^{HT_1} = pK_a^{\circ} - \rho_{im} \cdot \sigma_X - \rho_{am} \cdot \sigma_Y \qquad \text{eq 2.8}$$

$$pK_a^{HT_2} = pK_a^{\circ} - \rho_{am} \cdot \sigma_X - \rho_{im} \cdot \sigma_Y \qquad \text{eq 2.9}$$

The parameters Ka^{HT1} and Ka^{HT2} in eq 2.7 can be replaced by the terms obtained from eq 2.8 and 2.9, respectively. Eventually, eq 2.10 is obtained which shows the relation between p*Ka* and Hammett substituent constants. In the case of symmetrical triazenes, where $\sigma_X = \sigma_Y$, eq 2.10 reduces to eq 2.11.

$$pK_a = pK_a^{\circ} - \log\left(\frac{10^{(\rho_{im}+\rho_{am})\cdot(\sigma_x+\sigma_y)}}{10^{(\rho_{im}\cdot\sigma_x+\rho_{am}\cdot\sigma_y)} + 10^{(\rho_{am}\cdot\sigma_x+\rho_{im}\cdot\sigma_y)}}\right) \qquad \text{eq 2.10}$$

$$pK_a = pK_a^{\circ} - \log(0.5) - (\rho_{im} + \rho_{am}) \cdot \sigma \qquad \text{eq 2.11}$$

Figure 2.3 represents a plot of acid dissociation equilibrium constants (p*Ka*) of substituted symmetrical *trans*-triazenes vs. σ (or σ^{-}).[10] It clearly shows that the p*Ka* value decreases with increasingly stronger electron-withdrawing substituents. It is also shown that an

excellent linear relationship between p*Ka* and σ is obtained but with two points obviously off the line (4-CN and 4-NO_2 substituents). This is not unexpected, since there is a direct mesomeric interaction between the charge at N(3) in the triazeno moiety with 4-CN and 4-NO_2 groups. Thus, σ^- values are used to account for such through-conjugation.[11] It is important to mention that σ^- values for *para* and *meta* electron-donating substituents and for *meta* electron-withdrawing substituents are essentially the same as the ordinary σ values. Compared to the p*Ka* values for the other substituted triazenes shown in Figure 2.3, the acid dissociation constants for 4-CN and 4-NO_2 containing substrates do not correlate well with either σ or σ^- values. This observation is not unprecedented. Indeed, a similar correlation has been observed in the case of symmetrically mono and disubstituted diphenyltriazenes in 20% ethanol aqueous solutions.[12] The Yukawa-Tsuno modification of the Hammett equation (eq 2.12) has been applied to the acid dissociation of diphenyltriazenes, where r represents the enhance resonance effect parameter.[11]

$$pK_a = pK_a^\circ - \rho \cdot [\sigma + r\,(\sigma^- - \sigma)] \qquad \text{eq. 2.12}$$

The parameter σ in eq 2.11 can be replaced by $[\sigma + r\,(\sigma^- - \sigma)]$ (i.e., as in 2.12), so that eq 2.11 yields eq 2.13. Thus, one can apply eq 2.13 to the acid dissociation of substituted symmetrical *trans*-triazenes in 30% THF aqueous solution. Regression analysis to Figure 2.3 according to eq 2.13 leads to values of 13.8 ± 0.1, 4.6 ± 0.2 and 0.43 ± 0.05 for pK_a°, $(\rho_{im} + \rho_{am})$, and r, respectively. These values should be taken cautiously because r results indeed from only two points off the σ line. The resulting $[\sigma + r\,(\sigma^- - \sigma)]$ value for 4-CN substituent is 0.81 ± 0.05, whereas for 4-NO_2 substituent $[\sigma + r\,(\sigma^- - \sigma)]$ is 0.99 ± 0.05.

$$pK_a = pK_a^\circ - \log(0.5) - (\rho_{im} + \rho_{am}) \cdot [\sigma + r\,(\sigma^- - \sigma)] \qquad \text{eq 2.13}$$

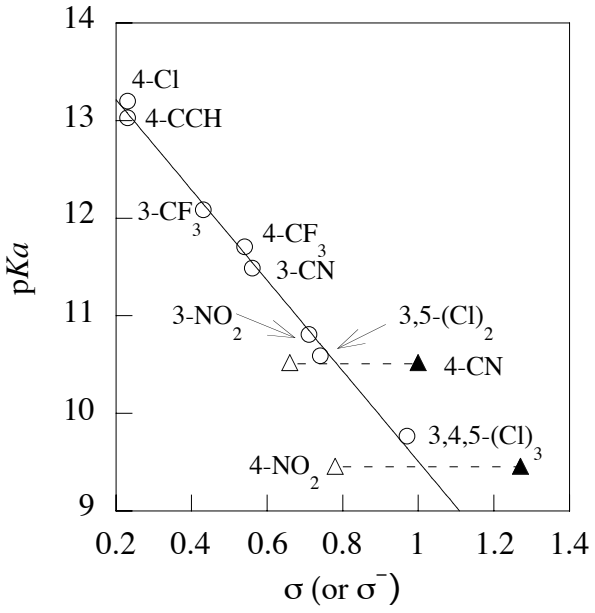

Figure 2.3 Plot of p*Ka* vs. Hammett substituent constants for substituted symmetrical *trans*-triazenes (open symbols, σ; closed symbols, σ^-). The straight line is obtained according to eq. 2.11, omitting data for 4-CN and 4-NO_2.

As already mentioned above, the Yukawa-Tsuno modification of the Hammett equation (i.e., eq 2.13) has been applied to the acid dissociation of 1,3-diphenyltriazenes in 20% ethanol aqueous solutions. Curve fitting of corresponding data according to eq 2.13 provides resulting values of 13.30, 3.26 and 0.78, for p*Ka*°, ρ, and r, respectively.[12] These results are comparable to those obtained in 30% THF aqueous solutions. The p*Ka*° and ρ values in 20% ethanol aqueous solutions are lower than that in 30% THF aqueous solutions. Meanwhile, the value of r is higher in 20% ethanol than that in 30% THF solutions. These evidently show that values of p*Ka*°, ρ, and r are solvent dependent. The dielectric constant of THF (i.e., ε(THF) = 7.6) is

lower than that of ethanol (i.e., ε(ethanol) = 24.3).[13] Since solvent-solute interactions increase with increasing dielectric constant, this implies that ethanol is more effective at solvating ions than THF is. Consequently, in any solvent that stabilizes ionic species (i.e., 20% ethanol vs. 30% THF aqueous solution), the values of p*Ka*° and ρ for the reaction decrease and the value of r increases.[14]

Figure 2.4 displays a plot of the acid dissociation equilibrium constants of unsymmetrical *trans*-triazenes (i.e., X = 4-CN and Y = 4-OCH_3, 4-Cl, 3-CF_3, 3,5-Cl_2, or 3,4,5-Cl_3) and Hammett substituent constants. Similarly to the case of symmetrical *trans*-triazenes case, the trend displayed in Figure 2.4 obviously shows that acidity increases with increasingly stronger electron-withdrawing Y-substituents. Since an excellent linear relationship between p*Ka* and σ_Y is obtained, it implies that in eq 2.10, the value of ρ_{im} is (experimentally) indistinguishable from the value of ρ_{am}. Thus, eq 2.10 simplifies to eq 2.14. A linear fitting according to eq 2.14 leads to values of 12.08 ± 0.05 and 2.29 ± 0.08, for (p*Ka*° - $\rho \cdot \sigma_{X=CN}$) and ρ, respectively.

$$pK_a = pK_a^\circ - \log(0.5) - \rho \cdot (\sigma_X + \sigma_Y) \qquad \text{eq 2.14}$$

Interestingly, the slope obtained from substituted symmetrical *trans*-triazenes (4.6 ± 0.2) is twice the slope obtained from unsymmetrical *trans*-triazenes (2.29 ± 0.08). This seems reasonable. The slope for substituted symmetrical *trans*-triazenes associates to the sum of the two reaction constants, ρ_{im} and ρ_{am} (eq 2.11), whereas the slope for unsymmetrical *trans*-triazenes corresponds to the value of ρ (eq 2.14). As a consequence, it is concluded that the ρ_{im} and ρ_{am} values cannot be distinguished experimentally.

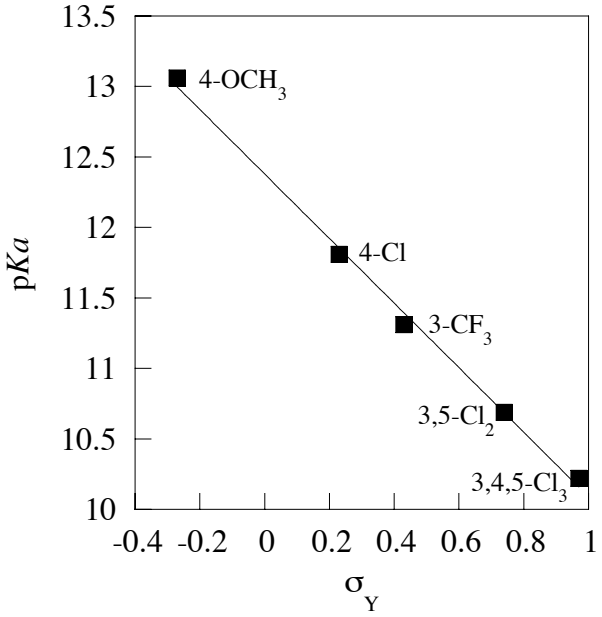

Figure 2.4 Plot of p*Ka* vs. Hammett substituent constants for unsymmetrical *trans*-triazenes where X = 4-CN and Y = 4-OCH_3, 4-Cl, 3-CF_3, 3,5-Cl_2, or 3,4,5-Cl_3.

The parameter $\sigma_{X=CN}$ can be calculated from the obtained value for (pKa^o - $\rho \cdot \sigma_{X=CN}$) using the pKa^o resulting from Figure 2.3 (i.e., 13.8 ± 0.1) and the value of ρ from Figure 2.4 (i.e., 2.29 ± 0.08). Thus, $\sigma_{X=CN}$ is determined to be 0.75 ± 0.07, which is in agreement with the $[\sigma + r(\sigma^- - \sigma)]$ value previously calculated for 4-CN of 0.81 ± 0.05. Since 4-CN and 4-NO_2 substituents are able to conjugate with the charge at N(3), it is important to use their $[\sigma + r(\sigma^- - \sigma)]$ values to correlate the p*Ka* values and substituent constants. Consequently, as represented in Figure 2.5, the plot between the acid dissociation equilibrium constants in 30% THF aqueous solution of the substrates of this and previous studies and the sum of the substituents constants (i.e., $\sigma_X + \sigma_Y$) yields an excellent straight line. According to eq 2.14, the linear fitting leads to the values of 2.33 ± 0.04 and 13.88 ± 0.05 for ρ and pKa^o. In fact, the value of ρ is consistent with that obtained in the unsymmetrical *trans*-triazene case

(2.29 ± 0.08), which is half the ρ obtained in the symmetrical *trans*-triazene case (4.6 ± 0.2). Also, the obtained p*Ka*° value from this fitting is in an excellent agreement with that obtained from symmetrical *trans*-triazenes (13.8 ± 0.1).

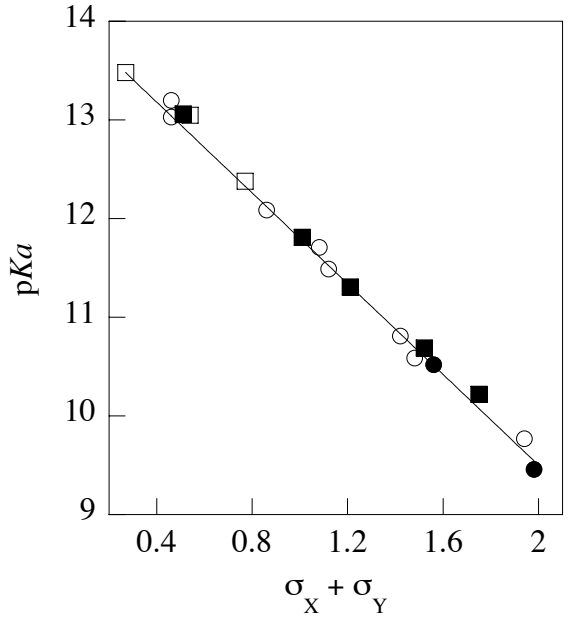

Figure 2.5 Plot of p*Ka* vs. Hammett substituent constants for substituted symmetrical *trans*-triazenes (❍), symmetrical *trans*-triazenes containing 4-CN or 4-NO_2 substituents (●), unsymmetrical *trans*-triazenes (❑), and unsymmetrical *trans*-triazenes containing a 4-CN group (■).

Finally, as it is shown in Scheme 2.5, the tautomeric equilibrium constant, K_T, between tautomers HT_1 and HT_2 is defined in eq 2.15. Eq 2.16 can be obtained when one substitutes eq 2.4 and eq 2.5 into eq 2.15 and takes the logarithm. As it is mentioned earlier, the ρ_{im} and ρ_{am} values are experimentally indistinguishable. This means that the values of pKa^{HT_1} and pKa^{HT_2}, defined in eq 2.8 and eq 2.9, respectively, are comparable, and hence, the calculated

value of K_T is close to 1. This observation is indeed consistent with results obtained experimentally as mentioned in Section 1.1.3, which show that K_T values are typically in the range of 0.1 to 10.

$$K_T = \frac{[HT_2]}{[HT_1]} \qquad \text{eq 2.15}$$

$$pK_T = pK_a^{HT_1} - pK_a^{HT_2} \qquad \text{eq 2.16}$$

2.2.2 Conclusions

The p*Ka* values for the substrates of this and of previous studies in 30% THF aqueous solution clearly depend on the electronic character of the substituents attached to the phenyl rings. It is found that a Hammett relationship can be applied to quantitatively correlate p*Ka* values and substituent constants. The p*Ka* values for 4-CN and 4-NO_2 containing *trans*-triazenes, however, do not correlate well with either σ or σ^- values when these two p*Ka* values are compared to the rest of the series. As a result, the Yukawa-Tsuno modification of the Hammett equation (eq 2.13) is introduced, i.e., the parameter σ is replaced by $[\sigma + r(\sigma^- - \sigma)]$. Thus, the resulting $[\sigma + r(\sigma^- - \sigma)]$ values for 4-CN and 4-NO_2 are 0.81 ± 0.05, and 0.99 ± 0.05, respectively. It is also indicated that the parameters pKa^o, ρ, and r are solvent dependent. The better the solvating capability of the solvent, the lower the pKa^o and ρ values and the higher the value of r. The correlation between acid dissociation constants and the sum of substituent constants for *trans*-1,3-diphenyltriazenes leads to a ρ value of 2.33 ± 0.04. This ρ value is in agreement with that obtained for unsymmetrical 4-cyano containing *trans*-

substrates (2.29 ± 0.08) and half the ρ value obtained for symmetrical substrates (4.6 ± 0.2), which corresponds to ($\rho_{im} + \rho_{am}$). However, ρ_{im} and ρ_{am} for 1,3-diphenyltriazenes could not be distinguished experimentally.

References

(1) Hill, D. T.; Stanley, K. G.; Williams, J. E. K.; Loev, B.; Fowler, P. J. *J. Med. Chem.* **1983**, *26*, 865-869.

(2) Campbell, T. W.; Day, B. F. *Chem. Rev.* **1951**, *48*, 299-317.

(3) Zollinger, H. *Azo and Diazo Chemistry: Aliphatic and Aromatic Compounds*; Interscience Publishers: New York, 1961, Chapter 8.

(4) Clayden, J.; Greeves, N.; Warren, S.; Wothers, P. *Organic Chemistry*; Oxford University Press: Oxford, 2001, pp (a) 597-598; (b) 559-560.

(5) Stefane, B.; Kocevar, M.; Polanc, S. *J. Org. Chem.* **1997**, *62*, 7165-7169.

(6) Vernin, G.; Siv, C.; Metzger, J.; Párkányi, C. *Synthesis* **1977**, 691-693.

(7) Albert, A.; Serjeant, E. P. *The Determination of Ionization Constants*; 3rd ed.; Chapman and Hall: New York, 1984, Chapter 4.

(8) Chen, N.; Barra, M.; Lee, I.; Chahal, N. *J. Org. Chem.* **2002**, *67*, 2271-2277.

(9) Zhang, H. M. Sc. Thesis, University of Waterloo, 2004.

(10) σ and σ^- values were taken from Hansch, C., Leo, A., and Taft, R. W. *Acc. Chem. Res.*, **1991**, *91*, 165-195.

(11) Jones, R. A. Y. In *Physical and Mechanistic Organic Chemistry*; Cambridge University Press: Cambridge, 1984, pp 45-50.

(12) Benes, J.; Beránek, V.; Zimprich, J.; Vetesnik, P. *Collect. Czech. Chem. Commun.* **1977**, *42*, 702-710.

(13) Lide, D. R., Ed. *Handbook of Chemistry and Physics; 77th ed.*; CRC Press: Boca Raton, 1996-1997, p 8-100.

(14) Ritchie, C. D. In *Physical Organic Chemistry : The Fundamental Concepts*; 2nd ed.; Marcel Dekker, Inc.: New York, 1990, p 95.

Chapter 3. Restricted Rotation around the N(2)-N(3) Bond of Cis-1,3-Diphenyltriazenes

3.1 Background

As already mentioned in Section 1.1.4, the mechanism of thermal *cis*-to-*trans* isomerization of both symmetrical and unsymmetrical 1,3-diphenyltriazenes in aqueous media involves two consecutive processes: restricted rotation around the N(2)-N(3) bond, followed by a 1,3-prototropic rearrangement catalyzed by general acids and bases.[1-3] The rate-controlling step is dependent on the pH of the solution. In alkaline solutions, at pH < 10 the 1,3-prototropic rearrangement is the rate-controlling step. On the other hand, at pH > 10, hindered rotation around the N(2)-N(3) bond is the rate-determining step. In this Chapter, the latter process is of interest. For symmetrical triazenes, only one rate constant for restricted rotation is measured. On the other hand, for unsymmetrical triazenes, which exist as pair of tautomers, two rate constants for restricted rotation around the N(2)-N(3) bond are determined, one value per tautomeric form.[3] Restricted rotation around the N(2)-N(3) bond is explained very well in terms of a 1,3-dipolar resonance form (Scheme 1.7). Based on this model, the more stable the charges on the 1,3-dipolar resonance form are, the lower the corresponding rate constant for restricted rotation is. The correlation of rate constants for restricted rotation around the N(2)-N(3) bond of *cis*-triazenes with Hammett substituent constants is carried out by means of an extended Hammett equation. This type of correlation analysis is of general interest to understand the electronic factors contributing to restricted rotation and to be able to predict and modulate the rate of such a process. A systematic study on the rate constants for restricted

rotation around the N(2)-N(3) bond of compounds **9** and **10** is carried out in 30% (v/v) THF aqueous NaOH solution using a home-built laser-flash photolysis system. Interestingly, only in the case of cyano-containing substrates, the observed rate constants (ascribed to restricted rotation around the N(2)-N(3) bond) are found to be pH dependent. This is attributed to the change in ionization state of the corresponding substrates. Further evidence for this assignment is obtained from solvent isotope effects.

3.2 Results and Discussion

As shown in the representative kinetic traces in Figure 3.1, laser excitation (at 355 nm) of target *trans*-triazenes in NaOH solutions leads to instantaneous bleaching (i.e., ΔA value is negative), attributed to photoinduced *trans*-to-*cis* isomerization of the corresponding substituted *trans*-**9** or *trans*-**10**. A negative ΔA occurs due to the fact that the absorptivity of *cis*-isomers is lower than that of *trans*-isomers at the monitoring wavelength.[4] The instantaneous bleaching is followed by complete recovery of the initial absorbance of the solution, attributed to the thermal *cis*-to-*trans* isomerization. This process is determined by the rate of restricted rotation around the N(2)-N(3) bond of the corresponding substrates under the experimental condition of this work (i.e., 30% (v/v) THF aqueous NaOH solution).

For symmetrical substituted triazenes **9**, only one first-order kinetic process is observed (e.g., Figure 3.1 left), so that the recovery traces can be satisfactorily described by a mono exponential function. For unsymmetrical substituted triazenes **10**, on the other hand, the recovery traces can be satisfactorily described by a bi-exponential function since two first-order kinetic processes are observed (e.g., Figure 3.1 right), which is attributed to the presence of two pairs of *cis*-isomers (i.e., one pair of *cis*-conformers per tautomeric *trans* form)

that react at different rates (as shown in Scheme 1.12). These observations are consistent with previous studies.[1-3]

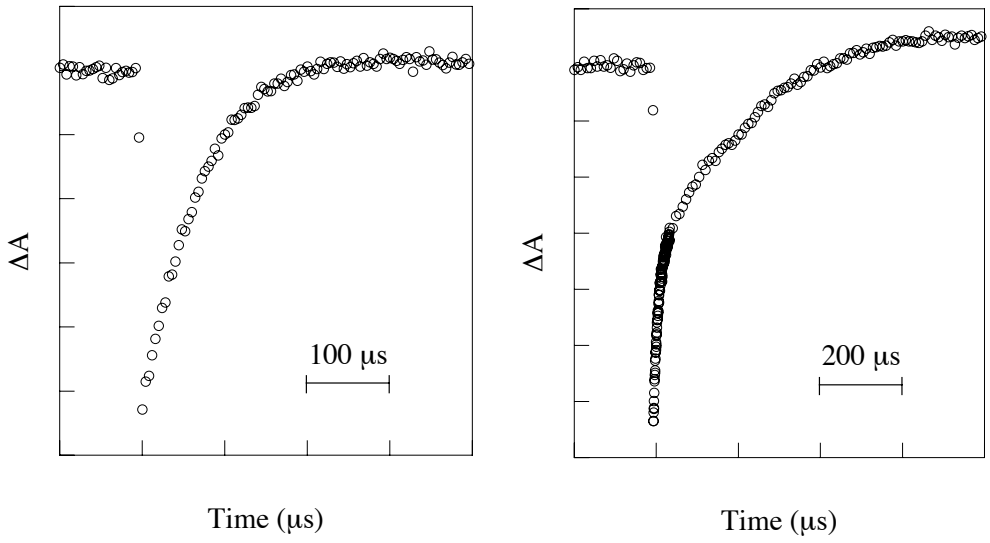

Figure 3.1 Kinetic traces recorded at 480 nm and 470 nm, respectively, for **9b** (*left*, [NaOH] = 0.200 M) and **10b** (*right*, [NaOH] = 0.0525 M) in 30% (v/v) THF aqueous NaOH solutions.

Recovery traces are collected using sets of solutions at different NaOH concentrations. Resulting observed rate constants (k_{obs}) are summarized in Appendix A (symmetrical triazenes) and Appendix B (unsymmetrical triazenes). These observed rate constants are ascribed to restricted rotation around the N(2)-N(3) bond. It is important to note that for unsymmetrical triazenes, k_{obs}^{f} and k_{obs}^{s} denote the observed rate constants corresponding to the fast and slow processes, respectively. Except for cyano-containing triazenes (see below), k_{obs} values are independent of hydroxide ion concentration (Tables A1, A3-4, A8-9 and B8-9) and correspond indeed to k_{rot} (and k'_{rot}) in Schemes 1.10 and 1.12. Tables 3.1 and 3.2 summarize the averaged k_{rot} values obtained from this and previous studies for symmetrical substituted triazenes (**9**) and

unsymmetrical substituted triazenes (**10**), respectively. For unsymmetrical substituted triazenes, the rate constant values given in Table 3.2 are assigned to each tautomeric form according to the 1,3-dipolar resonance model. As mentioned in the previous section, based on the 1,3-dipolar resonance model, the more stable the charges on the 1,3-dipolar resonance form are, the smaller the corresponding rate constant for restricted rotation is. Thus, for each unsymmetrical compound, the tautomer bearing the (more) electron-withdrawing group at N(1) will have a higher energy barrier for rotation (i.e., lower rate constant for rotation) compared to the tautomer with the (more) electron-donating group at N(1).

Table 3.1 Rate constants for restricted rotation in symmetrical substituted *cis*-1,3-diphenyltriazenes in 30% (v/v) THF:H_2O solution.[a]

9	X	k_{rot} (10^4 s^{-1})	**9**	X	k_{rot} (10^4 s^{-1})[c]
a	3,4-$(CH_3)_2$	8.0 ± 0.3	**j**	4-OCH_3	9.9 ± 0.4
b	4-CCH	1.57 ± 0.07	**k**	4-CH_3	6.9 ± 0.2
c	3-CF_3	0.79 ± 0.01	**l**	4-H	5.1 ± 0.2
d	3-CN	0.91 ± 0.02[b]	**m**	4-Cl	1.8 ± 0.1
f	3,5-$(Cl)_2$	0.60 ± 0.01	**n**	4-CF_3	1.2 ± 0.1
g	3,4,5-$(Cl)_3$	0.32 ± 0.01	**o**	4-CN	7.7 ± 0.2[d,e]

[a]μ = 0.5 M (NaCl) at 21 °C. [b](*Ka*/*Kw*) = (3.7 ± 0.4). [c]Values taken from ref. 2. [d]Value of k_{rot}^{-}. [e](*Ka*/*Kw*) = (47 ± 5).

Table 3.2 Rate constants for restricted rotation in unsymmetrical substituted *cis*-1,3-diphenyltriazenes in 30% (v/v) THF:H_2O solution.[a]

10	X[b]	Y[b]	k_{rot} (10^4 s^{-1})	**10**	X[b]	Y[b]	k_{rot} (10^4 s^{-1})
c	4-CN	3-CF_3	0.58 ± 0.07	**g**	4-CH_3O	4-CH_3	12.0 ± 0.4
d	4-Cl	4-CN	4 ± 1		4-CH_3	4-CH_3O	3.52 ± 0.07
	4-CN	4-Cl	0.40 ± 0.02	**h**	4-CH_3O	4-H	24 ± 2[d]
e	4-CH_3O	4-CN	24 ± 7		4-H	4-CH_3O	2.33 ± 0.08[d]
	4-CN	4-CH_3O	< 0.2[c]	**i**	4-CH_3O	4-CF_3	40 ± 3[c]
f	4-Cl	4-CF_3	5.2 ± 0.2		4-CF_3	4-CH_3O	0.26 ± 0.03[d]
	4-CF_3	4-Cl	0.488 ± 0.006	**j**	4-H	4-CF_3	14 ± 1[d]
					4-CF_3	4-H	0.54 ± 0.02[d]

[a]μ = 0.5 M (NaCl) at 21 °C. [b]X and Y represent the groups at the phenyl rings attached to N(1) and N(3), respectively, as shown in Chart 1.2 [c]The slowest rate constant that can be determined with the laser-flash photolysis system employed in this study is *ca.* 2000 s^{-1}. [d]Values taken from ref. 3.

A structure-reactivity analysis of the restricted rotation around the N(2)-N(3) bond is carried out employing a multiple-substituent Hammett equation. As mentioned in section 1.2, the Hammett equation is used to describe the electronic influence of *meta* and *para* substituents on the side chain reactions of benzene derivatives. However, the simple Hammett equation is not enough to describe the studied system since the substituents of the substrates of this study

are in different rings. Therefore, an extended Hammett equation as expressed in eq 3.1 is employed,

$$\log(k_{rot}) = \log(k_{rot}^{H}) + \rho_{im}\sigma_{im} + \rho_{am}\sigma_{am} \qquad \text{eq 3.1}$$

where k_{rot}^{H} and k_{rot} represent the rate constants for restricted rotation of the parent compound (i.e., 1,3-diphenyltriazene) and substituted compound, respectively, σ_{im} and σ_{am} are the σ values for substituents at the phenyl rings bonded to N(1) and N(3), respectively, and ρ_{im} and ρ_{am} are the Hammett reaction constants for N(1) and N(3), respectively. Figure 3.2 displays the double variable fitted Hammett plot of rate constants, summarized in Tables 3.1 and 3.2, for restricted rotation around the N(2)-N(3) bond of symmetrical *cis*-1,3-diphenyltriazenes (❍) and unsymmetrical *cis*-1,3-diphenyltriazenes (●) vs. the corresponding substituent constants.[5] By comparing all these rate constants for restricted rotation around the N(2)-N(3) bond, it is noticed that the rate constants diminish not only as the electron withdrawing character of the aryl group at N(1) increases, but also as the electron donating character of the aryl group at N(3) increases. The quality of the double variable fitting is reasonably good (R = 0.966).

Eq 3.1 implies that the presence of a substituent in one ring does not influence the sensitivity of the reaction to the substituent in the other ring. The cross interaction parameter ($\rho_{im\cdot am}$) is negligible, since the distance between the two substituents in the phenyl rings does not change in the rate-determining step.[6] The fact that the Hammett plot of rate constants vs. the corresponding substituent constants for symmetrical triazenes is linear (as clearly represented by the set of open circles diagonally lined up in Figure 3.2) strongly indicates that the cross interaction is indeed negligible. The curve fitting according to eq 3.1 leads to log (k_{rot}^{H}), ρ_{im}, and ρ_{am} values of 4.63 ± 0.03, -1.88 ± 0.08, and 0.70 ± 0.08, respectively, which

are consistent with the preliminary results from a previous study (namely, 4.68 ± 0.03, -1.93 ± 0.08, and 0.82 ± 0.08).[3] The sign of ρ_{im} and ρ_{am} can be very well explained based on the 1,3-dipolar resonance form (Scheme 1.7). Rotation around the N(2)-N(3) bond decreases electron delocalization along the nitrogen chain. Accordingly, the sign of ρ_{im} is negative, indicating that the electron density on N(1) decreases on rotation on going from ground state to transition state. On the other hand, the sign of ρ_{am} is positive, indicating that the electron density on N(3) increases on rotation on going from ground state to transition state. Furthermore, the absolute value of ρ_{im} is larger than the absolute value of ρ_{am}. This implies that restricted rotation around the N(2)-N(3) bond of substituted triazenes is more sensitive to the electronic character of the aryl group at N(1) than to the electronic character of the aryl group at N(3), as originally inferred from previous studies.[2,3]

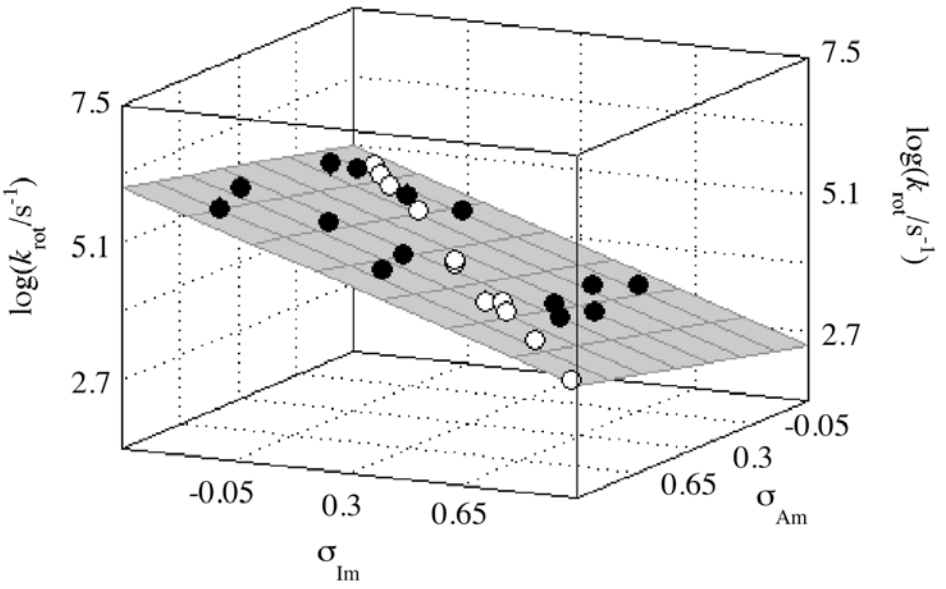

Figure 3.2 Multiple-substituent Hammett plot of rate constants for restricted rotation around the N(2)-N(3) bond in symmetrical (○) and unsymmetrical (●) *cis*-1,3-diphenyltriazenes.

It is necessary to highlight that Figure 3.2 presents not only data for symmetrical (Table 3.1) and unsymmetrical (Table 3.2) non-cyano-containing *cis*-1,3-diphenyltriazenes, but also for cyano-containing substrates. As already mentioned, observed rate constants for cyano-containing compounds are dependent on the concentration of hydroxide ion (Appendix A, Table A6 for symmetrical cyano-containing substrates; Appendix B, Tables B1-2, B4, and B6-8, for unsymmetrical cyano-containing substrates). Figure 3.3 displays observed rate constants for restricted rotation of two symmetrical cyano-containing compounds (i.e., **9d**, X = 3-CN, *left*, and **9o**, X = 4-CN, *right*, respectively) vs. NaOH concentration. The non-linear relationships shown in Figure 3.3 are attributed to a change in the ionization of the substrates. The pH dependency is therefore interpreted in terms of the reaction mechanism illustrated in Scheme 3.1.

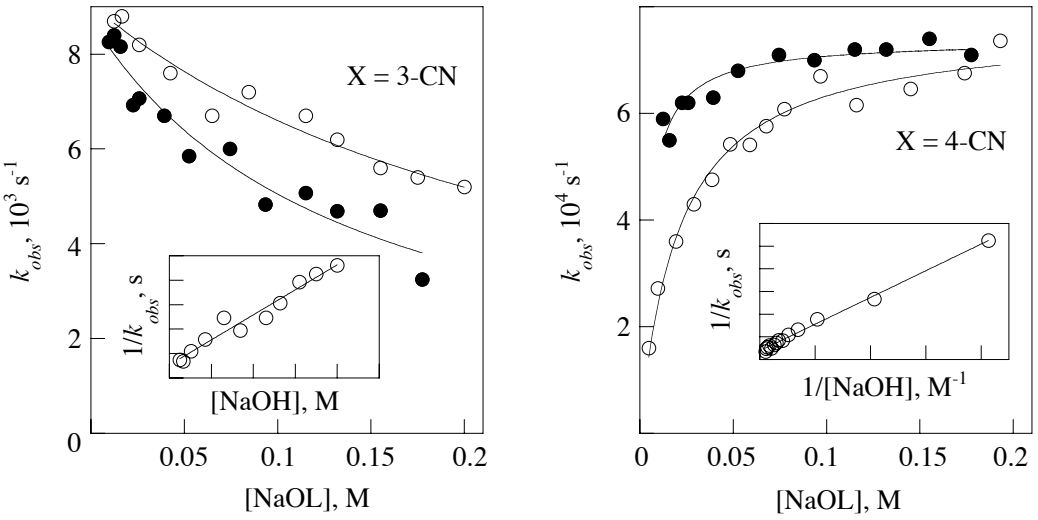

Figure 3.3 Plot of observed rate constant vs. [NaOL] (L = H or D) for restricted rotation around the N(2)-N(3) bond in *cis*-**9d** (*left*) and *cis*-**9o** (*right*) in 30% (v/v) THF:H_2O solution (❍) and 30% (v/v) THF:D_2O solution (●). Inset: reciprocal (*left*) and double reciprocal (*right*) plots for data in 30% (v/v) THF:H_2O solution.

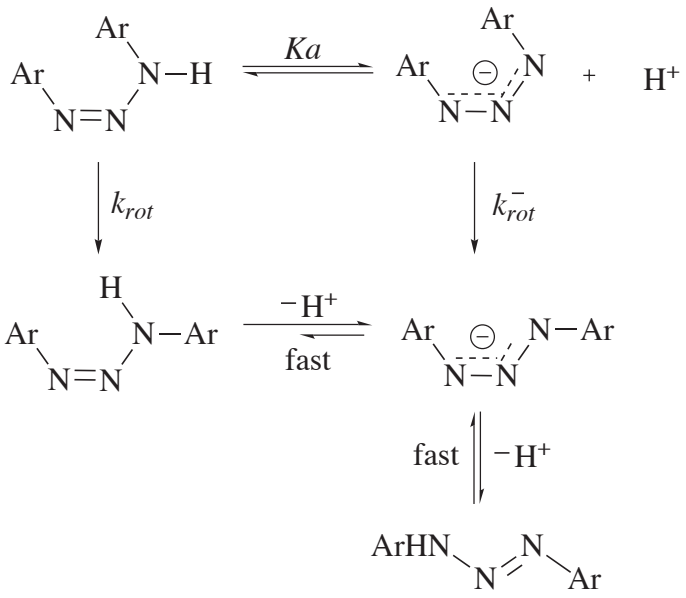

Scheme 3.1 *Cis*-to-*trans* isomerization mechanism for cyano-containing compounds.

The resulting expression of k_{obs} for the reaction mechanism shown in Scheme 3.1 is given in eq 3.2, where k_{rot} and k_{rot}^{-} represent the rate constants for restricted rotation of neutral and anionic *cis*-1,3-diphenyltriazene forms, respectively, while *Ka* corresponds to the *cis*-triazene acid dissociation equilibrium constant, and *Kw* denotes the self-dissociation equilibrium constant for water.

$$k_{obs} = \frac{k_{rot}^{-} \cdot Ka/Kw \cdot [OH^-] + k_{rot}}{1 + Ka/Kw \cdot [OH^-]} \qquad \text{eq 3.2}$$

According to Scheme 3.1, the partial double bond character of the N(2)-N(3) bond in the anionic form is expected to increase relative to that of the neutral form due to an increase in charge delocalization. Thus, the rate constant for rotation of the anionic form, k_{rot}^{-}, would be expected to be lower than that for the neutral form, k_{rot}. As a consequence, the values

of k_{obs} for restricted rotation around the N(2)-N(3) bond are expected to decrease with increasing pH. In fact, this is the case as seen in Figure 3.3 (*left*) for *cis*-**9d**. As illustrated in the inset of Figure 3.3 (*left*), the plot of the reciprocal rate constant for *cis*-**9d** vs. NaOH concentration is linear**,** which indicates ($k_{rot}^{-} \cdot Ka/Kw \cdot [OH^-]$) << k_{rot} in eq 3.2. As a result, eq 3.2 simplifies to eq 3.3. A nonlinear fitting of corresponding data (Appendix A, Table A6) to eq 3.3, leads to k_{rot} and Ka/Kw values given in Table 3.1 (entry 4).

$$k_{obs} = \frac{k_{rot}}{1 + Ka/Kw \cdot [OH^-]} \qquad \text{eq 3.3}$$

On the contrary, for k_{obs} to increase with pH as seen in the case of Figure 3.3 (*right*), the rate constant for restricted rotation of the anionic form, k_{rot}^{-}, must indeed be higher than that of the neutral form, k_{rot}. This would imply that upon deprotonation of the amino group, the partial double bond character of the N(2)-N(3) bond in the anionic form is lower than that in the neutral form. It is therefore inferred that the negative charge concentrates on the 4-cyano substituent attached to phenyl ring at N(3) rather than on the triazeno moiety. Hopkinson and Lien report in 1978 a*b initio* calculations on amines with unsaturated bonds adjacent to the nitrogen atom.[7] These calculations show that upon deprotonation, amines can undergo significant geometric rearrangements so that most of the negative charge of the anion concentrates at the more electronegative substituent.[7] It is interesting to note here that 1,3-bis(4-nitrophenyl)triazene (**9p**) can exist in both a normal and an *aci* (quinonoid nitronic acid) form (**12**).[8] Unfortunately, a comparison of data with nitro-containing 1,3-diphenyltriazenes (i.e., X = 4-NO_2 or 3-NO_2 in Chart 1.1), to support the role of valence tautomerization and direct resonance interaction in anionic *cis*-1,3-diphenyltriazenes, is

precluded since no isomerization can be detected with nitro-containing 1,3-diphenyltriazenes in NaOH aqueous solutions.[2]

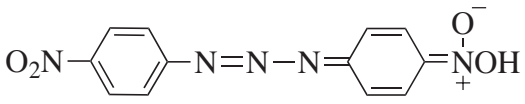

12

As shown in the inset of Figure 3.3 (*right*), the double reciprocal plot for restricted rotation of *cis*-**9o** in 30% v/v THF:H_2O solution is linear. This implies (k_{rot}^{-}·*Ka*/*Kw*·[OH^-]) >> k_{rot} and hence, eq 3.4 is obtained. The k_{rot}^{-} and *Ka*/*Kw* values resulting from a nonlinear fitting of corresponding data[9] according to eq 3.4 are given in Table 3.1 (entry 12).

$$k_{obs} = \frac{k_{rot}^{-} \cdot Ka/Kw \cdot [OH^-]}{1 + Ka/Kw \cdot [OH^-]} \qquad \text{eq 3.4}$$

Evidence for the change in the ionization state of symmetrical cyano-containing *cis*-1,3-diphenyltriazenes, as displayed in Scheme 3.1, is obtained from solvent kinetic isotope effects (SKIE) studies. SKIE refer to a change in rate constants when the solvent is replaced with an isotopically substituted form of it.[10a] In this study, SKIE are determined by taking the ratio of rate constants for restricted rotation around the N(2)-N(3) bond of *cis*-1,3-diphenyltriazenes in non-deuterated and deuterated aqueous media (i.e., $(k_{obs})_H$ in 30% (v/v) THF:H_2O solutions vs. $(k_{obs})_D$ in 30% (v/v) THF:D_2O solutions). A normal isotope

effect results when the ratio of rate constants in non-deuterated and deuterated solvents is larger than 1.[10b] An inverse isotope effect, on the other hand, results when the ratio of rate constants in non-deuterated and deuterated solvents is indeed lower than 1.[10b] The corresponding k_{obs} data in 30% (v/v) THF:D_2O solutions for symmetrical triazenes are given in Appendix A, Tables A2, A5, A7, and A10, whereas for unsymmetrical triazenes are given in Appendix B, Tables B3 and B5. Figure 3.3 (*left*) shows that *cis*-**9d** (where X = 3-CN) isomerizes faster in 30% (v/v) THF:H_2O (❍) than that in 30% (v/v) THF:D_2O (●). This indicates that a normal isotope effect is observed. Conversely, for Figure 3.3 (*right*), *cis*-**9o** (where X = 4-CN) isomerizes faster in 30% (v/v) THF:D_2O than that in 30% (v/v) THF:H_2O. This implies that an inverse isotope effect is observed. The non-linear fitting of data for **9d** and **9o** in 30% (v/v) THF:D_2O solutions, according to eq 3.3 and eq 3.4, respectively, yields experimental values of rotational rate constants, $(k_{rot})_D$, and ionization constants, $(Ka/Kw)_D$, summarized in Table 3.3.

Table 3.3 Summary of values of $(k_{rot})_D$, $(Ka/Kw)_D$, $(k_{rot})_H/(k_{rot})_D$, and $(Ka/Kw)_H/(Ka/Kw)_D$ for symmetrical substituted *cis*-1,3-diphenyltriazenes.

9	X	$(k_{rot})_D$ (10^5 s^{-1})[a]	$(Ka/Kw)_D$[a]	$(k_{rot})_H/(k_{rot})_D$	$(Ka/Kw)_H/(Ka/Kw)_D$
a	3,4-$(CH_3)_2$	0.89 ± 0.03	---	0.90 ± 0.03	---
c	3-CF_3	0.080 ± 0.002	---	0.99 ± 0.03	---
d	3-CN	0.087 ± 0.003	7.3 ± 0.9	1.05 ± 0.04	0.51 ± 0.08
o	4-CN	0.74 ± 0.01[b]	232 ± 32	1.04 ± 0.03[c]	0.20 ± 0.04

[a]In 30% (v/v) THF:D_2O solution, μ = 0.5 M (NaCl) at 21 °C. [b]Value of $(k^-_{rot})_D$. [c]Value of $(k^-_{rot})_H/(k^-_{rot})_D$.

Entries 3 and 4 in Table 3.3 show that the isotope effect on the rate constant for restricted rotation for **9d** and **9o** is essentially unity (i.e., no SKIE are detected). Also, as shown in Table 3.3, SKIE of *ca.* 1 result in the case of non-cyano containing symmetrical substrates, i.e., entry 1 (**9a**, X = 3,4-$(CH_3)_2$) and entry 2 (**9c**, X = 3-CF_3). These results are consistent with the fact that restricted rotation around the N(2)-N(3) bond involves a single reactant molecule in the rate-determining step, and hence, relatively minor solvent reorganization is required. Indeed, solvent isotope effects on solvation shells are typically small.[11] It is important to point out here that a previous study, partially introduced in Section 1.1.2, on *cis*-1,3,-di(4-X-phenyl)triazenes shows that the activation entropy ($\Delta S^{\ddagger}$) for restricted rotation is very small.[12] Values given in Table 3.4 (if at all significant) clearly indicate that the N(2)-N(3) restricted rotation is not associated with significant entropy changes between the transition state and the reactant, in agreement with an unimolecular mechanism for the rotational process.

Table 3.4 Activation entropy for restricted rotation of *cis*-1,3-di(4-X-phenyl)triazenes in 30% (v/v) THF:H_2O solutions.[a]

X	CH_3O	CH_3	H	Cl	CF_3
$\Delta S^{\ddagger}$ (e.u.)[b]	-5.0 ± 0.4	-5 ± 1	-4 ± 2	-1.8 ± 0.7	-2 ± 1

[a]μ = 0.5 M (NaCl) at 21 °C. [b]Values taken from ref. 13.

The ionization constants ratios, $[(Ka/Kw)_H/(Ka/Kw)_D]$, for *cis*-**9d** and *cis*-**9o** summarized in Table 3.3 are clearly lower than one. These isotopic effect values are consistent with the following facts. (i) The self-dissociation constant of H_2O in pure water solution

(pKw_{H_2O} = 14.163) is larger than that of D_2O (pKw_{D_2O} = 15.132).[13a] The same trend (i.e., $(Kw)_H/(Kw)_D$ >1) is expected in 30% (v/v) THF aqueous solutions, although corresponding pKw_{H_2O} and pKw_{D_2O} values will be higher than in pure water, since the dielectric constant of THF (ε = 7.6) is lower than that of H_2O (ε = 78.54),[13b] In fact, in 32.5% (v/v) THF aqueous solution pKw_{H_2O} = 16.43.[14] (ii) The dissociation constants of weak acids are larger in H_2O than that in D_2O (i.e., $(Ka)_H/(Ka)_D$ >1).[15] For example, p*Ka* values in H_2O and in D_2O are, respectively, 4.73 and 5.25 for acetic acid, and 10.58 and 11.23 for proline.[15] Finally, (iii) the isotopic effect $(Ka)_H/(Ka)_D$ increases as the strength of the weak acid decreases (e.g., *ca.* 3.3 vs. 4.5 for acetic acid vs. proline),[15] which leads to $(Ka)_H/(Ka)_D < (Kw)_H/(Kw)_D$ since water is a weaker acid than target triazenes, and ultimately, to ionization constants ratios, $[(Ka/Kw)_H/(Ka/Kw)_D]$, lower than one.

The fact that the ionization constants ratio for *cis*-**9d** is larger than that for *cis*-**9o**, can also be explained by the factors mentioned above. *Cis*-1,3-diphenyltriazenes are expected to be less acidic than their corresponding *trans*-forms, as a result of a decrease in resonance interactions due to the nonplanar conformation of the former.[2] Indeed, p*Ka* values for *cis*-**9d** and *cis*-**9o** can be estimated from the obtained *Ka*/*Kw* values (given in Table 3.1) and the reported pKw_{H_2O} value in 32.5% (v/v) THF aqueous solution (16.43)[14]. The resulting values, i.e., *ca.* 15.7 and 14.6 for *cis*-**9d** and *cis*-**9o**, respectively, are higher than the measured p*Ka* values (summarized in Table 2.2) for *trans*-**9d** (i.e., 11.49 ± 0.02) and *trans*-**9o** (i.e., 10.52 ± 0.02). Thus, the resulting $(Ka)_H/(Ka)_D$ isotope effect for *cis*-**9d** would be larger than that for *cis*-**9o**.

In the case of unsymmetrical *cis*-1,3-diphenyltriazenes with a 4-CN group attached to one of the phenyl rings, two kinetic processes are observed under the experimental condition of

this study (i.e., 30% (v/v) THF aqueous NaOH solutions). These two processes are attributed to the presence of two pairs of *cis* isomers (i.e., one pair of *cis*-conformers per tautomeric *trans* form, as depicted in Scheme 1.12) that react at different rates, similarly to the case of unsymmetrical non-cyano containing substrates mentioned above. Observed rate constants (k_{obs}) are dependent on the concentration of hydroxide ions (Appendix B, Tables B1-2, B4, and B6-8). Interestingly, for each unsymmetrical substrate, the fast process is accelerated with increasing NaOH concentration (Figure 3.4), while the slow process is slowed down (Figure 3.5). Also, as displayed in Figure 3.4, at any given NaOH concentration, the observed rate constants corresponding to the fast process, k_{obs}^{f}, increase as the electron-donating character of the variable substituent increases. Based on the preliminary Hammett ρ values, and the 1,3-dipolar resonance form, the rate constants for restricted rotation around N(2)-N(3) are expected to decrease with increasingly stronger electron-withdrawing substituents bonded to N(1). Thus, data displayed in Figure 3.4 should represent the tautomeric *cis-s-cis* forms bearing the variable substituents and 4-CN substituent at the phenyl rings attached to N(1) and N(3), respectively (i.e., *cis*-1,3-diphenyltriazenes forms with X = 3,4,5-$(Cl)_3$, 3,4-$(Cl)_2$, 3-CF_3, 4-Cl, and 4-OCH_3 and Y = 4-CN). This assignment seems reasonable since the negative charge that results from deprotonation of the amino group in the triazeno moiety would delocalize into the nearby CN group, which would lead to a decrease in the double bond character of the N(2)-N(3) bond in the anionic form relative to that of the neutral form. Hence, the observed rate constant for restricted rotation k_{obs}^{f} increases with increasing pH.

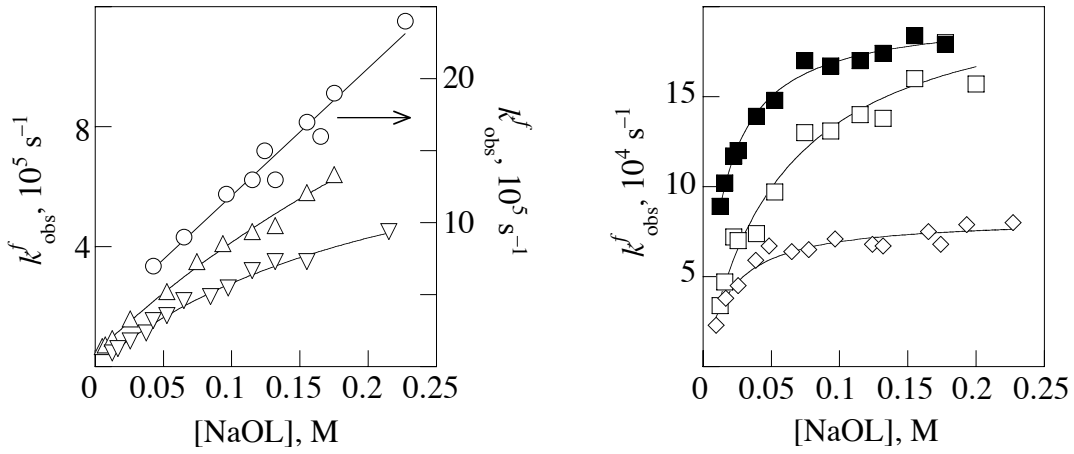

Figure 3.4 Plots of k^f_{obs} vs. [NaOL] (L = H or D) for restricted rotation of unsymmetrical *cis*-1,3-diphenyltriazenes with Y = 4-CN and X = 4-OCH_3 (○), 4-Cl (Δ), 3-CF_3 (∇), 3,5-Cl_2 (❑, ■) or 3,4,5-Cl_3 (◊); open symbols correspond to data in 30% (v/v) THF:H_2O solutions; closed symbol corresponds to 30% (v/v) THF:D_2O solution.

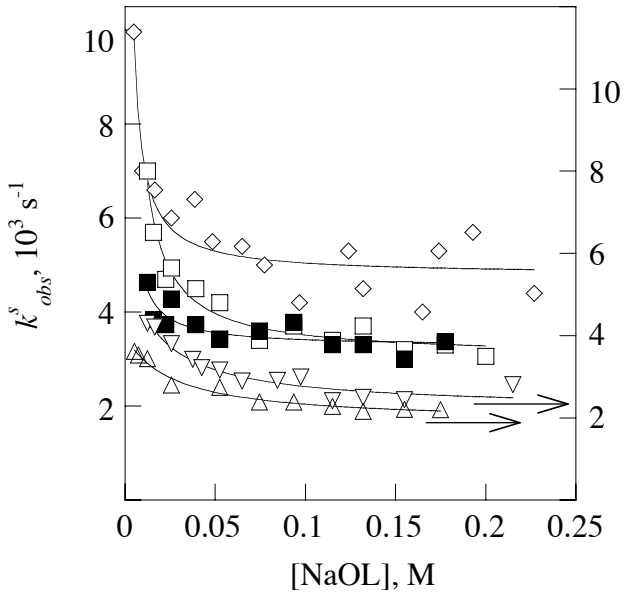

Figure 3.5 Plots of k^s_{obs} vs. [NaOL] (L = H or D) for restricted rotation of unsymmetrical *cis*-1,3-diphenyltriazenes with X = 4-CN and Y = 4-Cl (Δ), 3-CF_3 (∇), 3,5-Cl_2 (❑, ■) or 3,4,5-Cl_3 (◊); open symbols correspond to data in 30% v/v THF:H_2O solutions, closed symbol to 30% v/v THF:D_2O solution.

Figure 3.5, on the other hand, shows that at any given NaOH concentration, the observed rate constants corresponding to the slow process, k_{obs}^{s}, decrease as the electron-donating character of the variable substituent increases. According to the preliminary Hammett ρ values and 1,3-dipolar resonance form, the rate constants for restricted rotation around N(2)-N(3) are expected to increase with increasingly stronger electron-withdrawing substituents bonded to N(3). Thus, data displayed in Figure 3.5 are attributed to the tautomeric *cis-s-cis* forms bearing the 4-CN substituent and variable substituent in the phenyl rings attached to N(1) and N(3), respectively (i.e., *cis*-1,3-diphenyltriazenes forms with X = 4-CN and Y = 3,4,5-$(Cl)_3$, 3,4-$(Cl)_2$, 3-CF_3, 4-Cl, and 4-OCH_3). This assignment seems reasonable bearing in mind that a 4-CN substituent at N(1) stabilizes the 1,3-dipolar resonance form, leading to an increase of the N(2)-N(3) double bond character. Consequently, k_{obs}^{s} decreases with increasing pH. It is important to point out here that Figure 3.5 does not illustrate observed rate constants for restricted rotation of unsymmetrical *cis*-1,3-diphenyltriazene with X = 4-CN and Y = 4-OCH_3, since the observed values correspond indeed to the detection limit of the apparatus (i.e., *ca* 2000 s^{-1}).

The fact that two kinetic processes are being observed with unsymmetrical 4-CN containing substrates indicates the presence of (at least) two absorbing species of different reactivity. These would therefore imply that the primary *cis-s-cis* anionic (4-CN-containing) forms are not be the same ions and do not rapidly equilibrate, but rather undergo *cis*-to-*trans* isomerization. In contrast with the geometry of *trans*-triazenes (which are almost entirely planar),[16-19] the phenyl rings in *cis*-1,3-diphenyltriazenes are expected to be out of the plane because of steric hindrance. Thus, the primary anionic forms resulting from the ionization of tautomeric *cis-s-cis* 4-CN-containing triazenes may be stereoisomers with a different charge

distribution that links to the difference in dihedral angles of the two rings and to the degree of conjugation between the charge at N(3) in the triazeno moiety and the 4-CN substituent.

The linear plot displayed in Figure 3.4 for **10e** (where X = 4-OCH_3 and Y = 4-CN) implies that $(Ka/Kw \cdot [OH^-]) << 1$ in eq 3.2. Hence, eq 3.2 simplifies to eq 3.5. A linear fitting of corresponding data (Appendix B, Table B7) according to eq 3.5 yields values of k_{rot} (Table 3.2, entry 3) and of $(k_{rot}^- \cdot Ka/Kw)$ (Table 3.5, entry 5).

$$k_{obs} = k_{rot}^- \cdot Ka/Kw \cdot [OH^-] + k_{rot} \qquad \text{eq 3.5}$$

In the case of **10d** (where X = 4-Cl and Y = 4-CN), the non-linear fitting of corresponding data (Appendix B, Table B6) to eq 3.2 yields values of k_{rot} (Table 3.2), and k_{rot}^- and Ka/Kw (Table 3.4). Similar to the case of **9o** (X = 4-CN), in the case of data for Y = 4-CN and X = 3,4,5-Cl_3, 3,5-Cl_2, and 3-CF_3 displayed in Figure 3.4, the corresponding double reciprocal plots (not shown) are linear. This indicates that $(k_{rot}^- \cdot Ka/Kw \cdot [OH^-]) >> k_{rot}$ in eq 3.2, and therefore, eq 3.2 simplifies to eq 3.4, in agreement with the expected decrease in k_{rot} as X becomes a stronger electron-withdrawing group. Non-linear fittings of data for X = 3,4,5-Cl_3, 3,5-Cl_2, and 3-CF_3 (Appendix B, Tables B1-2, and B4, respectively) according to eq 3.4 provide the parameters summarized in Table 3.5.

Table 3.5 Rate constants for restricted rotation and acid dissociation equilibrium constants for anionic substituted unsymmetrical 4-CN-containing *cis*-1,3-diphenyltriazenes in 30% (v/v) THF:H_2O solution.[a]

10	X	Y	k_{rot}^{-} (10^5 s^{-1})	*Ka*/*Kw*
a	3,4,5-$(Cl)_3$	4-CN	0.83 ± 0.03	52 ± 8
	4-CN	3,4,5-$(Cl)_3$	0.048 ± 0.002	25 ± 3[b]
b	3,5-$(Cl)_2$	4-CN	2.2 ± 0.1	17 ± 3
	4-CN	3,5-$(Cl)_2$	0.031 ± 0.001	46 ± 3[b]
c	3-CF_3	4-CN	9.4 ± 0.9	4.2 ± 0.6
	4-CN	3-CF_3	0.022 ± 0.002	52 ± 23
d	4-Cl	4-CN	24 ± 9	1.8 ± 0.8
	4-CN	4-Cl	0.019 ± 0.001	37 ± 13
e	4-OCH_3	4-CN	92 ± 5[c]	<< 1

[a]μ = 0.5 M (NaCl) at 21 °C. [b]Value of (k_{rot} · *Kw*/*Ka*). [c]Value of (k_{rot}^{-} · *Ka*/*Kw*).

Plots displayed in Figure 3.5 for Y = 4-Cl and Y = 3-CF_3 are best fitted according to eq 3.2, while those for Y = 3,5-Cl_2 and 3,4,5-Cl_3 are best fitted to eq 3.6 (where (*Ka*/*Kw*·[OH^-]) >> 1 in eq 3.2). Resulting parameters are listed in Table 3.5, except for k_{rot} values for Y = 4-Cl and Y = CF_3, which are summarized in Table 3.2. It is important to indicate that the fitted parameters for Y = 4-Cl and 3-CF_3, as summarized in Table 3.5, should

be taken cautiously since the observed rate constants when [NaOH] > 0.1 M are very close to the detection limit of the apparatus (i.e., *ca* 2000 s^{-1}).

$$k_{obs} = k_{rot}^{-} + \frac{k_{rot}}{Ka/Kw \cdot [OH^-]} \qquad \text{eq 3.6}$$

Similarly to the case of *cis*-**9d** (X = 3-CN) and *cis*-**9o** (X = 4-CN), evidence for the assignment of the pH dependence observed with unsymmetrical 4-CN-containing *cis*-1,3-diphenyltriazenes comes from SKIE studies. As displayed in Figure 3.5, *cis*-**10b** (i.e., X = 4-CN, Y = 3,5-$(Cl)_2$) isomerizes faster in 30% (v/v) THF:H_2O solutions than that in 30% (v/v) THF:D_2O solutions. This indicates that a normal isotope effect is observed as in the case of *cis*-**9d**. Conversely, as in the case of *cis*-**9o**, the other tautomeric form of *cis*-**10b** (i.e., X = 3,5-$(Cl)_2$, Y = 4-CN), shown in Figure 3.4, isomerizes faster in 30% (v/v) THF:D_2O solutions than in 30% (v/v) THF:H_2O solutions (i.e., an inverse isotope effect is observed). The non-linear fittings of data for *cis*-**10b** (Appendix B, Table B3) according to eq 3.4 when X = 3,5-$(Cl)_2$, Y = 4-CN and to eq 3.6 when X = 4-CN, Y = 3,5-$(Cl)_2$ yield the parameters summarized in Table 3.6. Similar to the case of *cis*-**9a**, **9c-d**, and **9o**, for both tautomeric forms of *cis*-**10b** no SKIE are observed on the rate constants for restricted rotation (i.e., $(k_{rot}^{-})_H/(k_{rot}^{-})_D \approx 1$), in agreement with minimal solvent rearrangement for the unimolecular rotational process. Also, the ionization constants ratios as shown in Table 3.6 for *cis*-**10b** are lower than one, in agreement with the facts mentioned above (i.e., $(Kw)_H/(Kw)_D > 1$, $(Ka)_H/(Ka)_D > 1$, and $(Ka)_H/(Ka)_D < (Kw)_H/(Kw)_D$).

Table 3.6 Summary of values of $(k_{rot}^-)_D$, $(Ka/Kw)_D$, $(k_{rot}^-)_H/(k_{rot}^-)_D$, and $(Ka/Kw)_H/(Ka/Kw)_D$ for *cis*-**10b**.

X	Y	$(k_{rot}^-)_D$ ($10^3 s^{-1}$)	$(Ka/Kw)_D$	$(k_{rot}^-)_H/(k_{rot}^-)_D$	$(Ka/Kw)_H/(Ka/Kw)_D$
4-CN	3,5-$(Cl)_2$	3.3 ± 0.1	15 ± 3[b]	0.94 ± 0.07	0.33 ± 0.05
3,5-$(Cl)_2$	4-CN	200 ± 10	65 ± 4	1.10 ± 0.07	0.26 ± 0.05

[a]In 30% (v/v) THF:D_2O solution, μ = 0.5 M (NaCl) at 21 °C. [b]Value of $(k_{rot}{\cdot}Kw/Ka)$ from eq 3.6.

The correlation of values of k_{rot}^- (Table 3.5) for X = 4-CN and Y = variable substituent and their corresponding tautomeric forms (i.e., X = variable substituent and Y = 4-CN) vs. the corresponding Hammett substituent constants are displayed in Figure 3.6. The slope values, which correspond to the values of ρ_{im}^- and ρ_{am}^-, are -1.98 ± 0.03 and 0.54 ± 0.07, respectively. ρ_{im}^- and ρ_{am}^- denote the Hammett reaction constants for N(1) and N(3) for restricted rotation of anionic forms, respectively. Similarly to the case of neutral 1,3-diphenyltriazenes, the negative sign of ρ_{im}^-, (which indicates a decrease in the electron density on N(1) on rotation) and positive value of ρ_{am}^- (which indicates an increase in the electron density on N(3) on rotation) are fully consistent with the 1,3-dipolar resonance model (Scheme 1.7). As rotation around the N(2)-N(3) bond takes place, electron delocalization along the nitrogen chain reduces. Consequently, the electron density at N(1) and N(3) decreases and increases, respectively, on going from ground state to transition state. Moreover, the absolute value of ρ_{im}^- is clearly higher than that of ρ_{am}^-, demonstrating that the restricted rotation is more sensitive to the electronic character of the group attached to N(1) than to the group attached to N(3).

The correlation between the values of *Ka*/*Kw* (Table 3.4) for X = variable substituent and Y = 4-CN, and its corresponding σ_X constants are also displayed in Figure 3.6. As expected, it is clearly shown that the values of log(*Ka*/*Kw*) increase with increasingly stronger electron-withdrawing substituents. The value of the slope, which corresponds to ρ, is 1.97 ± 0.04. It is interesting to note that the latter value is comparable to the corresponding ρ□value (2.29 ± 0.08) obtained from unsymmetrical 4-cyano-containing *trans*-triazenes, described in Section 2.2.1.

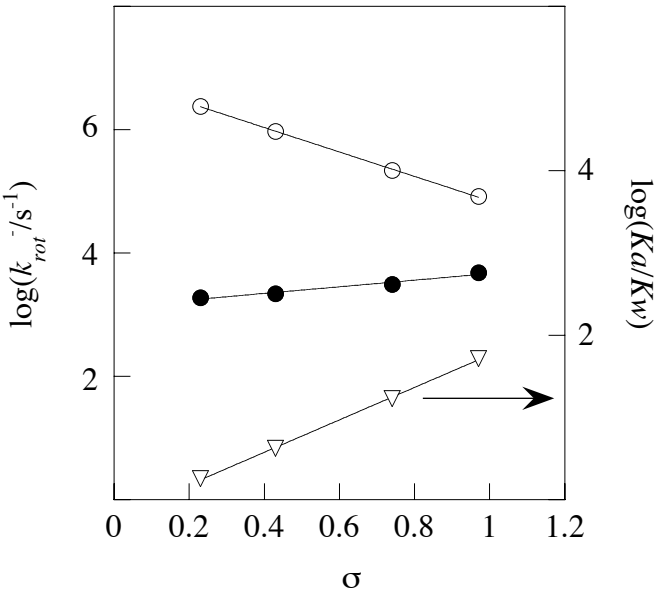

Figure 3.6 Plot of rate constants vs. Hammett substituent constants for restricted rotation of anionic *cis*-1,3-diphenyltriazenes (❍, for X = 4-CN and Y = variable substituent; ●, for X = variable substituent and Y = 4-CN) and plot of acid dissociation equilibrium constants vs. Hammett substituent constants for unsymmetrical 4-CN containing substrates (∇, for X = variable substituent and Y = 4-CN).

It is noticed that a similar correlation for values of *Ka*/*Kw* for the other tautomeric forms (i.e., X = 4-CN and Y = variable substituent) is precluded since only two values of *Ka*/*Kw* could be obtained. However, it is interesting to point out that these two values for Y = 4-Cl and 3-CF_3 are clearly higher than those for their tautomeric forms. This trend is consistent with studies on tautomeric equilibria of *trans*-1,3-diphenyltriazenes as described in Section 1.1.3, which show that *para* groups with an electron-withdrawing mesomeric effect favor the tautomer form having the N=N double bond closer to electron donating groups.[20-23]

3.3 Conclusions

It has been shown that laser excitation at 355 nm of target symmetrical and unsymmetrical 1,3-diphenyltriazenes in 30% (v/v) THF aqueous solutions leads to instantaneous photoinduced *trans*-to-*cis* isomerization, followed by thermal *cis*-to-*trans* isomerization. A quantitative analysis, performed by using a multiple-substituent Hammett equation, of the rate constants for restricted rotation around the N(2)-N(3) bond of target *cis*-1,3-diphenyltriazenes provides Hammett reactions constant (ρ) values of -1.88 ± 0.08 and 0.70 ± 0.08 for N(1) and N(3), respectively. The restricted rotation around the N(2)-N(3) bond of substituted triazenes is more sensitive to the electronic character of the aryl group at N(1) than to the electronic character of the aryl group at N(3). The study also shows that only in the case of cyano-containing substrates, the observed rate constants (k_{obs}), ascribed to restricted rotation around the N(2)-N(3) bond, depend on pH. This pH dependence is attributed to the change in substrate ionization. The pH dependency indicates that the charge distribution in the triazeno fragment is significantly influenced by mesomerically electron withdrawing groups. The correlation of rate constants for restricted rotation for the anionic forms of

cis-1,3-diphenyltriazenes yields values of -1.98 ± 0.03 and 0.54 ± 0.07 for ρ_{im} and ρ_{am}, respectively. Consistent with the case of neutral *cis*-1,3-diphenyltriazenes, the absolute value of ρ_{im} is higher than that of ρ_{am}, which indicates that the sensitivity of the reaction to the electronic character of the group attached to N(1) is greater than to that at N(3). The slope (which corresponds to ρ) obtained from the correlation of acid dissociation constants with Hammett substituent constants of unsymmetrical cyano-containing *cis*-1,3-diphenyltriazenes is comparable to that of unsymmetrical non-cyano-containing *trans*-1,3-diphenyltriazenes.

References

(1) Barra, M.; Chen, N. *J. Org. Chem.* **2000**, *65*, 5739-5744.

(2) Chen, N.; Barra, M.; Lee, I.; Chahal, N. *J. Org. Chem.* **2002**, *67*, 2271-2277.

(3) Zhang, H.; Barra, M. *J. Phys. Org. Chem.* **2005**, *6*, 498-503.

(4) Baro, J.; Dudek, D.; Luther, K.; Troe, J. *Ber. Bunsenges. Phys. Chem.* **1983**, 1161-1164.

(5) Hansch, C.; Leo, A.; Taft, R. W. *Chem. Rev.* **1991**, *91*, 165-195.

(6) Lee, I. *Adv. Phys. Org. Chem.* **1992**, *27*, 57-117.

(7) Hopkinson, A. C.; Lien, M. H. *Intl. J. Quant. Chem.* **1978**, *XIII*, 349-366.

(8) Benson, F. R. In *The High Nitrogen Compounds*; Wiley: New York, 1984, p 343.

(9) Observed rate constants for restricted rotation around N(2)-N(3) for *cis*-1,3-(4-cyano-phenyl)triazene in NaOH solution were taken from the supplementary material for ref. 2.

(10) Carroll, F. A. In *Perspectives on Structure and Mechanism in Organic Chemistry*; Brooks/Coles Publishing Company: California, 1998, p (a) 365; (b) 361.

(11) Albery, J. In *Proton Transfer Reactions*; Caldin, E. F., Gold, V., Eds.; John Wiley & Sons: New York, 1975, Chapter 9.

(12) Barra, M.; Srivastava, S.; Brockman, E. *J. Phys. Org. Chem.* **2004**, *17*, 1057-1060.

(13) Lide, D. R., Ed. *Handbook of Chemistry and Physics; 77th ed.*; CRC Press: Boca Raton, 1996-1997, p (a) 8-80; (b) 8-100.

(14) Wooley, E. M.; Tomkins, J.; Hepler, L. G. *J. Sol. Chem.* **1972**, *1*, 341 - 351.

(15) Delgado, R.; Fraústo Da Silva, J. J. R.; Amorim, M. T. S.; Cabral, M. F.; Chaves, S.; Costa, J. *Anal. Chim. Acta* **1991**, 271-282.

(16) Gladkova, V. F.; Kondrashev, Y. D. *Sov. Phys.-Crystallogr.* **1972**, *16*, 806-809.

(17) Zhang, D.-C.; Fei, Z.-H.; Zhang, T.-Z.; Zhang, Y.-Q.; Yu, K.-B. *Acta Crystallogr., Sect. C: Cryst. Struct. Commun.* **1999**, *C55*, 102-104.

(18) Hörner, M.; Bresolin, L.; Bordinhao, J.; Hartmann, E.; Strähle, J. *Acta Crystallogr., Sect. C: Cryst. Struct. Commun.* **2003**, *C59*, O426-O427.

(19) Karadyi, N.; Cakmak, S.; Odabasoglu, M.; Büyükgüngör, O. *Acta Crystallogr., Sect. C: Cryst. Struct. Commun.* **2005**, *C61*, O303-O305.

(20) Iwamura, H.; Albert, K.; Rieker, A. *Tetrahedron Lett.* **1976**, *17*, 2627-2630.

(21) Borisov, E. V.; Peregudov, A. S.; Postovoi, S. A.; Fedin, E. I.; Kravtsov, D. N. *Bull. Acad. Sci. USSR, Div. Chem. Sci.* **1986**, *35*, 499-502.

(22) Shcherbakova, O. V.; Kravtsov, D. N.; Peregudov, A. S.; Borisov, Y. A. *Russ. Chem. Bull.* **1998**, *47*, 1835-1386.

(23) Mitsuhashi, T.; Simamura, O. *Chem. Ind. (London)* **1964**, 578-579.

Chapter 4. Experimental

4.1 Synthetic Methods

4.1.1 Materials and Instruments

The following reactants were purchased from Aldrich Chem. Co and used as received: sodium hexanitrocobaltate(III) (SHNC), isoamyl nitrite (97%), 4-aminobenzonitrile (98%), 3-aminobenzonitrile (99%), 4-(trifluoromethyl)aniline hydrochloride (97%), 3-(trifluoromethyl)aniline (99%), *m*-anisidine (97%), 4-ethynylaniline (97%), 3,5-dichloroaniline (98%), 3,4,5-trichloroaniline, 3,4-dimethylaniline (98%), 3-nitroaniline, *p*-*N*,*N*-dimethylaminoaniline, and sodium deutroxide. In addition, *p*-nitroaniline, ACS grade petroleum ether (60 – 80 ºC), 37% (w/v) hydrochloric acid, sodium acetate, ACS grade chloroform, sodium hydroxide, and ACS grade methanol were all purchased from BDH and used as received. *p*-Anisidine (Eastman), *p*-chloroaniline (Baker), sodium nitrite (Sigma, Analytical grade), triethyl orthoformate (98%, Lancaster), acetone (Caledon Labs), and ethanol (Commercial Alcohols) were also used as received. Benzene, ethyl acetate and hexane were all obtained from EMD, and used as received. Deionized water was used for synthesis of triazenes.

^{1}H NMR spectra were recorded on a Bruker AC-300 (300MHz) NMR spectrometer. Chemical shifts are reported in parts per million (ppm) relative to solvent signals (i.e., δ 2.49 for DMSO-*d*6, and δ 2.05 for acetone-*d*6). Deurated solvents used for ^{1}H NMR, i.e., acetone-*d6* (D, 99.9%), DMSO-*d6* (D, 99.9%), chloroform-*d* (D, 99.9%), and D_2O (D, 99.9%), were purchased from Cambridge Isotope Laboratories, Inc. Electron impact mass spectra (EI MS) and high-resolution mass spectrometry (HRMS) were performed at the University of Waterloo on a JEOL HX110 mass spectrometer.

Melting points (mp) were determined on a MEL-TEMP melting point apparatus. Column chromatography was carried out using silica gel (70-230 mesh). Thin layer chromatography was performed on Whatman flexible TLC plates with 250 μm UV_{254} silica gel coating on polyester backing.

4.1.2 Synthesis of Symmetrical Triazenes

4.1.2.1 1,3-Bis(3,4-dimethylphenyl)triazene (9a)

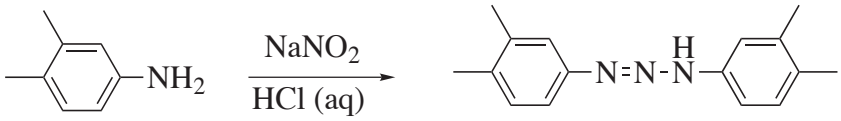

In a 25 mL round-bottom flask, 3,4-dimethylaniline (0.50 g, 4.1 mmol) was mixed with 37% (w/v) hydrochloric acid (0.54 mL, 17.9 mmol) and water (4.1 mL). This round-bottom flask was placed in an ice bath. A pre-cooled sodium nitrite solution (0.17 g of $NaNO_2$ in 1.0 mL of water) was then added slowly to the round-bottom flask keeping constant stirring to obtain 3,4-dimethylphenyl diazonium ions. After the addition of $NaNO_2$ was completed, the solution was kept stirring for 10 minutes and then the pH was adjusted to *ca*. 6 by adding 18% (w/v) sodium acetate aqueous solution. A bright yellow precipitate began to form immediately. The reaction mixture was kept stirring for 20 minutes. The bright yellow precipitate was filtered out, washed with cold water, and dried in vacuum overnight at room temperature. The raw product was purified by recrystallization using petroleum ether (60 - 80°C) to yield the desired product as small dark-orange needles (119 mg; yield 60%). To the best of our knowledge, no physical data have been reported for 1,3-bis(3,4-dimethylphenyl)triazene; mp 142 - 144 ºC; ^{1}H NMR (300 MHz, acetone-*d*6): 2.22 (s, 3H, C**H**$_3$), 2.26 (s, 3H, C**H**$_3$), 7.11 (d, 2H, *meta* **H** to

NNNH, J = 8.1 Hz), 7.19 (dd, 2H, *para* **H** to CH_3, J = 1.8 and 8.1 Hz), 7.26 (br, 2H, *ortho* **H** to NNNH and CH_3), 10.99 (s, 1H, N**H**); MS m/z (rel. intensity) (EI): 253 (M, 9), 225 (36), 133 (41), 105 (100), 77 (19); HRMS calc. for $C_{16}H_{19}N_3$: 253.1579, found: 253.1587.

4.1.2.2 1,3-Bis(4-ethynylphenyl)triazene (9b)

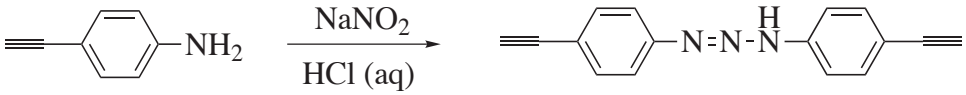

In a 25 mL round-bottom flask, 4-ethynylaniline (0.585 g, 5 mmol) was mixed with 37% (w/v) hydrochloric acid (0.65 mL, 21.4 mmol) and water (5 mL). This round-bottom flask was placed in an ice bath. A pre-cooled sodium nitrite solution (0.21 g of $NaNO_2$ in 1.25 mL of water) was then added slowly to the round-bottom flask keeping constant stirring to obtain 4-ethynylphenyl diazonium ions. After the addition of $NaNO_2$ was completed, the solution was kept stirring for 60 minutes and then the pH was adjusted to *ca*. 6 by adding 18% (w/v) sodium acetate aqueous solution. A reddish precipitate began to form immediately. The reaction mixture was kept stirring overnight. The reddish precipitate was filtered out, washed with cold water, and dried in vacuum overnight at room temperature. A dark red powder raw product was obtained. The raw product was purified by column chromatography (using benzene as eluent) followed by recrystallization using hexane to afford the desired product as shiny light-orange needles (210 mg; yield 60%). To the best of our knowledge, no physical data have been reported for 1,3-bis(4-ethynylphenyl)triazene; mp 143.5 - 144 ºC; ^{1}H NMR (300 MHz, acetone-*d*6): 3.65 (s, 2H, CC**H**), 7.52 (s, 8H, Ar**H**), 11.64 (s, 1H, N**H**); MS m/z (rel. intensity) (EI): 245 (M, 11), 129 (61), 101 (100); HRMS calc. for $C_{16}H_{11}N_3$: 245.0953, found: 245.0947.

4.1.2.3 1,3-Bis[3-(trifluoromethyl)phenyl]triazene (9c)

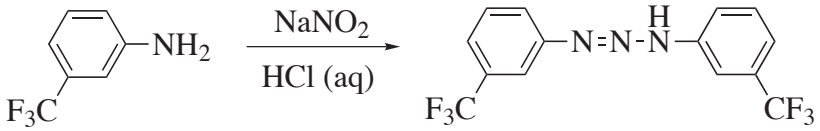

In a 25 mL round-bottom flask, 3-(trifluoromethyl)aniline (0.81 g, 5 mmol) was mixed with 37% (w/v) hydrochloric acid (0.65 mL, 21.4 mmol) and water (5 mL). This round-bottom flask was placed in an ice bath. A pre-cooled sodium nitrite solution (0.21 g of $NaNO_2$ in 1.3 mL of water) was then added slowly to the round-bottom flask keeping constant stirring to obtain 3-(trifluoromethyl)phenyl diazonium ions. After the addition of $NaNO_2$ was completed, the solution was kept stirring for 60 minutes and then the pH was adjusted to *ca*. 6 by adding 18% (w/v) sodium acetate aqueous solution. A light-yellow precipitate began to form immediately. The reaction mixture was kept stirring for one hour. The yellow precipitate was filtered out, washed with cold water, and dried in vacuum overnight at room temperature. The raw product was purified by recrystallization using hexane to afford the desired product as golden-brown fine needles (600 mg; yield 72%); mp 116 - 117 ºC (lit. mp[1] 115 - 116 ºC); ^{1}H NMR (300 MHz, DMSO-*d*6): 7.51 (d, 2H, *para* **H** to CF_3, J = 7.9 Hz), 7.63 (t, 2H, *meta* **H** to CF_3, J = 7.9 Hz), 7.69 (s, 2H, *ortho* **H** to NNNH & CF_3), 7.77 (d, 2H, *para* **H** to NNNH, J = 7.9 Hz), 12.92 (br, 1H, N**H**).

4.1.2.4 1,3-Bis(3-cyanophenyl)triazene (9d)

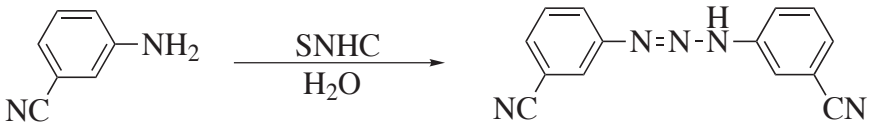

Synthesis of 1,3-bis(3-cyanophenyl)triazene was done by one-pot nitrosation of *m*-nitroaniline with SHNC, which acted as nitrosation agent in aqueous solution. To a solution containing SHNC (303.5 mg, 0.75 mmol) and 5 mL of water, *m*-cyanoaniline (118.1 mg, 1 mmol) was added. The reaction mixture was stirred at room temperature for 40 hours. The yellowish raw product was filtered off and washed thoroughly with cold water. The raw product was purified by recrystallization using a 2:1 mixture of chloroform and hexane to afford the desired product as pale yellow powder (83.1 mg; yield 67%); mp 185 - 186 ºC; ^{1}H NMR (300 MHz, acetone-*d*6): 7.60 (m, 4H, *para* **H** and *meta* **H** to CN), 7.85 (d, 2H, *para* **H** to NNNH, J = 7.7 Hz), 7.96 (s, 2H, *ortho* **H** to NNNH and CN), 11.89 (s, 1H, N**H**).

4.1.2.5 1,3-Bis(3-nitrophenyl)triazene (9e)

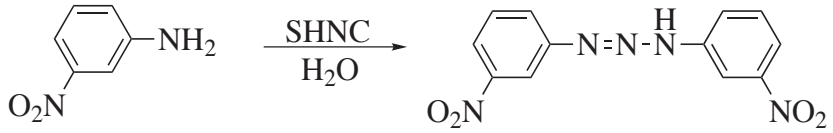

Synthesis of 1,3-bis(3-nitrophenyl)triazene was done by one-pot nitrosation of *m*-nitroaniline with SHNC, which acted as nitrosation agent in aqueous solution. To a solution containing SHNC (607.8 mg, 1.5 mmol) and 10 mL of water, *m*-nitroaniline (276.8 mg, 2 mmol) was added. The reaction mixture was stirred at room temperature for 72 hours. The yellowish raw product was filtered off and washed thoroughly with cold water. The obtained raw product was dried under vacuum for five hours to afford a pale yellow solid. The crude product was then recrystallized from acetone to yield a fine yellow powder (143.5 mg; yield 50%); mp 191 – 192 ºC (lit. mp[2] 198.5 - 199.5 ºC); ^{1}H NMR (300 MHz, DMSO-*d*6): 7.70

(t, 2H, *meta* **H** to NO_2, J = 7.1 Hz), 7.91 (d, 2H, *ortho* **H** to NNNH, J = 7.1 Hz), 8.02 (br, 2H, *para* **H** to NNNH), 8.18 (s, 2H, *ortho* **H** to NO_2 and NNNH), 13.15 (s, 1H, N**H**).

4.1.2.6 1,3-Bis(3,5-dichlorophenyl)triazene (9f)

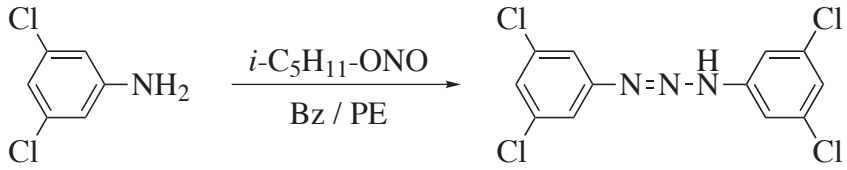

Isoamyl nitrite (0.88 g, 7.5 mmol) was added dropwise to a stirred solution of 3,5-dichloroaniline (0.81 g, 5 mmol) in a mixture of petroleum ether (10 mL) and benzene (5 mL). The reaction mixture was kept at room temperature for two and a half hours, and the solvent was then removed on a rotary evaporator. The raw product was purified by recrystallization using hexane and then acetone to afford the desired product as pale orange powder (80 mg; yield 10%); mp 178 - 180 ºC (lit. mp[3] 184 - 186 ºC); ^{1}H NMR (300 MHz, acetone-*d*6): 7.27 (br, 2H, *para* **H** to NNNH), 7.53 (s, 4H, *ortho* **H** to NNNH), 11.88 (s, 1H, N**H**); MS m/z (rel. intensity) (EI): 333 (M [$^{35}Cl_4$], 3), 173 (47), 145 (100), HRMS calc. for $C_{12}H_7{}^{35}Cl_4N_3$: 332.9394, found: 332.9400.

4.1.2.7 1,3-Bis(3,4,5-trichlorophenyl)triazene (9g)

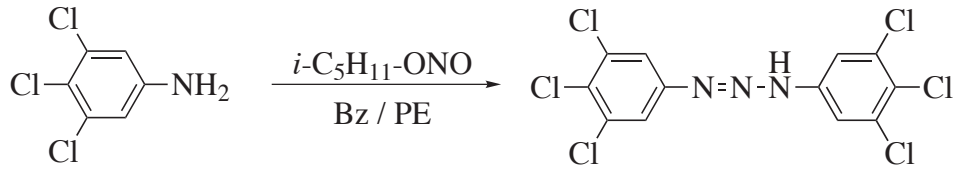

Isoamyl nitrite (0.22 g, 1.9 mmol) was added dropwise to a stirred solution of 3,4,5-trichloroaniline (0.25 g, 1.27 mmol) in a mixture of petroleum ether (2.5 mL) and benzene (1.3 mL). The reaction mixture was kept at room temperature for two and a half hours, and the solvent was then removed on a rotary evaporator. The raw product was recrystallized using petroleum ether (60 – 80 °C) to afford the desired product as yellow powder (100.9 mg; yield 35%); mp 182 - 183 ºC (lit. mp[2] 199 - 200 ºC); ^{1}H NMR (300 MHz, DMSO-*d*6): 7.75 (s, 4H, *ortho* **H** to NNNH), 13.06 (s, 1H, N**H**).

4.1.2.8 Attempted Synthesis of 1,3-Bis(3-methylphenyl)triazene (9h) by the Classical Diazonium Method

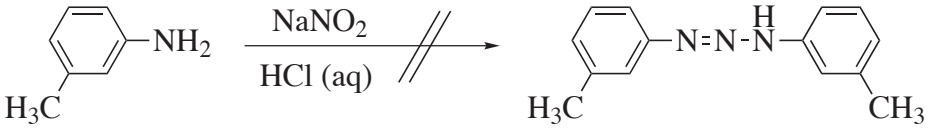

In a 25 mL round-bottom flask, 3-methylaniline (0.54 g, 5 mmol) was mixed with 37% (w/v) hydrochloric acid (0.64 mL, 21.2 mmol) and water (5 mL). This round-bottom flask was placed in an ice bath. A pre-cooled sodium nitrite solution (0.21 g of $NaNO_2$ in 1.3 mL of water) was then added slowly to the round-bottom flask keeping constant stirring to obtain 3-methylphenyl diazonium ions. After the addition of $NaNO_2$ was completed, the solution was kept stirring for 30 minutes and then the pH was adjusted to *ca*. 6 by adding 20% (w/v) sodium acetate aqueous solution. A purple precipitate in an orange solution began to form immediately. The reaction mixture was kept stirring for one hour. The purple precipitate was filtered out, washed with cold water, and dried in vacuum overnight at room temperature. The purple raw product was purified by recrystallization using petroleum ether (60 – 80 ºC). The

desired product (i.e., triazene) is not afforded, instead the azo compound shown below (where $R_1 = CH_3$, $R_2 = NH_2$, and $R_3 = CH_3$) is formed as a dark purple solid (335.2 mg; yield 60%); mp 205 - 206 ºC; ^{1}H NMR (300 MHz, DMSO-*d*6): 2.39 (s, 3H, *para* C**H**$_3$ to N=N and *meta* to NH_2), 2.58 (s, 3H, *meta* C**H**$_3$ to N=N), 6.90 (br, 2H, *ortho* **H** to NH_2 and *para* **H** to NH_2), 7.27 (br, 1H, *meta* **H** to CH_3), 7.41 (br, 1H, *para* **H** to N=N), 7.66 (m, 3H, *ortho* **H** to N=N), 8.62 (br, 2H, N**H**$_2$)

The orange filtrate solution was evaporated and dried in vacuum overnight at room temperature. The raw product was purified by column chromatography (using 7:1 benzene:ethyl acetate as eluent), to yield the azo compound where $R_1 = NH_2$, $R_2 = CH_3$, and $R_3 = CH_3$ as a dark orange solid (64 mg; yield 11%); mp 72 - 74 ºC; ^{1}H NMR (300 MHz, DMSO-*d*6): 2.36 (s, 3H, *meta* C**H**$_3$ to NH_2), 2.54 (s, 3H, *meta* C**H**$_3$ to N=N), 5.99 (s, 2H, N**H**$_2$), 6.45 (dd, 1H, *para* **H** to CH_3 and *ortho* to NH_2, J = 2.3 and 8.6 Hz), 6.50 (d, 1H, *ortho* **H** to CH_3 and NH_2, J = 2.3 Hz), 7.20 (d, 1H, *para* **H** to N=N, J = 7.4 Hz), 7.35 (t, 1H, *meta* **H** to N=N and CH_3, J = 7.4 Hz), 7.53 (m, 3H, *ortho* **H** to N=N).

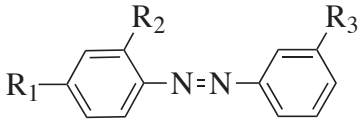

4.1.2.9 Attempted Synthesis of 1,3-Bis(3-methylphenyl)triazene (9h) by SHNC Method

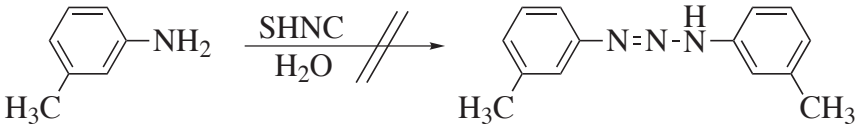

To a solution containing SHNC (1.41 g, 3.5 mmol) and 23 mL of water, 3-methylaniline (500 mg, 4.7 mmol) was added. The reaction mixture was stirred at room temperature for 8 hours. A black product formed. It was filtered off, washed thoroughly with cold water and dried under vacuum overnight to afford a mixture of black and yellow solids. The crude product was purified by means of preparative TLC (using 5:1 benzene:ethyl acetate as eluents) to yield an orange solid (21 mg; yield 5.3%). Instead of the formation of desired triazene, the azo compound shown above (R_1 = NH_2, R_2 = CH_3, and R_3 = CH_3) is obtained; mp 72 - 74 ºC; ^{1}H NMR (300 MHz, DMSO-*d*6): 2.38 (s, 3H, *meta* C**H**$_3$ to NH_2), 2.53 (s, 3H, *meta* C**H**$_3$ to N=N), 5.99 (s, 2H, N**H**$_2$), 6.45 (dd, 1H, *para* **H** to CH_3 and *ortho* to NH_2, J = 2.1 and 8.4 Hz), 6.49 (d, 1H, *ortho* **H** to CH_3 and NH_2, J = 2.1 Hz), 7.20 (d, 1H, *para* **H** to N=N, J = 7.9 Hz), 7.37 (t, 1H, *meta* **H** to N=N and CH_3, J = 7.9 Hz), 7.52 (m, 3H, *ortho* **H** to N=N).

4.1.2.10 Attempted Synthesis of 1,3-Bis(3-methylphenyl)triazene (9i)

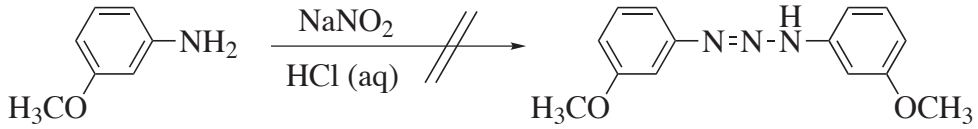

In a 25 mL round-bottom flask, 3-methoxyaniline (0.62 g, 5 mmol) was mixed with 37% (w/v) hydrochloric acid (0.64 mL, 21.2 mmol) and water (5 mL). This round-bottom flask was placed in an ice bath. A pre-cooled sodium nitrite solution (0.21 g of $NaNO_2$ in 1.3 mL of water) was then added slowly to the round-bottom flask keeping constant stirring to obtain 3-methoxyphenyl diazonium ions. After the addition of $NaNO_2$ was completed, the solution was kept stirring for 30 minutes and then the pH was adjusted to *ca*. 6 by adding 20% (w/v) sodium acetate aqueous solution. A brown precipitate began to form immediately. The reaction

mixture was kept stirring for one hour. The brown precipitate was filtered out, washed with cold water, and dried in vacuum overnight at room temperature. The raw product was purified by recrystallization using ethanol. The desired product (i.e., triazene) is not afforded, instead the azo compound shown above (R_1 = NH_2, R_2 = OCH_3, and R_3 = OCH_3) is formed as a dark brown solid (304.5 mg; yield 47%); mp 160 - 162 ºC; ^{1}H NMR (300 MHz, DMSO-*d*6): 3.85 (s, 3H, *meta* OC**H**$_3$ to NH_2), 3.90 (s, 3H, *meta* OC**H**$_3$ to N=N), 6.17(br, 2H, N**H**$_2$), 6.21 (dd, 1H, **H** *ortho* to NH_2 and *para* to OCH_3, J = 2.1 and 8.8 Hz), 6.31 (d, 1H, *ortho* **H** to NH_2 and OCH_3, J = 2.1 Hz), 6.94 (dd, 1H, *para* **H** to N=N, J = 2.1 and 7.7 Hz), 7.21 (t, 1H, *ortho* **H** to N=N and OCH_3, J = 2.1 Hz), 7.28 (d, 1H, **H** *ortho* to N=N and *para* to OCH_3, J = 7.7 Hz), 7.38 (t, 1H, *meta* **H** to N=N and OCH_3, J = 7.7 Hz), 7.52 (d, 1H, *meta* **H** to NH_2, J = 8.8 Hz).

4.1.3 Synthesis of Unsymmetrical Triazenes

4.1.3.1 3,4,5-Trichloro-4-cyano-1,3-diphenyltriazene (10a)

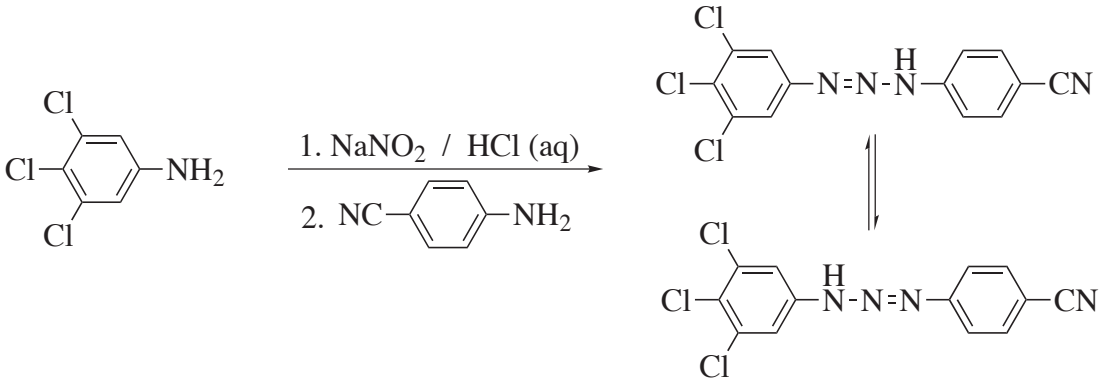

In a 25 mL round-bottom flask, 3,4,5-trichloroaniline (165.6 mg, 0.843 mmol) was mixed with 37% (w/v) hydrochloric acid (80 μL, 2.53 mmol) and water (1.94 mL). This round-bottom flask was placed in an ice bath. A pre-cooled sodium nitrite solution (0.06 g of $NaNO_2$ in 0.56 mL of water) was then added slowly to the round-bottom flask keeping constant stirring to

obtain 3,4,5-trichlorophenyl diazonium ions. After the addition of $NaNO_2$ was completed, the solution was kept stirring for 65 minutes and then the pH was adjusted to *ca*. 6 by adding 18% (w/v) sodium acetate aqueous solution. In a 50 mL round-bottom flask, 4-cyanoaniline (99.6 mg, 0.843 mmol) was dissolved in *ca*. 2.8 mL of methanol. The flask was placed in an ice bath and stirred vigorously. Afterwards, the solution contained in the 25 mL round-bottom flask was added drop-by-drop to the 50 mL round-bottom flask over a period of 35 minutes. A dark yellow precipitate began to form immediately. After this addition, the reaction mixture was kept stirring for three and a half hours. The bright yellow precipitate was filtered out, washed with cold water and dried in vacuum overnight at room temperature. The raw product was purified by recrystallization using ethanol to afford the product as a bright yellow powder (131.7 mg; yield 50%). To the best of our knowledge, no physical data have been reported for 3,4,5-trichloro-4-cyano-1,3-diphenyltriazene; mp 229 – 230 ºC; ^{1}H NMR (300 MHz, DMSO-*d*6): 7.58 (d, 2H, *meta* **H** to CN, J = 8.4 Hz), 7.75 (s, 2H, *ortho* **H** to Cl), 7.81(d, 2H, *ortho* **H** to CN, J = 8.4 Hz), 13.17 (s, 1H, N**H**); MS m/z (rel. intensity) (EI): 324(M [$^{35}Cl_3$], 9), 207 (45), 179 (100), 130 (31), 102 (65); HRMS calc. for $C_{13}H_7{}^{35}Cl_3N_3$: 323.9736; found: 323.9734.

4.1.3.2 3,5-Dichloro-4-cyano-1,3-diphenyltriazene (10b)

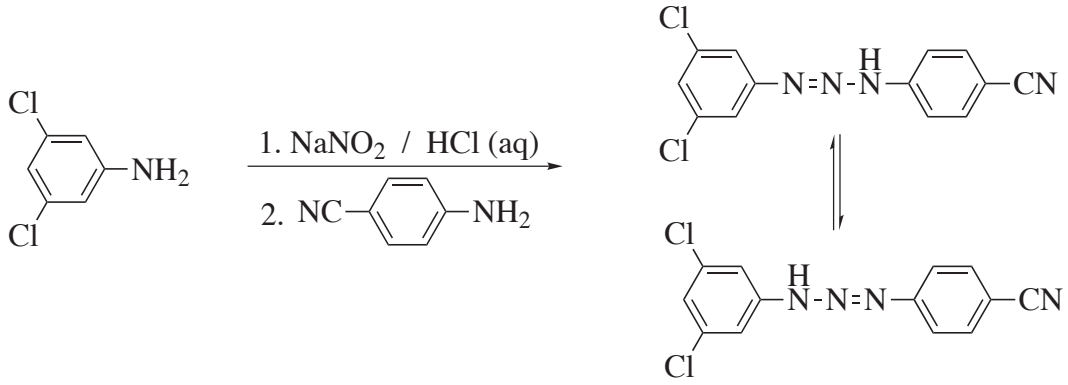

In a 25 mL round-bottom flask, 3,5-dichloroaniline (324.5 mg, 2 mmol) was mixed with 37% (w/v) hydrochloric acid (0.5 mL, 16.5 mmol) and water (4.6 mL). This round-bottom flask was placed in an ice bath. A pre-cooled sodium nitrite solution (0.16 g of $NaNO_2$ in 1.34 mL of water) was then added slowly to the round-bottom flask keeping constant stirring to obtain 3,5-dichlorophenyl diazonium ions. After the addition of $NaNO_2$ was completed, the solution was kept stirring for 65 minutes and then the pH was adjusted to *ca*. 6 by adding 18% (w/v) sodium acetate aqueous solution. In a 50 mL round-bottom flask, 4-cyanoaniline (236.7 mg, 2 mmol) was dissolved in 6.7 mL of methanol. The flask was placed in an ice bath and stirred vigorously. Afterwards, the solution contained in the 25 mL round-bottom flask was added drop-by-drop to the 50 mL round-bottom flask over a period of 45 minutes. A bright yellow precipitate began to form immediately. After this addition, the reaction mixture was kept stirring for 20 hours. The bright yellow precipitate was poured into 100 mL of cold water, then filtered out, and washed with cold water. The precipitate was dried in vacuum overnight at room temperature. The raw product was purified by recrystallization using ethanol to afford the product as a bright yellow solid (449.8 mg; yield 78%). To the best of our knowledge, no physical data have been reported for 3,5-dichloro-4-cyano-1,3-diphenyltriazene; mp 224 - 224.5ºC; ^{1}H NMR (300 MHz, DMSO-*d*6): 7.44 (s, 1H, *para* **H** to NNNH), 7.53 (s, 2H, *ortho* **H** to NNNH and Cl), 7.58 (d, 2H, *meta* **H** to CN, J = 8.5 Hz), 7.81 (d, 2H, *ortho* **H** to CN, J = 8.5 Hz), 13.13 (br, 1H, N**H**); MS m/z (rel. intensity) (EI): 290 (M [$^{35}Cl_2$], 2.5), 173 (47), 145 (87), 130 (100), 102 (24); HRMS calc. for $C_{13}H_8{}^{35}Cl_2N_4$: 290.0126; found: 290.0133.

4.1.3.3 4-Cyano-3′-trifluoromethyl-1,3-diphenyltriazene (10c)

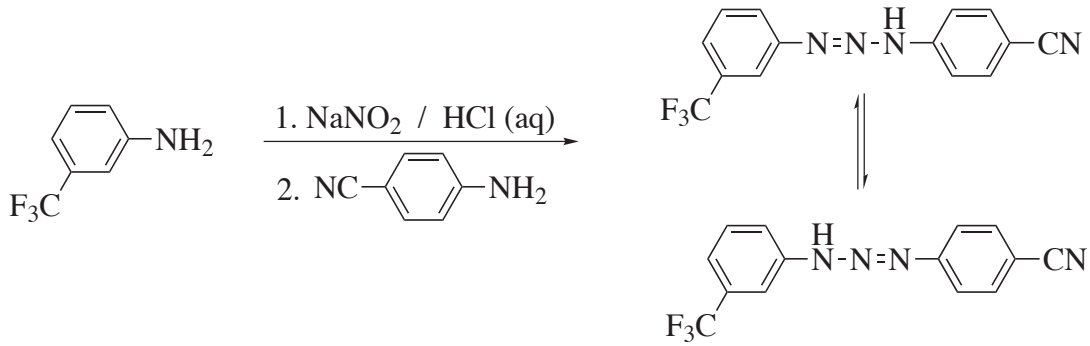

In a 25 mL round-bottom flask, 3-(trifluoromethyl)aniline (483.4 mg, 3 mmol) was mixed with 37% (w/v) hydrochloric acid (0.75 mL, 24.7 mmol) and water (7 mL). This round-bottom flask was placed in an ice bath. A pre-cooled sodium nitrite solution (0.22 g of $NaNO_2$ in 2 mL of water) was then added slowly to the round-bottom flask keeping constant stirring to obtain 3-(trifluoromethyl)phenyl diazonium ions. After the addition of $NaNO_2$ was completed, the solution was kept stirring for 90 minutes and then the pH was adjusted to *ca.* 6 by adding 18% (w/v) sodium acetate aqueous solution. In a 50 mL round-bottom flask, 4-cyanoaniline (354.4 mg, 3 mmol) was dissolved in 10 mL of methanol. The flask was placed in an ice bath and stirred vigorously. Afterwards, the solution in the 25 mL round-bottom flask was added drop-by-drop to the 50 mL round-bottom flask over a period of 55 minutes. A light yellow precipitate began to form immediately. After this addition, the reaction mixture was kept stirring for two hours. The light-yellow precipitate was filtered out, washed with cold water and dried in vacuum overnight at room temperature. The raw product was purified by column chromatography (using 2:1 benzene:ethyl acetate as eluent) and recrystallization using a mixture of chloroform and hexane (1:1) to afford the product as a yellow powder (39.7 mg; yield 5%). To the best of our knowledge, no physical data have been reported for

4-cyano-3′-trifluoromethyl-1,3-diphenyltriazene; mp 190 – 191 ºC; ^{1}H NMR (300 MHz, acetone-*d*6): 7.61(d, 1H, *para* **H** to CF_3), 7.69 (overlapping d and t, 3H, *meta* **H** to CN and *meta* **H** to CF_3), 7.80 (d, 2H, *ortho* **H** to CN), 7.86 (overlapping s and d, 2H, *para* **H** to NNNH and *ortho* **H** to CF_3 and NNNH), 11.95 (s, 1H, N**H**); MS m/z (rel. intensity) (EI): 290 (M, 9), 173 (27), 145 (100), 130 (19), 102 (45); HRMS calc. for $C_{14}H_9F_3N_4$: 290.0779, found: 290.0780.

4.1.3.4 4-Chloro-4′-cyano-1,3-diphenyltriazene (10d)

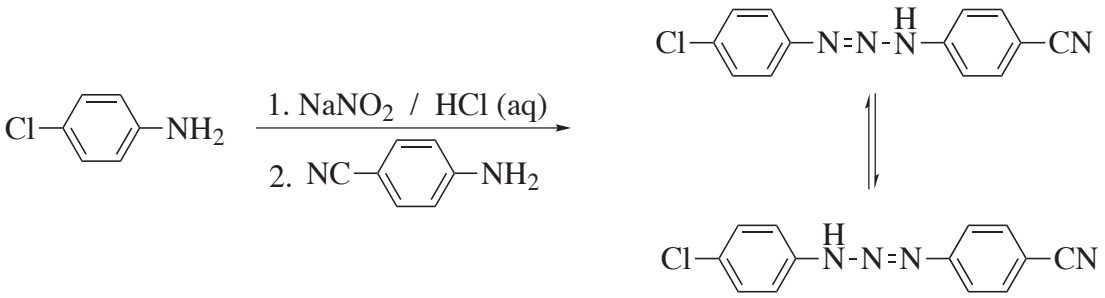

In a 25 mL round-bottom flask, 4-cyanoaniline (236.1 mg, 2 mmol) was mixed with 37% (w/v) hydrochloric acid (0.5 mL, 16.5 mmol) and water (4.6 mL). This round-bottom flask was placed in an ice bath. A pre-cooled sodium nitrite solution (0.16 g of $NaNO_2$ in 1.34 mL of water) was then added slowly to the round-bottom flask keeping constant stirring to obtain 4-cyanophenyl diazonium ions. After the addition of $NaNO_2$ was completed, the solution was kept stirring for 65 minutes and then the pH was adjusted to *ca*. 6 by adding 18% (w/v) sodium acetate aqueous solution. In a 50 mL round-bottom flask, 4-chloroaniline (255.2 mg, 2 mmol) was dissolved in 6.7 mL of methanol. The flask was placed in an ice bath and stirred vigorously. Afterwards, the solution contained in the 25 mL round-bottom flask was added drop-by-drop to the 50 mL round-bottom flask over a period of 55 minutes. An orange

precipitate began to form immediately. After this addition, the reaction mixture was kept stirring for 18 hours. The bright orange precipitate was poured into 100 mL of cold water, then filtered out, and washed with cold water. The precipitate was dried in vacuum overnight at room temperature. The raw product was purified by recrystallization using hexane to yield the product as shiny orange needles (278.8 mg; yield 55%). To the best of our knowledge, no physical data have been reported for 4-chloro-4′-cyano-1,3-diphenyltriazene; mp 154 – 155 ºC; ^{1}H NMR (300 MHz, acetone-*d*6): 7.45 (d, 2H, *ortho* **H** to Cl, J = 8.8 Hz), 7.60 (two overlapping d, 4H, *ortho* **H** to NNNH), 7.76(d, 2H, *ortho* **H** to CN, J = 8.8 Hz), 11.79 (s, 1H, N**H**); MS m/z (rel. intensity) (EI): 256 (M [^{35}Cl], 16), 139 (47), 111 (100), 102 (75); HRMS calc. for $C_{13}H_9{}^{35}ClN_4$: 256.0516; found: 256.0513.

4.1.3.5 4-Cyano-4′-methoxy-1,3-diphenyltriazene (10e)

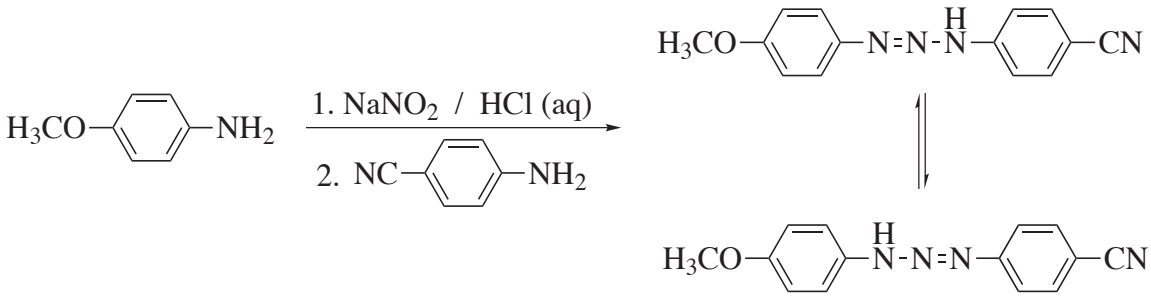

In a 25 mL round-bottom flask, 4-methoxyaniline (246.3 mg, 2 mmol) was mixed with 37% (w/v) hydrochloric acid (0.5 μL, 16.5 mmol) and water (4.6 mL). This round-bottom flask was placed in an ice bath. A pre-cooled sodium nitrite solution (0.16 g of $NaNO_2$ in 1.34 mL of water) was then added slowly to the round-bottom flask keeping constant stirring to obtain 4-methoxyphenyl diazonium ions. After the addition of $NaNO_2$ was completed, the solution was kept stirring for 75 minutes and then the pH was adjusted to *ca*. 6 by adding 18% (w/v)

sodium acetate aqueous solution. In a 50 mL round-bottom flask, 4-cyanoaniline (237.1 mg, 2 mmol) was dissolved in 6.7 mL methanol. The flask was placed in an ice bath and stirred vigorously. Afterwards, the solution contained in the 25 mL round-bottom flask was added drop-by-drop to the 50 mL round-bottom flask over a period of 60 minutes. A dark brown precipitate began to form immediately. After this addition, the reaction mixture was kept stirring overnight. The dark brown precipitate was filtered out, washed with cold water and dried in vacuum overnight at room temperature. The raw product was purified by recrystallization using ethanol to afford the product as shiny brown needles (318.4 mg; yield 65%). To the best of our knowledge, no physical data have been reported for 4-cyano-4′-methoxy-1,3-diphenyltriazene; mp 160 – 161 ºC; ^{1}H NMR (300 MHz, acetone-*d*6): 3.85 (s, 3H, OC**H**$_3$), 7.01 (d, 2H, *ortho* **H** to CH_3O, J = 8.8 Hz), 7.57 (two overlapping apparent doublets, 4H, *ortho* **H** to NNNH), 7.73 (d, 2H, *ortho* **H** to CN, J = 8.8 Hz), 11.46 (br, 1H, N**H**); MS m/z (rel. intensity) (EI): 252 (M, 45), 135 (70), 122 (72), 107 (100); HRMS calc. for $C_{14}H_{12}N_4O$: 252.1011; found: 252.1011.

4.1.3.6 4-Chloro-4′-trifluoromethyl-1,3-diphenyltriazene (10f)

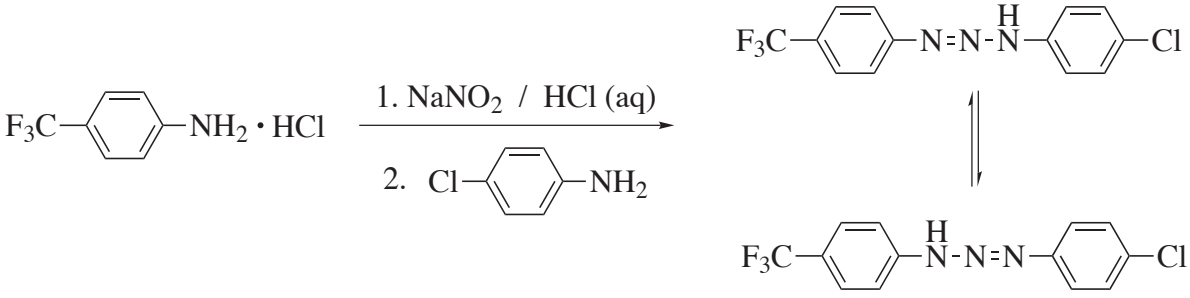

In a 25 mL round-bottom flask, 4-(trifluoromethyl)aniline hydrochloride (0.40 g, 2 mmol) was mixed with 37% (w/v) hydrochloric acid (0.50 mL, 16.5 mmol) and water (5 mL). This round-

bottom flask was placed in an ice bath. A pre-cooled sodium nitrite solution (0.14 g of $NaNO_2$ in 1.3 mL of water) was then added slowly to the round-bottom flask keeping constant stirring to obtain 4-(trifluoromethyl)phenyl diazonium ions. After the addition of $NaNO_2$ was completed, the solution was kept stirring for 60 minutes and then the pH was adjusted to *ca*. 6 by adding 18% (w/v) sodium acetate aqueous solution. In a 50 mL round-bottom flask, 4-chloroaniline (0.26 g, 2 mmol) was dissolved in 6.7 mL of methanol. The flask was placed in an ice bath and stirred vigorously. Afterwards, the solution contained in the 25 mL round-bottom flask was added drop-by-drop to the 50 mL round-bottom flask over a period of 40 minutes. A yellow precipitate began to form immediately. After this addition, the reaction mixture was kept stirring for two hours. The yellow precipitate was filtered out, washed with cold water and dried in vacuum overnight at room temperature. The raw product was purified by recrystallization using hexane to afford the product as yellow light solid (450 mg; yield 75%). To the best of our knowledge, no physical data have been reported for 4-chloro-4′-trifluoromethyl-1,3-diphenyltriazene; mp 125 - 126 ºC; ^{1}H NMR (300 MHz, DMSO-*d*6): 7.47 (d, 2H, *ortho* **H** to Cl, J = 8.5 Hz), 7.53 (d, 4H, *ortho* **H** to NNNH, J = 8.5 Hz), 7.71 (d, 2H, *ortho* **H** to CF_3, J = 8.5 Hz), 12.85 (s, 1H, N**H**); MS m/z (rel. intensity) (EI): 300(M [^{35}Cl], 100), 173(26), 162 (24), 139(11); HRMS calc. for $C_{13}H_{10}{}^{35}ClF_3N_3$: 300.0515, found: 300.0547.

4.1.3.7 4-Methoxy-4′-methyl-1,3-diphenyltriazene (10g)

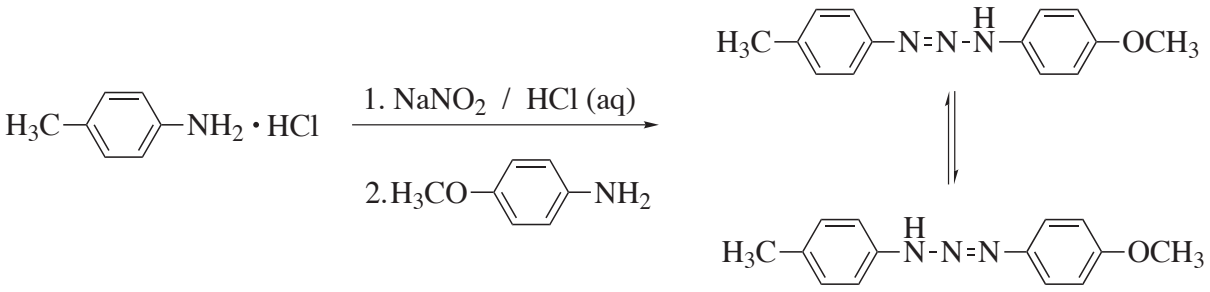

In a 25 mL round-bottom flask, 4-methylaniline hydrochloride (0.43 g, 3 mmol) was mixed with 37% (w/v) hydrochloric acid (0.75 mL, 24.7 mmol) and water (7 mL). This round-bottom flask was placed in an ice bath. A pre-cooled sodium nitrite solution (0.22 g of $NaNO_2$ in 2 mL of water) was then added slowly to the round-bottom flask keeping constant stirring to obtain 4-methylphenyl diazonium ions. After the addition of $NaNO_2$ was completed, the solution was kept stirring for 45 minutes and then the pH was adjusted to *ca*. 6 by adding 18% (w/v) sodium acetate aqueous solution. In a 50 mL round-bottom flask, 4-methoxyaniline (0.37 g, 3 mmol) was dissolved in 10 mL of methanol. The flask was placed in an ice bath and the solution was stirred vigorously. Subsequently, the diazonium ion solution contained in the 25 mL round-bottom flask was added drop-by-drop to the 50 mL round-bottom flask over a period of 45 minutes. A dark brown precipitate began to form immediately. The reaction mixture was kept stirring for two hours. The dark brown precipitate was filtered out, washed with cold water, and dried in vacuum overnight at room temperature. The raw product was purified by recrystallization using petroleum ether to afford the desired product as shiny brown needles (240 mg; yield 34%); mp 84 - 85 ºC (lit. mp[4] 87.5 ºC); ^{1}H NMR (300 MHz, DMSO-*d*6): 2.26 (s, 3H, C**H**$_3$), 3.76 (s, 3H, OC**H**$_3$), 6.95 (d, 2H, *ortho* **H** to CH_3O, J = 8.1 Hz), 7.14 (br, 2H, *ortho* **H** to CH_3), 7.41 (br, 4H, *ortho* **H** to NNNH), 12.12 (br, 1H, N**H**).

4.1.4 Synthesis of Amidines

Amidines, another class of amine derivatives, are compounds containing two different types of nitrogen atoms (i.e., –N=CH–N<).[5] The amidino group is the combination of an azomethine-like C=N double bond with an amide like C-N single bond. Due to the presence of

the C=N double bond, amidines can undergo reversible *cis-trans* isomerization.[6] Thus, besides triazenes, amidines have potential as photochromic materials.[5]

A series of symmetrical amidines (listed in Chart 4.1) were selected, based on their capability to absorb at 355 nm (excitation wavelength of the apparatus employed in this study). The chosen series of amidines have to be synthesized (see below for detailed description of the corresponding experimental conditions) since they are not commercially available. Mechanistic studies on the thermal *cis*-to-*trans* isomerization of chosen amidines were planned but unfortunately, no evidence for photoisomerization could be obtained. Thus, the *cis-trans* isomerization study on the amidine system was discontinued.

Chart 4.1 Target amidines

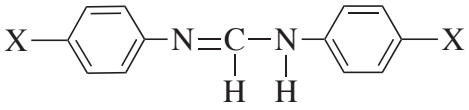

13

13	X	**13**	X
a	$N(CH_3)_2$	**d**	Cl
b	OCH_3	**e**	NO_2
c	CN		

4.1.4.1 N,N′-Di(p-N,N-dimethylaminophenyl)formamidine (13a)

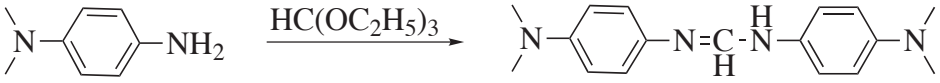

Synthesis of *N,N′*-di(*p-N,N*-dimethylaminophenyl)formamidine was done by mixing *p-N,N*-dimethylamino aniline (1.1814 g, 10 mmol) with triethyl orthoformate (0.83 mL, 5 mmol) in a 25 mL round bottom flask. This mixture was heated at 120 – 130 ºC for 13.5

hours and then cooled down. As the reaction mixture was cooled down to room temperature, yellow solid crude product was formed. The crude product was purified by recrystallization using ethanol to afford very shiny and very fine golden crystals (1.0359 g; 84% yield); mp 137.5-138 ºC (lit. mp[7] 139 ºC); ^{1}H NMR (300 MHz, chloroform-*d*): 2.90 (s, 12H, C**H**$_3$), 6.71 (d, 4H, *ortho* **H** to N(CH$_3$)$_2$, J = 8.8 Hz), 6.97 (d, 4H, *meta* **H** to N(CH$_3$)$_2$, J = 8.8 Hz), 8.62 (s, 1H, NC**H**NH).

4.1.4.2 N,N′-Di(p-methoxyphenyl)formamidine (13b)

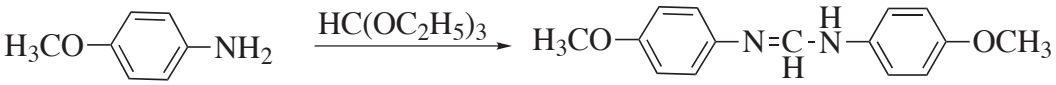

Synthesis of *N,N′*-di(*p*-methoxyphenyl)formamidine was done by mixing *p*-methoxyaniline (1.3545 g, 11 mmol) with triethyl orthoformate (2.0 mL, 11 mmol) in a 25 mL round bottom flask. This mixture was heated in an oil bath at 120 – 130 ºC for 5 hours. Afterwards, the reaction mixture was cooled down and as a result, a dark purple crystalline crude product was formed. The crude product was purified by recrystallization using ethanol to afford sparkling dark-purple prisms (0.2739 g; 20% yield); mp 114-115°C (lit. mp[8]112-113°C); ^{1}H NMR (300 MHz, chloroform-*d*): 3.77 (s, 6H, OC**H**$_3$), 6.83 (d, 4H, *ortho* **H** to CH$_3$O, J = 8.4 Hz), 6.96 (d, 4H, *meta* **H** to CH$_3$, J = 8.4 Hz), 8.01 (s, 1H, NC**H**NH).

4.1.4.3 N,N′-Di(p-cyanophenyl)formamidine (13c)

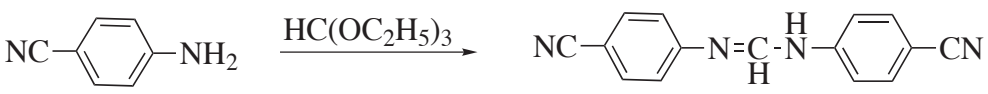

Synthesis of *N,N′*-di(*p*-cyanophenyl)formamidine was done by mixing *p*-cyanoaniline (1.1814 g, 10 mmol) with triethyl orthoformate (0.83 mL, 5 mmol) in a 25 mL round bottom flask. This mixture was heated at 120 – 130 ºC for 13.5 hours. A yellow solid crude product was formed after the reaction mixture was cooled down to room temperature. The crude product was purified using recrystallization using ethanol to afford golden crystals (1.0359 g; 84% yield); mp 216-217 ºC (lit. mp[9] 216-217 ºC); ^{1}H NMR (300 MHz, acetone-*d*6): 7.51 (br, 4H, *meta* **H** to CN), 7.70 (d, 4H, *ortho* **H** to CN, J = 8.6 Hz), 8.42 (br, 1H, NC**H**NH), 9.44 (s, 1H, NCHN**H**, signal disappears after addition of D_2O).

4.1.4.4 N,N′-Di(p-chlorophenyl)formamidine (13d)

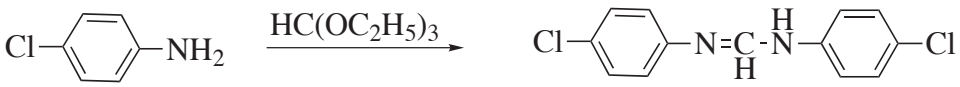

Synthesis of *N,N′*-di(*p*-chlorophenyl)formamidine was done by mixing *p*-chloroaniline (1.2814 g, 10 mmol) with triethyl orthoformate (1.7 mL, 10 mmol) in a 25 mL round bottom flask. This mixture was heated at 120 – 130 ºC for 5 hours and then cooled down. As a result, an off-white crude product was formed. The crude product was purified by recrystallization using ethanol to afford very shiny and very fine golden crystals (0.7524 g; 56.7% yield); mp 182 - 182.5 ºC (lit. mp[10] 184 ºC); ^{1}H NMR (300 MHz, chloroform-*d*): 7.00 (d, 4H, *meta* **H** to Cl, J = 8.7 Hz), 7.27 (d, 4H, *ortho* **H** to Cl, J = 8.7 Hz), 8.07 (s, 1H, NC**H**NH). ^{1}H NMR (300 MHz, acetone-*d6*): 7.30 (m, 8H), 8.18 (s, 1H, NC**H**NH), 8.89 (s, 1H, NCHN**H**, signal disappears after addition of D_2O).

4.1.4.5 N,N′-Di(p-nitrophenyl)formamidine (13e)

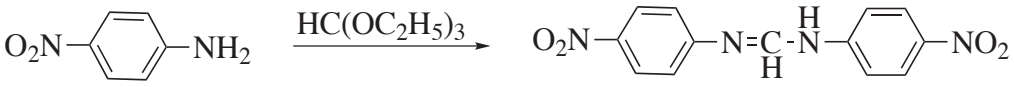

Synthesis of *N,N′*-di(*p*-nitrophenyl)formamidine was done by mixing the *p*-nitroaniline (1.3812 g, 10 mmol) with triethyl orthoformate (1.7 mL, 10 mmol) in a 25 mL round bottom flask. This mixture was heated at 95 ºC for a day. Afterwards, the reaction mixture was cooled down and a yellow solid crude product was formed. The crude product was purified by recrystallization using ethyl acetate to afford bright yellow crystals (0.9514 g; 70% yield); mp 241-242 ºC (lit. mp 236-237 ºC[11] and 245-246 ºC[12]); ^{1}H NMR (300 MHz, DMSO-*d*6): 7.43 (br, 4H, *meta* **H** to NO_2), 8.19 (d, 4H, *ortho* **H** to NO_2, J = 9.0 Hz), 8.56 (br, 1H, NC**H**NH), 10.8 (s, 1H, NCHN**H**, signal disappears after addition of D_2O).

4.2 Kinetic and pKa Studies

4.2.1 Reagents and Instruments

All triazenes employed were synthesized as described in the previous section. THF (Omnisolv grade) was purchased from EM Science. Before used, THF was purified by fractional distillation to remove the stabilizer 2,6-di-*tert*-butyl-4-methylphenol. Ultra pure water for the preparation of aqueous buffer solutions was obtained by passing deionized water through a Millipore Milli-Q system.

The measurements of pH were performed using an ATI Orion PerpHectT 350 digital pH meter. Ground state UV-visible spectra were recorded on a Varian Cary 1 Bio UV-visible spectrophotometer. Moreover, kinetic measurements on restricted rotation about the N(2)-N(3) bond of the triazenes were carried out using a home-built laser-flash photolysis (LFP) system.

Laser-Flash Photolysis is a useful method for investigating reactive intermediates generated by a laser pulse.[13] Short-lived intermediates can be characterized by means of their primary photochemical and photophysical processes. The photochemical phenomena may involve quenching reactions of transients and/or added substrates leading to product formation. Photophysical mechanisms involve intersystem crossing and energy transfer.[13]

The experimental setup of a LFP system is shown in Figure 4.1. The component parts of our LFP spectrometer include the cell holder and the monitoring light source (a xenon arc lamp with an output of 150 W). Additionally, there is an excitation source, which is an Nd:YAG laser (Continuum Surelite I-10) operating at 355 nm (4 – 6 ns pulses, < 10 mJ/pulse), optical quality lenses and filters, and a detector system, which consists of a monochromator and a photomultiplier tube (MC and PMT) combination. Finally, the LFP analysis/output devices are a digitizer and a computer. In the absence of the laser, the system resembles a single beam spectrophotometer. Further details on the laser system used for the purpose of this study are reported elsewhere.[14,15]

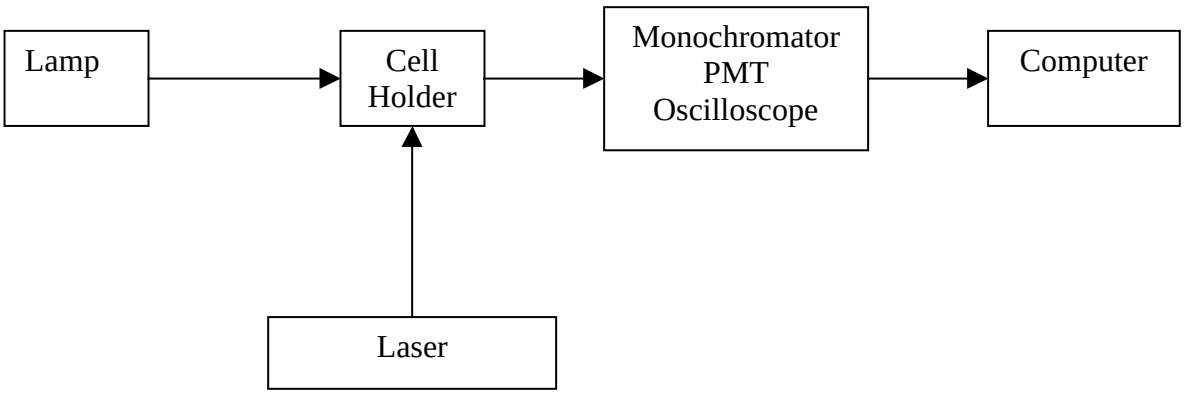

Figure 4.1 Experimental set up of a Laser-Flash Photolysis system.

4.2.2 Sample Preparations and Data Processing

For the determination of acid dissociation equilibrium constants, buffer aqueous solutions were made according to procedures described in the literature.[16] THF was added to the buffer solutions to reach 30% (v/v) concentration. After injection of an aliquot from a concentrated target triazene THF solution into the buffer solutions, spectra of the resulting solutions were collected on a UV-visible spectrometer. Values of p*Ka* for triazenes were obtained by using the general curve-fitting procedure of Kaleidagraph™ software (version 3.6.2 from Synergy Software) to fit data to eq 2.3.

Kinetic studies on the restricted rotation around the N(2)-N(3) bond of target triazenes were performed in NaOH solutions (concentrations ranging from 0.01 to 0.2 M) using 30% (v/v) THF:H_2O as solvent. The ionic strength of the solutions was kept constant at 0.5 M using NaCl as compensating electrolyte. The kinetic measurements were performed after the injection of an aliquot of the corresponding concentrated triazene THF solution to an alkaline solution containing all other components. All sample solutions for laser kinetic studies were air-equilibrated and kept at room temperature, i.e., 21 ± 1 °C. Sample solutions were kept in quartz cell constructed of 7 x 7 mm^2 Suprasil tubing. The concentration of the target triazenes in the laser kinetic samples was of the order of 10^{-5} M, so that the absorbance of the triazene solution at 355 nm (excitation wavelength) was in the 0.3 - 0.5 range.

For each sample solution, kinetic traces were recorded at different time ranges. These kinetic traces were then combined for analysis. Values for the observed rate constants were obtained by using the general curve-fitting procedure of Kaleidagraph™ software version 3.6.2 from Synergy Software. The kinetic traces for the target triazenes were fitted with either a single exponential or two-exponential functions. The general equation for the curve fittings is

shown in the following equation (eq 4.1), where ΔA_t is the change in absorbance measured at time t, ΔA_∞ is the change in absorbance at the end of the reaction (residual absorbance), n represents the total number of kinetic terms that are observed (i.e., 1 or 2), ΔA_i represents the contribution of process i, and k_i denotes the rate constant for process i. Finally, Figure 3.3 was generated using TableCurve 3D (version 4.0 from Systat Software, Inc.). Values for Hammett reaction constants were obtained by fitting to eq 3.1 using the general curve-fitting procedure of Kaleidagraph™ software (version 3.6.2 from Synergy Software).

$$\Delta A_t = \Delta A_\infty + \sum_{i=1}^{n} (\Delta A_i) e^{-k_i \cdot t} \qquad \text{eq 4.1}$$

References

(1) Hill, D. T.; Stanley, K. G.; Williams, J. E. K.; Loev, B.; Fowler, P. J. *J. Med. Chem.* **1983**, *26*, 865-869.

(2) Stefane, B.; Kocevar, M.; Polanc, S. *J. Org. Chem.* **1997**, *62*, 7165-7169.

(3) Vernin, G.; Siv, C.; Metzger, J.; Párkányi, C. *Synthesis* **1977**, 691-693.

(4) Mitsuhashi, T.; Simamura, O. *J. Chem. Soc.* **1970**, *B*, 705-711.

(5) Häfelinger, G. In *The Chemistry of Amidine and Imidates*; Patai, S., Ed.; John Wiley & Sons: New York, 1975, Chapter 1.

(6) Prevorsek, D. C. *J. Phys. Chem.* **1962**, *66*, 769-778.

(7) Saeed, A. A. H.; Selman, S. A. *Can. J. Spectrosc.* **1982**, *27*, 123-125.

(8) Kashima, C.; Shimizu, M.; Eto, T.; Omote, Y. *Bull. Chem. Soc. Jpn.* **1986**, *59*, 3317-3319.

(9) Crundwell, E. *J. Chem. Soc. Abstracts* **1956**, 368-371.

(10) Lewis, C. D.; Krupp, R. G.; Tieckelmann, H.; Post, H. W. *J. Org. Chem.* **1947**, *12*, 303-307.

(11) Walther, R. *J. Prakt. Chem.* **1896**, *53*, 472.

(12) Roberts, R. M.; DeWolfe, R. H.; Ross, J. H. *J. Amer. Chem. Soc.* **1951**, *73*, 2277-2281.

(13) Hadel, L. M. *In CRC Handbook of organic photochemistry*; CRC Press: Boca Raton, Fla, 1989; Vol. 1, 279-292.

(14) Barra, M.; Agha, K. A. *J. Photochem. Photobiol. A: Chem.* **1997**, *109*, 293-298.

(15) Sanchez, A. M.; Barra, M.; Rossi, R. H. *J. Org. Chem.* **1999**, *64*, 1604-1609.

(16) Lide, D. R., Ed. *Handbook of Chemistry and Physics; 77th ed.*; CRC Press: Boca Raton, 1996-1997, 8-42.

Appendix A. Observed rate constants for restricted rotation around the N(2)-N(3) bond for symmetrical substituted 1,3-diphenyltriazenes.

Table A1: 1,3-Bis(3,4-dimethylphenyl)triazene (**9a**) in NaOH solutions.[a]

[NaOH], M	k_{obs} (10^4 s^{-1})	[NaOH], M	k_{obs} (10^4 s^{-1})
0.0124	7.6 ± 0.1	0.0649	7.7 ± 0.1
0.0165	8.9 ± 0.1	0.132	7.3 ± 0.1
0.0258	8.5 ± 0.2		

[a]In 30% (v/v) THF:H_2O, μ = 0.5 M (NaCl), at T = 21°C. [**9a**] = 2.22 x 10^{-5} M

Table A2: 1,3-Bis(3,4-dimethylphenyl)triazene (**9a**) in NaOD solutions.[a]

[NaOD], M	k_{obs} (10^4 s^{-1})	[NaOD], M	k_{obs} (10^4 s^{-1})
0.0124	8.6 ± 0.1	0.132	8.3 ± 0.1
0.0225	9.8 ± 0.1	0.155	7.1 ± 0.1
0.0525	9.4 ± 0.1	0.178	6.7 ± 0.1
0.0935	8.4 ± 0.1		

[a]In 30% (v/v) THF:D_2O, μ = 0.5 M (NaCl), at T = 21°C. [**9a**] = 2.22 x 10^{-5} M

Table A3: 1,3-Bis(4-ethynylphenyl)triazene (**9b**) in NaOH solutions.[a]

[NaOH], M	k_{obs} (10^4 s^{-1})	[NaOH], M	k_{obs} (10^4 s^{-1})
0.0096	1.50 ± 0.04	0.115	1.50 ± 0.04
0.0124	1.63 ± 0.03	0.155	1.60 ± 0.03
0.0258	1.88 ± 0.04	0.200	1.31 ± 0.03
0.0649	1.60 ± 0.03		

[a]In 30% (v/v) THF:H_2O, μ = 0.5 M (NaCl), at T = 21°C. [**9b**] = 5.87 x 10^{-5} M

Table A4: 1,3-Bis(3-trifluoromethylphenyl)triazene **9c** in NaOH solutions.[a]

[NaOH], M	k_{obs} (10^3 s^{-1})	[NaOH], M	k_{obs} (10^3 s^{-1})
0.0124	8.1 ± 0.6	0.0649	8.0 ± 0.6
0.0165	8.2 ± 0.4	0.132	7.7 ± 0.3
0.0258	7.54 ± 0.07		

[a]In 30% (v/v) THF:H_2O, μ = 0.5 M (NaCl), at T = 21°C. [**9c**] = 3.54 x 10^{-5} M.

Table A5: 1,3-Bis(3-trifluoromethylphenyl)triazene (**9c**) in NaOD solutions.[a]

[NaOD], M	k_{obs} (10^3 s^{-1})	[NaOD], M	k_{obs} (10^3 s^{-1})
0.0124	7.9 ± 0.1	0.0745	7.3 ± 0.1
0.0158	8.6 ± 0.1	0.0935	7.9 ± 0.1
0.0225	8.8 ± 0.1	0.115	7.2 ± 0.1
0.0392	8.0 ± 0.1	0.132	6.0 ± 0.1
0.0525	8.0 ± 0.1		

[a]In 30% (v/v) THF:D_2O, μ = 0.5 M (NaCl), at T = 21°C. [**9c**] = 3.54 x 10^{-5} M

Table A6: 1,3-Bis(3-cyanophenyl)triazene (**9d**) in NaOH solutions.[a]

[NaOH], M	k_{obs} (10^3 s^{-1})	[NaOH], M	k_{obs} (10^3 s^{-1})
0.0124	8.7 ± 0.6	0.115	6.7 ± 0.4
0.0165	8.8 ± 0.6	0.132	6.2 ± 0.4
0.0258	8.2 ± 0.4	0.155	5.6 ± 0.2
0.0425	7.6 ± 0.4	0.175	5.4 ± 0.2
0.0649	6.7 ± 0.3	0.200	5.2 ± 0.2
0.0845	7.2 ± 0.7		

[a]In 30% (v/v) THF:H_2O, μ = 0.5 M (NaCl), at T = 21°C. [**9d**] = 2.33 x 10^{-5} M

Table A7: 1,3-Bis(3-cyanophenyl)triazene (**9d**) in NaOD solutions.[a]

[NaOH], M	k_{obs} (10^3 s^{-1})	[NaOH], M	k_{obs} (10^3 s^{-1})
0.0096	8.26 ± 0.07	0.0745	6.0 ± 0.1
0.0124	8.42 ± 0.09	0.0935	4.83 ± 0.07
0.0158	8.16 ± 0.07	0.115	5.07 ± 0.07
0.0225	6.93 ± 0.07	0.132	4.69 ± 0.09
0.0258	7.07± 0.08	0.155	4.7 ± 0.1
0.0392	6.7 ± 0.1	0.178	3.25 ± 0.08
0.0525	5.85 ± 0.08		

[a]In 30% (v/v) THF:D_2O, μ = 0.5 M (NaCl), at T = 21°C. [**9d**] = 2.33 x 10^{-5} M

Table A8: 1,3-Bis(3,5-dichlorophenyl)triazene (**9f**) in NaOH solutions.[a]

[NaOH], M	k_{obs} (10^3 s^{-1})	[NaOH], M	k_{obs} (10^3 s^{-1})
0.0124	5.55 ± 0.08	0.0845	6.4 ± 0.1
0.0165	6.4 ± 0.1	0.115	5.6 ± 0.1
0.0258	5.93 ± 0.07	0.155	5.7 ± 0.1
0.0425	6.3 ± 0.1	0.175	6.4 ± 0.1

[a]In 30% (v/v) THF:H_2O, μ = 0.5 M (NaCl), at T = 21°C. [**9f**] = 5.01 x 10^{-5} M

Table A9: 1,3-Bis(3,4,5-trichlorophenyl)triazene (**9g**) in NaOH solutions.[a]

[NaOH], M	k_{obs} (10^3 s^{-1})	[NaOH], M	k_{obs} (10^3 s^{-1})
0.0124	3.37 ± 0.07	0.0649	3.25 ± 0.07
0.0165	3.36 ± 0.06	0.132	3.03 ± 0.07
0.0258	3.08 ± 0.07	0.227	3.03 ± 0.08

[a]In 30% (v/v) THF:H_2O, μ = 0.5 M (NaCl), at T = 21°C. [**9g**] = 3.73 x 10^{-5} M

Table A10: 1,3-Bis(4-cyanophenyl)triazene (**9o**) in NaOD solutions.[a]

[NaOD], M	k_{obs} (10^4 s^{-1})	[NaOD], M	k_{obs} (10^4 s^{-1})
0.0124	5.9 ± 0.1	0.0745	7.1 ± 0.1
0.0158	5.5 ± 0.1	0.0935	7.0 ± 0.1
0.0225	6.2 ± 0.1	0.115	7.2 ± 0.1
0.0258	6.2 ± 0.1	0.132	7.2 ± 0.2
0.0392	6.3 ± 0.1	0.155	7.4 ± 0.1
0.0525	6.6 ± 0.1	0.178	7.1 ± 0.1

[a]In 30% (v/v) THF:D_2O, μ = 0.5 M (NaCl), at T = 21°C. [**9o**] = 9.02 x 10^{-5} M

Appendix B. Observed rate constants for restricted rotation around the N(2)-N(3) bond for unsymmetrical substituted 1,3-diphenyltriazenes.

Table B1: 3,4,5-Trichloro-4-cyano-1,3-diphenyltriazene (**10a**) in NaOH solutions.[a]

[NaOH], M	k_{obs}^{f} (10^4 s^{-1})	k_{obs}^{s} (10^3 s^{-1})	[NaOH], M	k_{obs}^{f} (10^4 s^{-1})	k_{obs}^{s} (10^3 s^{-1})
0.00967	2.3 ± 0.4	7 ± 1	0.0967	7.1 ± 0.3	4.2 ± 0.3
0.0124	2.7 ± 0.3	5.6 ± 0.8	0.124	6.8 ± 0.3	5.3 ± 0.3
0.0165	3.8 ± 0.2	6.6 ± 0.2	0.132	6.7 ± 0.2	4.5 ± 0.2
0.0258	4.5 ± 0. 2	6.0 ± 0.3	0.165	7.5 ± 0.3	3.6 ± 0.2
0.0387	5.9 ± 0.2	6.4 ± 0.2	0.174	6.8 ± 0.3	5.3 ± 0.4
0.0484	6.7 ± 0.3	5.5 ± 0.4	0.193	7.9 ± 0.4	6.1 ± 0.2
0.0649	6.4 ± 0.2	5.4 ± 0.3	0.227	8.0 ± 0.2	4.4 ± 0.2
0.0774	6.5 ± 0.3	5.0 ± 0.3			

[a]In 30% (v/v) THF:H_2O, μ = 0.5 M (NaCl), at T = 21°C. [**10a**] = 6.21 x 10^{-5} M

Table B2: 3,5-Dichloro-4-cyano-1,3-diphenyltriazene (**10b**) in NaOH solutions.[a]

[NaOH], M	k_{obs}^{f} (10^5 s^{-1})	k_{obs}^{s} (10^3 s^{-1})	[NaOH], M	k_{obs}^{f} (10^5 s^{-1})	k_{obs}^{s} (10^3 s^{-1})
0.0124	0.34 ± 0.02	7 ± 1	0.0935	1.31 ± 0.06	3.7 ± 0.1
0.0158	0.47 ± 0.01	5.7 ± 0.1	0.115	1.40 ± 0.01	3.4 ± 0.1
0.0225	0.72 ± 0.02	4.7 ± 0.1	0.132	1.38 ± 0.04	3.7 ± 0.2
0.0258	0.70 ± 0.06	4.94 ± 0.04	0.155	1.60 ± 0.07	3.20 ± 0.01
0.0392	0.74 ± 0.02	4.5 ± 0.1	0.178	1.8 ± 0.2	3.3 ± 0.2
0.0525	0.97 ± 0.06	4.2 ± 0.5	0.200	1.57 ± 0.07	3.06 ± 0.07
0.0745	1.30 ± 0.06	3.4 ± 0.1			

[a]In 30% (v/v) THF:H_2O, μ = 0.5 M (NaCl), at T = 21°C. [**10b**] = 5.1 x 10^{-5} M

Table B3: 3,5-Dichloro-4-cyano-1,3-diphenyltriazene (**10b**) in NaOD solutions.[a]

[NaOD], M	k_{obs}^{f} (10^5 s^{-1})	k_{obs}^{s} (10^3 s^{-1})	[NaOD], M	k_{obs}^{f} (10^5 s^{-1})	k_{obs}^{s} (10^3 s^{-1})
0.0124	0.89 ± 0.02	4.63 ± 0.08	0.0745	1.70 ± 0.05	3.60 ± 0.06
0.0158	1.02 ± 0.03	3.83 ± 0.07	0.0935	1.67 ± 0.05	3.76 ± 0.06
0.0225	1.17 ± 0.03	3.73 ± 0.07	0.115	1.70 ± 0.06	3.31 ± 0.06
0.0258	1.20 ± 0.03	4.28 ± 0.07	0.132	1.74 ± 0.06	3.31 ± 0.06
0.0392	1.39 ± 0.04	3.73 ± 0.07	0.155	1.84 ± 0.06	3.00 ± 0.05
0.0525	1.48 ± 0.04	3.43 ± 0.06	0.178	1.79 ± 0.06	3.37 ± 0.06

[a]In 30% (v/v) THF:D_2O, μ = 0.5 M (NaCl), at T = 21°C. [**10b**] = 5.1 x 10^{-5} M

Table B4: 4-Cyano-3′-trifluoromethyl-1,3-diphenyltriazene (**10c**) in NaOH solutions.[a]

[NaOH], M	k_{obs}^{f} (10^5 s^{-1})	k_{obs}^{s} (10^3 s^{-1})	[NaOH], M	k_{obs}^{f} (10^5 s^{-1})	k_{obs}^{s} (10^3 s^{-1})
0.0124	0.46 ± 0.08	4.3 ± 0.2	0.0845	2.34 ± 0.07	2.91 ± 0.08
0.0165	0.60 ± 0.07	4.21 ± 0.06	0.0975	2.62 ± 0.09	2.99 ± 0.07
0.0258	0.86 ± 0.02	3.8 ± 0.2	0.115	3.2 ± 0.1	2.42 ± 0.08
0.0375	1.12 ± 0.03	3.42 ± 0.07	0.132	3.50 ± 0.09	2.5 ± 0.2
0.0425	1.54 ± 0.06	3.22 ± 0.08	0.155	3.5 ± 0.1	2.44 ± 0.08
0.0525	1.70 ± 0.06	3.16 ± 0.08	0.215	4.5 ± 0.1	2.81 ± 0.06
0.0649	2.2 ± 0.4	2.7 ± 0.2			

[a]In 30% (v/v) THF:H_2O, μ = 0.5 M (NaCl), at T = 21°C. [**10c**] = 5.71 x 10^{-5} M

Table B5: 4-Cyano-3′-trifluoromethyl-1,3-diphenyltriazene (**10c**) in NaOD solutions.[a]

[NaOD], M	k_{obs}^{f} (10^5 s^{-1})	k_{obs}^{s} (10^3 s^{-1})	[NaOD], M	k_{obs}^{f} (10^5 s^{-1})	k_{obs}^{s} (10^3 s^{-1})
0.0124	1.37 ± 0.05	3.32 ± 0.05	0.0975	5.5 ± 0.3	1.36 ± 0.04
0.0375	3.5 ± 0.1	2.60 ± 0.05	0.132	6.2 ± 0.6	1.51 ± 0.06
0.0525	4.2 ± 0.2	1.48 ± 0.04	0.175	6.9 ± 0.5	2.05 ± 0.07

[a]In 30% (v/v) THF:D_2O, μ = 0.5 M (NaCl), at T = 21°C. [**10c**] = 5.16 x 10^{-5} M

Table B6: 4-Chloro-4-cyano-1,3-diphenyltriazene (**10d**) in NaOH solutions.[a]

[NaOH], M	k_{obs}^{f} (10^5 s^{-1})	k_{obs}^{s} (10^3 s^{-1})	[NaOH], M	k_{obs}^{f} (10^5 s^{-1})	k_{obs}^{s} (10^3 s^{-1})
0.00525	0.67 ± 0.02	3.62 ± 0.05	0.0935	4.1 ± 0.2	2.39 ± 0.05
0.00745	0.73 ± 0.02	3.53 ± 0.05	0.115	4.5 ± 0.2	2.28 ± 0.07
0.0124	0.93 ± 0.02	3.44 ± 0.06	0.132	4.7 ± 0.2	1.97 ± 0.04
0.0258	1.59 ± 0.04	2.80 ± 0.07	0.155	5.8 ± 0.2	2.21 ± 0.07
0.0525	2.5 ± 0.1	2.74 ± 0.04	0.175	6.5 ± 0.3	2.56 ± 0.04
0.0745	3.5 ± 0. 1	2.39 ± 0.06	0.200	6.3 ± 0.2	2.16 ± 0.05

[a]In 30% (v/v) THF:H_2O, μ = 0.5 M (NaCl), at T = 21°C. [**10d**] = 5.29 x 10^{-5} M

Table B7: 4-Cyano-4′-methoxy-1,3-diphenyltriazene (**10e**) in NaOH solutions.[a]

[NaOH], M	k_{obs}^{f} (10^6 s^{-1})	k_{obs}^{s} (10^3 s^{-1})	[NaOH], M	k_{obs}^{f} (10^6 s^{-1})	k_{obs}^{s} (10^3 s^{-1})
0.0096	0.20 ± 0.02	2.20 ± 0.03	0.115	1.3 ± 0.2	2.29 ± 0.03
0.0124	0.19 ± 0.03	2.24 ± 0.03	0.124	1.5 ± 0.2	1.98 ± 0.04
0.0165	0.26 ± 0.02	2.20 ± 0.03	0.132	1.3 ± 0.3	2.08 ± 0.05
0.0258	0.32 ± 0.04	2.22 ± 0.04	0.155	1.7 ± 0.4	2.12 ± 0.05
0.0425	0.7 ± 0.1	2.09 ± 0.03	0.165	1.6 ± 0.2	1.89 ± 0.04
0.0649	0.9 ± 0.1	2.15 ± 0.03	0.175	1.9 ± 0.2	2.08 ± 0.04
0.0845	0.73 ± 0.09	2.34 ± 0.05	0.227	2.4 ± 0.5	2.19 ± 0.07
0.0960	1.2 ± 0.1	1.88 ± 0.03			

[a]In 30% (v/v) THF:H_2O, μ = 0.5 M (NaCl), at T = 21°C. [**10e**] = 5.42 x 10^{-5} M

Table B8: 4-Chloro-4′-trifluoromethyl-1,3-diphenyltriazene (**10f**) in NaOH solutions.[a]

[NaOH], M	k_{obs}^{f} (10^4 s^{-1})	k_{obs}^{s} (10^3 s^{-1})	[NaOH], M	k_{obs}^{f} (10^4 s^{-1})	k_{obs}^{s} (10^3 s^{-1})
0.0258	5.5 ± 0.7	5.1 ± 0.2	0.115	5.4 ± 0.6	4.7 ± 0.3
0.0425	4.9 ± 0.5	4.9 ± 0.2	0.155	5.6 ± 0.6	4.8 ± 0.2
0.0845	5.2 ± 0.7	5.0 ± 0.3	0.175	4.4 ± 0.3	4.8 ± 0.2

[a]In 30% (v/v) THF:H_2O, μ = 0.5 M (NaCl), at T = 21°C. [**10f**] = 4.61 x 10^{-5} M

Table B9: 4-Methoxy-4′-methyl-1,3-diphenyltriazene (**10g**) in NaOH solutions.[a]

[NaOH], M	k_{obs}^{f} (10^5 s^{-1})	k_{obs}^{s} (10^4 s^{-1})
0.0165	1.3 ± 0.1	3.5 ± 0.5
0.0258	1.1 ± 0.1	3.6 ± 0.9
0.0649	1.3 ± 0.2	3.7 ± 0.6
0.132	1.2 ± 0.1	3.3 ± 0.6
0.227	1.1 ± 0.2	3.5 ± 0.8

[a]In 30% (v/v) THF:H_2O, μ = 0.5 M (NaCl), at T = 21°C. [**10g**] = 2.12 x 10^{-5} M